

TROPICAL FOCK-GONCHAROV COORDINATES FOR SL_3 -WEBS ON SURFACES II: NATURALITY

DANIEL C. DOUGLAS AND ZHE SUN

ABSTRACT. In a companion paper [DS20], we constructed nonnegative integer coordinates $\Phi_{\mathcal{T}}(\mathcal{W}_{3,\widehat{S}}) \subseteq \mathbb{Z}_{\geq 0}^N$ for the collection $\mathcal{W}_{3,\widehat{S}}$ of reduced SL_3 -webs on a finite-type punctured surface \widehat{S} , depending on an ideal triangulation \mathcal{T} of \widehat{S} . We show that these coordinates are natural with respect to the choice of triangulation, in the sense that if a different triangulation \mathcal{T}' is chosen, then the coordinate change map relating $\Phi_{\mathcal{T}}(\mathcal{W}_{3,\widehat{S}})$ to $\Phi_{\mathcal{T}'}(\mathcal{W}_{3,\widehat{S}})$ is a tropical \mathcal{A} -coordinate cluster transformation. We can therefore view the webs $\mathcal{W}_{3,\widehat{S}}$ as a concrete topological model for the Fock-Goncharov-Shen positive integer tropical points $\mathcal{A}_{\mathrm{PGL}_3,\widehat{S}}^+(\mathbb{Z}^t)$.

1. INTRODUCTION

For a finitely generated group Γ and a suitable Lie group G , a primary object of study in higher Teichmüller theory [Wie18] is the G -character variety

$$\mathcal{R}_{G,\Gamma} = \{\rho : \Gamma \longrightarrow G\} // G$$

consisting of group homomorphisms from the group Γ to the Lie group G , considered up to conjugation. Here, the double bar indicates that the quotient is being taken in the algebro-geometric sense of geometric invariant theory [MFK94].

We are interested in studying the character variety $\mathcal{R}_{\mathrm{SL}_3,S} := \mathcal{R}_{\mathrm{SL}_3,\pi_1(S)}$ in the case where the group $\Gamma = \pi_1(S)$ is the fundamental group of a finite-type punctured surface S with negative Euler characteristic, and where the Lie group $G = \mathrm{SL}_3$ is the special linear group.

Sikora [Sik01] associated to any SL_3 -web W in the surface S (Figure 1) a trace regular function $\mathrm{Tr}_W \in \mathcal{O}(\mathcal{R}_{\mathrm{SL}_3,S})$ on the SL_3 -character variety. A theorem of Sikora-Westbury [SW07] implies that the preferred subset $\mathcal{W}_{3,S}$ of reduced SL_3 -webs indexes, by taking trace functions, a linear basis for the algebra $\mathcal{O}(\mathcal{R}_{\mathrm{SL}_3,S})$ of regular functions on the SL_3 -character variety.

In a companion paper [DS20], we constructed explicit nonnegative integer coordinates for this SL_3 -web basis $\mathcal{W}_{3,S}$. In particular, we identified $\mathcal{W}_{3,S}$ with the set of solutions in $\mathbb{Z}_{\geq 0}^N$ of finitely many Knutson-Tao inequalities [KT99] and modulo 3 congruence conditions. These coordinates depend on a choice of an ideal triangulation \mathcal{T} of the punctured surface S .

In the present article, we prove that these web coordinates satisfy a surprising naturality property with respect to this choice of ideal triangulation \mathcal{T} . Specifically, if another ideal triangulation \mathcal{T}' is chosen, then the induced coordinate change map takes the form of a tropicalized \mathcal{A} -coordinate cluster transformation [FZ02, FG06].

Date: September 15, 2022.

This work was partially supported by the U.S. National Science Foundation grants DMS-1107452, 1107263, 1107367 “RNMS: GEometric structures And Representation varieties” (the GEAR Network). The first author was also partially supported by the U.S. National Science Foundation grants DMS-1406559 and 1711297, and the second author by the China Postdoctoral Science Foundation grant 2018T110084, the FNR AFR Bilateral grant COALAS 11802479-2, and the Huawei Young Talents Program at IHES.

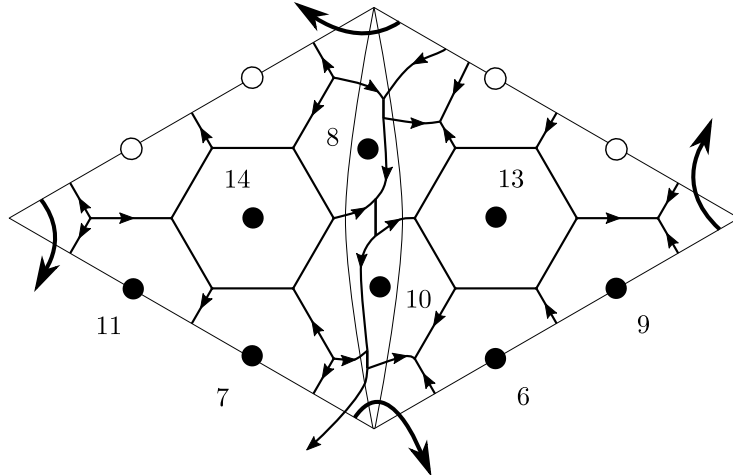


FIGURE 1. Positive tropical integer \mathcal{A} -coordinates for a reduced SL_3 -web on the once punctured torus, with respect to an ideal triangulation \mathcal{T} .

1.1. Global aspects.

More precisely, let \widehat{S} be a marked surface, namely a compact oriented surface together with a finite subset $M \subseteq \partial\widehat{S}$ of preferred points, called marked points, lying on some of the boundary components of \widehat{S} . By a puncture we mean a boundary component of \widehat{S} containing no marked points, which is thought of as shrunk down to a point. We say the surface $\widehat{S} = S$ is non-marked if $M = \emptyset$. We always assume that \widehat{S} admits an ideal triangulation \mathcal{T} , namely a triangulation whose vertex set is equal to the set of punctures and marked points. See §2.1.

1.1.1. Fock-Goncharov duality.

Fock-Goncharov [FG06] introduced a pair of mutually dual moduli spaces $\mathcal{X}_{\mathrm{PGL}_n, \widehat{S}}$ and $\mathcal{A}_{\mathrm{SL}_n, \widehat{S}}$ (as well as for more general Lie groups). In the case $\widehat{S} = S$ of non-marked surfaces, the spaces $\mathcal{X}_{\mathrm{PGL}_n, S}$ and $\mathcal{A}_{\mathrm{SL}_n, S}$ are variations of the PGL_n - and SL_n -character varieties; for $n = 2$, they generalize the enhanced Teichmüller space [FG07a] and the decorated Teichmüller space [Pen87], respectively. Fock-Goncharov duality is a canonical mapping

$$\mathbb{I} : \mathcal{A}_{\mathrm{SL}_n, S}(\mathbb{Z}^t) \longrightarrow \mathcal{O}(\mathcal{X}_{\mathrm{PGL}_n, S}),$$

from the discrete set $\mathcal{A}_{\mathrm{SL}_n, S}(\mathbb{Z}^t)$ of tropical integer points of the moduli space $\mathcal{A}_{\mathrm{SL}_n, S}$ to the algebra $\mathcal{O}(\mathcal{X}_{\mathrm{PGL}_n, S})$ of regular functions on the moduli space $\mathcal{X}_{\mathrm{PGL}_n, S}$, satisfying enjoyable properties; for instance, the image of \mathbb{I} should form a linear basis for the algebra of functions $\mathcal{O}(\mathcal{X}_{\mathrm{PGL}_n, S})$. In the case $n = 2$, Fock-Goncharov gave a concrete topological construction of duality by identifying the tropical integer points with laminations on the surface.

There are various ways to formulate Fock-Goncharov duality. A closely related version is

$$\mathbb{I} : \mathcal{A}_{\mathrm{PGL}_n, S}(\mathbb{Z}^t) \longrightarrow \mathcal{O}(\mathcal{X}_{\mathrm{SL}_n, S})$$

(compare [FG06, Theorem 12.3 and the following Remark] for $n = 2$). There are also formulations of duality in the setting of marked surfaces \widehat{S} , where the moduli spaces $\mathcal{X}_{\mathrm{PGL}_n, \widehat{S}}$ and $\mathcal{X}_{\mathrm{SL}_n, \widehat{S}}$ are replaced [GS15, GS19] by slightly more general constructions $\mathcal{P}_{\mathrm{PGL}_n, \widehat{S}}$ and $\mathcal{P}_{\mathrm{SL}_n, \widehat{S}}$.

Investigating Fock-Goncharov duality has led to many exciting developments. By employing powerful conceptual methods (scattering diagrams, broken lines, Donaldson-Thomas transformations), works such as [GHKK18, GS19] have established general formulations

of duality. On the other hand, explicit higher rank constructions, in the spirit of Fock-Goncharov's topological approach in the case $n = 2$, are not as well understood.

Following [GS15] (see also [FG06, Proposition 12.2]), we focus on the positive points $\mathcal{A}_{\mathrm{PGL}_n, \widehat{S}}^+(\mathbb{Z}^t) \subseteq \mathcal{A}_{\mathrm{PGL}_n, \widehat{S}}(\mathbb{Z}^t)$, defined with respect to the tropicalized Goncharov-Shen potential $P^t : \mathcal{A}_{\mathrm{PGL}_n, \widehat{S}}(\mathbb{Z}^t) \rightarrow \mathbb{Z}$ by $\mathcal{A}_{\mathrm{PGL}_n, \widehat{S}}^+(\mathbb{Z}^t) = (P^t)^{-1}(\mathbb{Z}_{\geq 0})$. These positive tropical integer points play an important role in a variation of the previously mentioned duality,

$$(*) \quad \mathbb{I} : \mathcal{A}_{\mathrm{PGL}_n, \widehat{S}}^+(\mathbb{Z}^t) \longrightarrow \mathcal{O}(\mathcal{R}_{\mathrm{SL}_n, \widehat{S}})$$

(see [GS15, Conjecture 10.11 and Theorem 10.12, as well as Theorems 10.14, 10.15 for $G = \mathrm{PGL}_2$]). Here, the space $\mathcal{R}_{\mathrm{SL}_n, \widehat{S}}$, introduced in [GS15, §10.2] (they denote it by $\mathrm{Loc}_{\mathrm{SL}_n, \widehat{S}}$), is a generalized (twisted) version of the SL_n -character variety $\mathcal{R}_{\mathrm{SL}_n, S}$ valid for marked surfaces \widehat{S} .

Because PGL_n is not simply connected, the moduli space $\mathcal{A}_{\mathrm{PGL}_n, \widehat{S}}$ does not have a cluster structure; however, it does admit a positive structure. The tropical spaces $\mathcal{A}_{\mathrm{PGL}_n, \widehat{S}}(\mathbb{Z}^t)$ and $\mathcal{A}_{\mathrm{PGL}_n, \widehat{S}}^+(\mathbb{Z}^t)$ are thus defined; moreover, they can be seen as subsets of the real tropical space $\mathcal{A}_{\mathrm{SL}_n, \widehat{S}}(\mathbb{R}^t)$, thereby inheriting a tropical cluster structure. Our goal is to construct, in the case $n = 3$, a concrete topological model for the space $\mathcal{A}_{\mathrm{PGL}_3, \widehat{S}}^+(\mathbb{Z}^t)$ of positive tropical integer points, which also exhibits this tropical cluster structure.

See §2 for a brief overview of the underlying Fock-Goncharov-Shen theory.

1.1.2. Topological indexing of linear bases.

One of our guiding principles is that tropical integer points should correspond to topological objects generalizing laminations [Thu97] on surfaces in the case $n = 2$. Such so-called higher laminations can be studied from many points of view, blending ideas from geometry, topology, and physics; see, for instance, [FKK13, Xie13, GS15, Le16]. In the present article, we focus attention on one of the topological approaches to studying higher laminations, via webs [Kup96, Sik01, CKM14]; see also [GMN13]. Webs are certain n -valent graphs-with-boundary embedded in the surface \widehat{S} (considered up to equivalence in $\widehat{S} - M$). Webs also appear naturally in the context of quantizations of character varieties via skein modules and algebras [Tur89, Wit89, Prz91, Sik05].

We begin by reviewing the case $n = 2$. For a marked surface \widehat{S} , define the set $\mathcal{L}_{2, \widehat{S}}$ of (bounded) 2-laminations on \widehat{S} so that $\ell \in \mathcal{L}_{2, \widehat{S}}$ is a finite collection of mutually-non-intersecting simple loops and arcs on \widehat{S} such that (i) there are no contractible loops; and, (ii) arcs end only on boundary components of \widehat{S} containing marked points, and there are no arcs contracting to a boundary interval without marked points.

In the case where the surface $\widehat{S} = S$ is non-marked, a 2-lamination $\ell \in \mathcal{L}_{2, S}$ corresponds to a trace function $\mathrm{Tr}_\ell \in \mathcal{O}(\mathcal{R}_{\mathrm{SL}_2, S})$, namely the regular function on the character variety $\mathcal{R}_{\mathrm{SL}_2, S}$ defined by sending $\rho : \pi_1(S) \rightarrow \mathrm{SL}_2$ to the product $\prod_\gamma \mathrm{Tr}(\rho(\gamma))$ of the traces along the components γ of ℓ . It is well-known [Bul97, PS00] that the trace functions Tr_ℓ , varying over the 2-laminations $\ell \in \mathcal{L}_{2, S}$, form a linear basis for the algebra $\mathcal{O}(\mathcal{R}_{\mathrm{SL}_2, S})$ of regular functions on the SL_2 -character variety.

On the opposite topological extreme, consider the case where the surface $\widehat{S} = \widehat{D}$ is a disk with k marked points m_i on its boundary, cyclically ordered. For each i , assign a positive integer n_i to the i -th boundary interval located between the marked points m_i and m_{i+1} . This determines a subset $\mathcal{L}_{2, \widehat{D}}(n_1, \dots, n_k) \subseteq \mathcal{L}_{2, \widehat{D}}$ consisting of the 2-laminations

ℓ having geometric intersection number equal to n_i on the i -th boundary interval. It follows from the Clebsch-Gordan theorem (see, for instance, [Kup96, §2.2,2.3]) that the subset $\mathcal{L}_{2,\widehat{D}}(n_1, \dots, n_k)$ of 2-laminations indexes a linear basis for the space of SL_2 -invariant tensors $(V_{n_1} \otimes \dots \otimes V_{n_k})^{\mathrm{SL}_2}$, where V_{n_i} is the unique n_i -dimensional irreducible representation of SL_2 .

For a general marked surface \widehat{S} , Goncharov-Shen's moduli space $\mathcal{R}_{\mathrm{SL}_2, \widehat{S}}$ simultaneously generalizes both (a twisted version of) the character variety $\mathcal{R}_{\mathrm{SL}_2, S}$ for non-marked surfaces $\widehat{S} = S$, as well as the spaces of invariant tensors $(V_{n_1} \otimes V_{n_2} \otimes \dots \otimes V_{n_k})^{\mathrm{SL}_2}$ for marked disks $\widehat{S} = \widehat{D}$. By [GS15, Theorem 10.14], the set of 2-laminations $\mathcal{L}_{2, \widehat{S}}$ canonically indexes a linear basis for the algebra of functions $\mathcal{O}(\mathcal{R}_{\mathrm{SL}_2, \widehat{S}})$ on the generalized character variety for the marked surface \widehat{S} , closely related to the linear bases in the specialized cases $\widehat{S} = S$ and $\widehat{S} = \widehat{D}$.

We now turn to the case $n = 3$. In the setting of the disk $\widehat{S} = \widehat{D}$ with k marked points on its boundary, the integers n_i are replaced with highest weights λ_i of irreducible SL_3 -representations V_{λ_i} , and the object of interest is the space $(V_{\lambda_1} \otimes V_{\lambda_2} \otimes \dots \otimes V_{\lambda_k})^{\mathrm{SL}_3}$ of SL_3 -invariant tensors. Kuperberg [Kup96] proved that the set $\mathcal{W}_{3, \widehat{D}}(\lambda_1, \dots, \lambda_k)$ of non-convex non-elliptic 3-webs W on \widehat{D} , matching certain fixed topological boundary conditions corresponding to the weights λ_i , indexes a linear basis for the invariant space $(V_{\lambda_1} \otimes V_{\lambda_2} \otimes \dots \otimes V_{\lambda_k})^{\mathrm{SL}_3}$ (so can be thought of as the SL_3 -analogue of the subset $\mathcal{L}_{2, \widehat{D}}(n_1, \dots, n_k) \subseteq \mathcal{L}_{2, \widehat{D}}$).

On the other hand, for non-marked surfaces $\widehat{S} = S$, Sikora [Sik01] defined, for any 3-web W on S , a trace function Tr_W on the character variety $\mathcal{R}_{\mathrm{SL}_3, S}$, generalizing the trace functions Tr_ℓ for 2-laminations $\ell \in \mathcal{L}_{2, S}$ (Sikora also defined $\mathrm{Tr}_W \in \mathcal{O}(\mathcal{R}_{\mathrm{SL}_n, S})$ for any n -web W). A theorem of Sikora-Westbury [SW07] implies that the subset $\mathcal{W}_{3, S}$ of non-elliptic 3-webs W indexes, by taking trace functions Tr_W , a linear basis for the algebra of regular functions $\mathcal{O}(\mathcal{R}_{\mathrm{SL}_3, S})$ on the SL_3 -character variety.

For a general marked surface \widehat{S} , Frohman-Sikora's work [FS22], motivated by Kuperberg [Kup96], suggests that a good definition for the (bounded) 3-laminations is the set $\mathcal{W}_{3, \widehat{S}}$ of reduced 3-webs W on \widehat{S} , which in particular are allowed to have boundary; see §3. Indeed, by [FS22, Proposition 4], this set $\mathcal{W}_{3, \widehat{S}}$ forms a linear basis for the reduced SL_3 -skein algebra. As for non-marked surfaces S , where skein algebras quantize character varieties, we suspect that Frohman-Sikora's reduced SL_3 -skein algebra is a quantization of Goncharov-Shen's generalized SL_3 -character variety $\mathcal{R}_{\mathrm{SL}_3, \widehat{S}}$. In particular, we suspect that the set $\mathcal{W}_{3, \widehat{S}}$ indexes a canonical linear basis for the algebra of regular functions $\mathcal{O}(\mathcal{R}_{\mathrm{SL}_3, \widehat{S}})$, generalizing the case $n = 2$ [GS15, Theorem 10.14]; see [FS22, Conjecture 23].

1.1.3. Tropical coordinates for higher laminations.

Let a positive integer cone be a subset of $\mathbb{Z}_{\geq 0}^k$ closed under addition and containing zero.

As in [FG06, FG07a], in the case $n = 2$, given a choice of ideal triangulation \mathcal{T} , with N_2 edges, of the marked surface \widehat{S} , one assigns N_2 nonnegative integer coordinates to a given 2-lamination $\ell \in \mathcal{L}_{2, \widehat{S}}$ by taking the geometric intersection numbers of ℓ with the edges of the ideal triangulation \mathcal{T} . This assignment determines an injective coordinate mapping

$$\Phi_{\mathcal{T}}^{(2)} : \mathcal{L}_{2, \widehat{S}} \hookrightarrow \mathbb{Z}_{\geq 0}^{N_2}$$

on the set of 2-laminations $\mathcal{L}_{2, \widehat{S}}$. Moreover, the image of $\Phi_{\mathcal{T}}^{(2)}$ is a positive integer cone in $\mathbb{Z}_{\geq 0}^{N_2}$, which is characterized as the set of solutions of finitely many inequalities and parity

conditions of the form

$$a + b - c \geq 0 \quad \text{and} \quad a + b - c \in 2\mathbb{Z} \quad (a, b, c \in \mathbb{Z}_{\geq 0}).$$

Moreover, these integer coordinates are natural with respect to the choice of \mathcal{T} , in the sense that if a different ideal triangulation \mathcal{T}' is chosen, then the induced coordinate transformation is the SL_2 tropical \mathcal{A} -coordinate cluster transformation [FG07a, Figure 8]. These natural coordinates provide an identification $\mathcal{L}_{2,\widehat{S}} \cong \mathcal{A}_{\mathrm{PGL}_2,\widehat{S}}^+(\mathbb{Z}^t)$ as in [GS15, Theorem 10.15]. Taken together, [GS15, Theorems 10.14, 10.15] constitute a compelling topological version of the duality (*) in the case $n = 2$; see [GS15, the two paragraphs after Theorem 10.15].

Our main result generalizes these natural coordinates to the setting $n = 3$.

More precisely, given an ideal triangulation \mathcal{T} of a marked surface \widehat{S} , put N_3 to be twice the number of edges (including boundary edges) of \mathcal{T} plus the number of triangles of \mathcal{T} . Recall the set $\mathcal{W}_{3,\widehat{S}}$ of (equivalence classes of) reduced 3-webs on \widehat{S} , discussed above.

Theorem 1.1. *Given an ideal triangulation \mathcal{T} of the marked surface \widehat{S} , there is an injection*

$$\Phi_{\mathcal{T}} : \mathcal{W}_{3,\widehat{S}} \hookrightarrow \mathbb{Z}_{\geq 0}^{N_3}$$

satisfying the property that the image of $\Phi_{\mathcal{T}}$ is a positive integer cone in $\mathbb{Z}_{\geq 0}^{N_3}$ which is characterized as the set of solutions of finitely many Knutson-Tao rhombus inequalities [KT99] and modulo 3 congruence conditions of the form

$$a + b - c - d \geq 0 \quad \text{and} \quad a + b - c - d \in 3\mathbb{Z} \quad (a, b, c, d \in \mathbb{Z}_{\geq 0}).$$

Moreover, these coordinates are natural with respect to the action of the mapping class group of the surface \widehat{S} . More precisely, if a different ideal triangulation \mathcal{T}' is chosen, then the coordinate change map relating $\Phi_{\mathcal{T}}$ and $\Phi_{\mathcal{T}'}$ is given by the SL_3 tropical \mathcal{A} -coordinate cluster transformation of [FZ02, FG06], expressed locally as in Equations (1)-(5); see Figure 2.

See Theorems 3.9, 4.3, and 4.19. The construction of $\Phi_{\mathcal{T}}$ (Theorem 3.9) was done in [DS20].

This construction was motivated by earlier work of Xie [Xie13] and Goncharov-Shen [GS15].

In particular, Goncharov-Shen used the Knutson-Tao rhombus inequalities associated to an ideal triangulation \mathcal{T} of \widehat{S} to index the set of positive \mathcal{A} tropical integer points, which they showed parametrizes a linear basis for the algebra of regular functions $\mathcal{O}(\mathcal{R}_{\mathrm{SL}_3,\widehat{S}})$; see [GS15, §3.1 and Theorem 10.12 (stated for more general Lie groups)]. Their parametrization is not mapping class group equivariant; see the remark in [GS15, page 614] immediately after the aforementioned theorem. In [GS19] they construct equivariant bases using the abstract machinery of [GHKK18]. Theorem 1.1 provides a concrete model indexing the set $\mathcal{A}_{\mathrm{PGL}_3,\widehat{S}}^+(\mathbb{Z}^t)$ of positive tropical integer points, also based on the Knutson-Tao inequalities, which in addition is equivariant with respect to the action of the mapping class group. This natural indexing $\mathcal{W}_{3,\widehat{S}} \cong \mathcal{A}_{\mathrm{PGL}_3,\widehat{S}}^+(\mathbb{Z}^t)$ provided by Theorem 1.1 generalizes the $n = 2$ case [GS15, Theorem 10.15].

We think of the web coordinates of Theorem 1.1 as positive tropical integer \mathcal{A} -coordinates. We call the positive integer cone $\Phi_{\mathcal{T}}(\mathcal{W}_{3,\widehat{S}}) \subseteq \mathbb{Z}_{\geq 0}^{N_3}$ the SL_3 Knutson-Tao-Goncharov-Shen cone with respect to the ideal triangulation \mathcal{T} of \widehat{S} .

These tropical web coordinates were constructed for some simple examples, such as the eight triangle webs shown in Figure 11 below, in [Xie13]. They also appeared implicitly in [SWZ20, Theorem 8.22], in the geometric context of eruption flows on the $\mathrm{PGL}_n(\mathbb{R})$ -Hitchin

component ($n = 3$). Xie [Xie13] checked the mapping class group equivariance, in the above sense, of these coordinates on a handful of examples.

Frohman-Sikora [FS22] independently constructed nonnegative integer coordinates for the set $\mathcal{W}_{3,\widehat{S}}$ of reduced 3-webs. Their coordinates are related to, but different than, the coordinates of Theorem 1.1.

As an application, Kim [Kim20] constructed an explicit SL_3 -version of Fock-Goncharov duality using the tropical web coordinates of Theorem 1.1, in the setting of non-marked surfaces $\widehat{S} = S$. We expect that Kim's approach, together with the SL_3 -quantum trace map [Dou21, Kim20], will lead to an explicit SL_3 -version of quantum Fock-Goncharov duality [FG09]; see [AK17] for the $n = 2$ case.

As another application, Ishibashi-Kano [IK22] generalized the coordinates of Theorem 1.1 to an SL_3 -version of shearing coordinates for (unbounded) 3-laminations.

To end this subsection, we briefly recall from [DS20] the construction of the coordinate map $\Phi_{\mathcal{T}}$ from Theorem 1.1; see §3. Given the ideal triangulation \mathcal{T} , form the split ideal triangulation $\widehat{\mathcal{T}}$ by replacing each edge E of \mathcal{T} with two parallel edges E' and E'' ; in other words, fatten each edge E into a bigon. One then puts a given reduced 3-web $W \in \mathcal{W}_{3,\widehat{S}}$ into good position with respect to the split ideal triangulation $\widehat{\mathcal{T}}$. The result is that most of the complexity of the 3-web W is pushed into the bigons (Figure 8), whereas over each triangle there is only a single (possibly empty) honeycomb together with finitely many arcs lying on the corners (Figure 9). Once the 3-web W is in good position, its coordinates $\Phi_{\mathcal{T}}(W) \in \mathbb{Z}_{\geq 0}^{N_3}$ are readily computed. For an example in the once punctured torus, see Figure 1.

1.2. Local aspects.

The first new contribution of the present work is a proof of the naturality statement appearing in Theorem 1.1; see §4. This is a completely local statement, since any two ideal triangulations \mathcal{T} and \mathcal{T}' are related by a sequence of diagonal flips inside ideal squares. It therefore suffices to check the desired tropical coordinate change formulas for a single square:

- (1)
$$x_i = x'_i \quad (i = 1, 2, \dots, 8),$$
- (2)
$$\max\{x_2 + y_3, y_1 + x_3\} - y_2 = z_2,$$
- (3)
$$\max\{y_1 + x_6, x_7 + y_3\} - y_4 = z_4,$$
- (4)
$$\max\{x'_1 + z_4, x'_8 + z_2\} - y_1 = z_1,$$
- (5)
$$\max\{z_2 + x'_5, z_4 + x'_4\} - y_3 = z_3.$$

See Figure 2 for the notation.

Given a 3-web $W \in \mathcal{W}_{3,\widehat{S}}$ in good position with respect to \mathcal{T} , the restriction $W|_{\square}$ of W to a triangulated ideal square $(\square, \mathcal{T}|_{\square}) \subseteq (\widehat{S}, \mathcal{T})$ falls into one of 42 families $\mathcal{W}_{\mathcal{T}|_{\square}}^k \subseteq \mathcal{W}_{3,\square}$ for $k = 1, 2, \dots, 42$. Depending on which family $\mathcal{W}_{\mathcal{T}|_{\square}}^k$ the restricted web $W|_{\square}$ belongs to, there is an explicit topological description of how $W|_{\square}$ rearranges itself into good position after the flip; see §5. These local 42 families of 3-webs in the square have a geometric interpretation, leading to our second main result.

Let $\widehat{S} = \square$ be a disk with four marked points, namely an ideal square, and let \mathcal{T} be a choice of diagonal of \square . Theorem 1.1 says that the set $\mathcal{W}_{3,\square}$ of reduced 3-webs in \square embeds

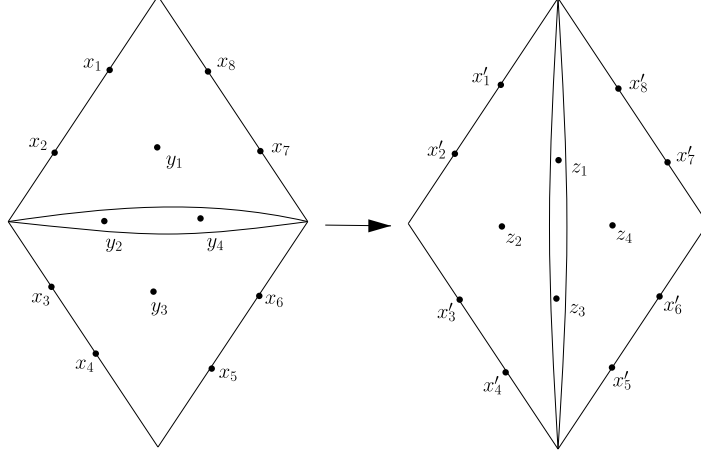


FIGURE 2. Local SL_3 tropical \mathcal{A} -coordinate cluster transformation, corresponding to a diagonal flip $\mathcal{T} \rightarrow \mathcal{T}'$ in the square. See Equations (1)-(5).

via $\Phi_{\mathcal{T}}$ as a positive integer cone inside $\mathbb{Z}_{\geq 0}^{12}$. This cone possesses a finite subset of irreducible elements spanning it over $\mathbb{Z}_{\geq 0}$, called its Hilbert basis [Hil90, Sch81]; see §6.

Theorem 1.2. *The Knutson-Tao-Goncharov-Shen cone $\Phi_{\mathcal{T}}(\mathcal{W}_{3,\square}) \subseteq \mathbb{Z}_{\geq 0}^{12}$ associated to the triangulated ideal square (\square, \mathcal{T}) has a Hilbert basis consisting of 22 elements, corresponding via $\Phi_{\mathcal{T}}$ to 22 reduced 3-webs $W_{\mathcal{T}}^i \in \mathcal{W}_{3,\square}$ for $i = 1, 2, \dots, 22$.*

Moreover, the positive integer cone

$$\Phi_{\mathcal{T}}(\mathcal{W}_{3,\square}) = \bigcup_{k=1}^{42} \mathcal{C}_{\mathcal{T}}^k \subseteq \mathbb{Z}_{\geq 0}^{12}$$

can be decomposed into 42 sectors $\mathcal{C}_{\mathcal{T}}^k$: (I) each sector is generated over $\mathbb{Z}_{\geq 0}$ by 12 of the 22 Hilbert basis elements, and (II) adjacent sectors are separated by a codimension 1 wall. These sectors $\mathcal{C}_{\mathcal{T}}^k$ are in one-to-one correspondence with the 42 families $\mathcal{W}_{\mathcal{T}}^k \subseteq \mathcal{W}_{3,\square}$ of 3-webs in the square, discussed above.

Lastly, each family $\mathcal{W}_{\mathcal{T}}^k \subseteq \mathcal{W}_{3,\square}$ contains 12 distinguished 3-webs $W_{\mathcal{T}}^{i(k,j)} \in \{W_{\mathcal{T}}^i\}_{i=1,2,\dots,22}$ for $j = 1, 2, \dots, 12$, corresponding to the 12 Hilbert basis elements generating the sector $\mathcal{C}_{\mathcal{T}}^k$. We refer to the set $\{W_{\mathcal{T}}^{i(k,j)}\}_{j=1,2,\dots,12}$ of these 12 distinguished 3-webs as the topological type of the sector $\mathcal{C}_{\mathcal{T}}^k$. Then, two sectors $\mathcal{C}_{\mathcal{T}}^k$ and $\mathcal{C}_{\mathcal{T}}^{k'}$ are adjacent if and only if their topological types differ by exactly one distinguished 3-web; see Figure 3.

See Theorems 6.10 and 7.21.

We like to think of Theorem 1.2 as expressing a topological wall-crossing phenomenon. Investigating whether it could be related to other wall-crossing phenomena appearing in cluster geometry [KS08] might be an interesting problem for future research.

For a related appearance of Hilbert bases, in the $n = 2$ setting, see [AF17].

The proof of Theorem 1.2 is geometric in nature and might be of independent interest. Recall [FG06] there are two dual sets of coordinates for the two dual moduli spaces of interest, respectively, the \mathcal{A} -coordinates and the \mathcal{X} -coordinates, as well as their tropical counterparts. For a triangulated ideal square (\square, \mathcal{T}) , via the mapping $\Phi_{\mathcal{T}}$ each 3-web $W \in \mathcal{W}_{3,\square}$ is assigned 12 positive tropical integer \mathcal{A} -coordinates $\Phi_{\mathcal{T}}(W) \in \mathbb{Z}_{\geq 0}^{12}$. We show that there are also assigned to W four internal tropical integer \mathcal{X} -coordinates valued in \mathbb{Z} , two associated to

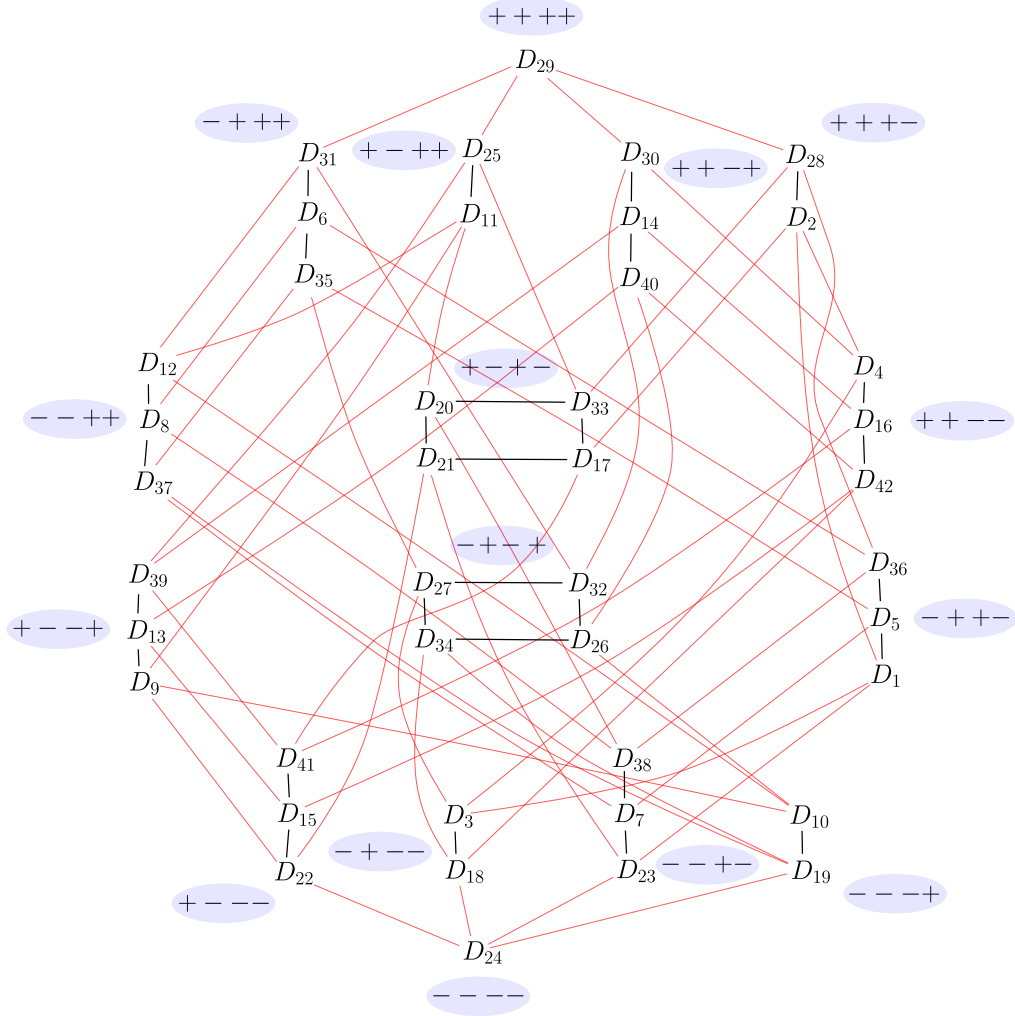


FIGURE 3. Sectors and walls in the Knutson-Tao-Goncharov-Shen (KTGS) cone $\Phi_{\mathcal{T}}(\mathcal{W}_{3,\square}) \subseteq \mathbb{Z}_{\geq 0}^{12}$ for a triangulated ideal square (\square, \mathcal{T}) . More precisely, displayed is a corresponding sector decomposition $\{D_i\}_{i=1,2,\dots,42}$ of (a projection to \mathbb{R}^4 of a real version of) an isomorphic cone in $\mathbb{Z}_+^8 \times \mathbb{Z}^4$, obtained from the KTGS cone via a transformation defined using the 4 tropical integer \mathcal{X} -coordinates. The sectors D_i are grouped depending on which orthant of \mathbb{R}^4 they belong to. These sectors are the vertices of a 4-valent graph, where two sectors are connected by an edge if and only if they share a wall; equivalently, their topological types differ by a single web. See Theorem 1.2.

the unique internal edge of \mathcal{T} and one for each triangle of \mathcal{T} ; see Figure 23 below. We find that the decomposition of the \mathcal{A} -cone $\Phi_{\mathcal{T}}(\mathcal{W}_{3,\square}) \subseteq \mathbb{Z}_{\geq 0}^{12}$ into 42 sectors is mirrored by a corresponding decomposition of the \mathcal{X} -lattice \mathbb{Z}^4 into 42 sectors; see Figure 3. We think of this as a manifestation of Fock-Goncharov's tropicalized canonical map:

$$p^t : \mathcal{W}_{3,\square} \cong \Phi_{\mathcal{T}}(\mathcal{W}_{3,\square}) \cong \mathcal{A}_{\text{PGL}_{3,\square}}^+(\mathbb{Z}^t)_{\mathcal{T}} \subseteq \mathcal{A}_{\text{SL}_{3,\square}}(\mathbb{R}^t)_{\mathcal{T}} \xrightarrow{\text{canonical}} \mathcal{X}_{\text{PGL}_{3,\square}}(\mathbb{R}^t)_{\mathcal{T}}.$$

The image of the map p^t is $\mathcal{X}_{\text{PGL}_{3,\square}}(\mathbb{Z}^t)_{\mathcal{T}} \cong \mathbb{Z}^4$, and p^t maps sectors of the positive integer cone $\Phi_{\mathcal{T}}(\mathcal{W}_{3,\square}) \cong \mathcal{A}_{\text{PGL}_{3,\square}}^+(\mathbb{Z}^t)_{\mathcal{T}}$ to sectors of the integer lattice $\mathcal{X}_{\text{PGL}_{3,\square}}(\mathbb{Z}^t)_{\mathcal{T}} \cong \mathbb{Z}^4$. See §7.

ACKNOWLEDGEMENTS

We are profoundly grateful to Dylan Allegretti, Francis Bonahon, Charlie Frohman, Sasha Goncharov, Linhui Shen, Daping Weng, Tommaso Cremaschi, and Subhadip Dey for many very helpful conversations and for generously offering their time as this project developed.

Much of this work was completed during very enjoyable visits to Tsinghua University in Beijing, supported by a GEAR graduate internship grant, and the University of Southern California in Los Angeles. We would like to take this opportunity to extend our enormous gratitude to these institutions for their warm hospitality (and tasty dinners!).

2. BACKGROUND ON FOCK-GONCHAROV-SHEN THEORY AND TROPICAL POINTS

In this section, we recall some theoretical preliminaries in order to discuss the set $\mathcal{A}_{\mathrm{PGL}_3, \hat{S}}^+(\mathbb{Z}^t)$ of positive tropical integer PGL_3 -points, including the Fock-Goncharov \mathcal{A} -moduli space and the Goncharov-Shen potential.

2.1. Marked surfaces, ideal triangulations, and rhombi.

A *marked surface* \hat{S} is a pair (S, m_b) where S is a compact oriented finite-type surface with at least one boundary component, and $m_b \subseteq \partial S$ is a finite set of *marked points* on ∂S . Let $m_p \subseteq \{\text{components of } \partial S\}$ be the set of *punctures*, defined as the subset of boundary components without marked points; as is common in the literature, for the remainder of the article we identify such unmarked boundary components in m_p with the (actual) punctures obtained by removing them and shrinking the resulting hole down to a point.

We assume the Euler characteristic condition $\chi(S) < d/2$, where d is the number of components of $\partial S - m_b$ limiting to a marked point. (For example, $d = 3$ for a once punctured disk with three marked points on its boundary.) This topological condition is equivalent to the existence of an *ideal triangulation* \mathcal{T} of \hat{S} , namely a triangulation whose set of vertices is equal to $m_b \cup m_p$; the vertices of \mathcal{T} are called *ideal vertices*.

For simplicity, we always assume that \mathcal{T} does not contain any *self-folded triangles*. That is, we assume each triangle of \mathcal{T} has three distinct sides. (Our results should generalize, essentially without change, to allow for self-folded triangles.)

Given an ideal triangulation \mathcal{T} of \hat{S} , we define the *ideal 3-triangulation* \mathcal{T}_3 of \mathcal{T} to be the triangulation of \hat{S} obtained by subdividing each ideal triangle Δ of \mathcal{T} into 9 triangles; see Figure 4 below. The 3-triangulation \mathcal{T}_3 has as many ideal vertices as \mathcal{T} , and has N *non-ideal vertices*, where N is defined in Notation 2.1 below.

A *pointed ideal triangle* is a triangle Δ in an ideal triangulation \mathcal{T} together with a preferred ideal vertex; Δ is called a *pointed ideal 3-triangle* when subdivided as part of the associated 3-triangulation \mathcal{T}_3 .

Given a pointed ideal 3-triangle, we may talk about the three associated *rhombi*; see Figure 5 below. In the figure, the red rhombus is called the *corner rhombus*, and the yellow and green rhombi are called the *interior rhombi*. Each rhombus has two *acute vertices* and two *obtuse vertices*. Note that exactly one of these eight vertices, the *corner vertex*, is an ideal vertex of \mathcal{T}_3 ; specifically, the top (acute) vertex of the corner rhombus. (We will see below that the other vertices correspond to Fock-Goncharov \mathcal{A} -coordinates.)

Notation 2.1.

- (1) The natural number N is defined as twice the total number of edges (including boundary edges) of \mathcal{T} plus the number of triangles of \mathcal{T} . (Note that N is what we called N_3 in §1.)
- (2) It will be convenient to denote the nonnegative real numbers by $\mathbb{R}_+ := \mathbb{R}_{\geq 0}$ and the nonnegative integers by $\mathbb{Z}_+ := \mathbb{Z}_{\geq 0}$. Similarly, put $\mathbb{R}_- := \mathbb{R}_{\leq 0}$ and $\mathbb{Z}_- := \mathbb{Z}_{\leq 0}$.

2.2. SL_3 -decorated local systems.

Although not strictly required for the main theorems of the article, the material of this section and the following one §2.3 is intended to emphasize the important conceptual concepts guiding the rest of the paper.

Let E be a 3-dimensional vector space.

2.2.1. \mathcal{A} -coordinates.

Definition 2.2 (Decorated flags). A *flag* F in E is a maximal filtration of vector subspaces of E ,

$$\{0\} = F^{(0)} \subseteq F^{(1)} \subseteq F^{(2)} \subseteq F^{(3)} = E, \quad \dim F^{(i)} = i,$$

denoted by $(F^{(1)}, F^{(2)})$.

A *decorated flag* (F, φ) is a pair consisting of a flag F and a collection φ of 2 nonzero vectors

$$\varphi = (\check{f}_i \in (F^{(i)}/F^{(i-1)}) - \{0 + F^{(i-1)}\}; \quad i = 1, 2).$$

The collection of decorated flags is denoted by \mathcal{A} .

We can think of \mathcal{A} as a homogeneous set as follows. Let $\mathrm{GL}(E)$ be the general linear group, and let $\mathrm{SL}(E) \subseteq \mathrm{GL}(E)$ be the special linear group consisting of transformations with determinant 1. The group $\mathrm{SL}(E)$ acts transitively on \mathcal{A} by left translation. Then \mathcal{A} can be identified with the quotient set $\mathrm{SL}(E)/U$ for any maximal unipotent subgroup U of $\mathrm{SL}(E)$ (that is, in some basis β of E , we have that U consists of upper triangular matrices with 1's on the main diagonal, namely unipotent matrices).

We fix a volume form $\Omega \in \Lambda^3(E)$ on E . Then, a decorated flag $(F, \varphi) \in \mathcal{A}$ determines a unique element $\check{f}_3 \in F^{(3)}/F^{(2)} = E/F^{(2)}$ satisfying the property that $\Omega(f_1 \wedge f_2 \wedge \check{f}_3) = 1$ for all $f_i \in F^{(i)}$, $i = 1, 2, 3$, such that $f_i + F^{(i-1)} = \check{f}_i \in F^{(i)}/F^{(i-1)}$. A *basis for (F, φ) with respect to the volume form Ω* is a choice of such a basis (f_1, f_2, \check{f}_3) for the vector space E .

Definition 2.3 (\mathcal{A} -moduli space $\mathcal{A}_{\mathrm{SL}_3, \widehat{S}}$ [FG06, §2]). Fix a base point x_0 in \widehat{S} , which henceforth will be suppressed in the notation. Let α_i be an oriented peripheral closed curve around a puncture $p_i \in m_p$. A *decorated SL_3 -local system* on \widehat{S} is a pair (ρ, ξ) consisting of

- a surface group representation $\rho \in \mathrm{Hom}(\pi_1(\widehat{S}), \mathrm{SL}_3)$ with unipotent monodromy along each peripheral curve α_i ; and,
- a *flag map* $\xi : m_b \cup m_p \rightarrow \mathcal{A}$, such that each peripheral monodromy $\rho(\alpha_i)$ fixes the decorated flag $\xi(p_i) \in \mathcal{A}$. Note that the decorated flags assigned to the marked points m_b can be chosen arbitrarily.

Two decorated SL_3 -local systems $(\rho_1, \xi_1), (\rho_2, \xi_2)$ are equivalent if and only if there exists some $g \in \mathrm{SL}_3$ such that $\rho_2 = g\rho_1 g^{-1}$ and $\xi_2 = g\xi_1$. We denote the moduli space of equivalence classes of decorated SL_3 -local systems on \widehat{S} by $\mathcal{A}_{\mathrm{SL}_3, \widehat{S}}$.

Remark 2.4. More precisely, the flag map ξ should be defined equivariantly at the level of the universal cover \widetilde{S} , and satisfy certain genericity conditions. These technicalities will be suppressed throughout our discussion.

Notation 2.5. Let $V_{\mathcal{T}}$ (resp. $V_{\mathcal{T}_3}$) be the set of vertices of \mathcal{T} (resp. \mathcal{T}_3). Note that $V_{\mathcal{T}} = m_b \cup m_p \subseteq V_{\mathcal{T}_3}$.

$$I_3 := \{ V \in V_{\mathcal{T}_3} - V_{\mathcal{T}} \mid V \text{ lies on an edge of } \mathcal{T} \} \text{ and } J_3 := V_{\mathcal{T}_3} - (V_{\mathcal{T}} \cup I_3).$$

We adopt the following vertex labelling conventions:

- We denote a vertex $V \in I_3$ on an oriented ideal edge (a, b) of \mathcal{T} by $v_{a,b}^{i,3-i} = v_{b,a}^{3-i,i}$, where $i = 1$ or 2 is the least number of edges of \mathcal{T}_3 from V to b (see Figure 4).
- We denote a vertex $V \in I_3 \cup J_3$ on a triangle (a, b, c) oriented counterclockwise by $v_{a,b,c}^{i,j,k}$, where the three nonnegative integers i, j, k summing to 3 are the least number of edges of \mathcal{T}_3 from V to \overline{bc} , from V to \overline{ac} , and from V to \overline{ab} , respectively, where \overline{bc} , \overline{ac} , \overline{ab} denote the unoriented edges of \mathcal{T} (see Figure 4).

Definition 2.6 (\mathcal{A} -coordinates [FG06, §9]). Fix an ideal triangulation \mathcal{T} of \widehat{S} and its 3-triangulation \mathcal{T}_3 . Consider a vertex $V \in I_3 \cup J_3$ contained in a counterclockwise oriented ideal triangle $\Delta = (a, b, c)$, as in Figure 5. In the sense described above, choose bases, with respect to the fixed volume form Ω ,

$$(a_1, a_2, a_3), (b_1, b_2, b_3), (c_1, c_2, c_3) \in E^3$$

for the generic decorated flags $\xi_\rho(a), \xi_\rho(b), \xi_\rho(c) \in \mathcal{A}$. For a decorated local system $(\rho, \xi) \in \mathcal{A}_{\text{SL}_3, \widehat{S}}$, the *Fock-Goncharov \mathcal{A} -coordinate* at $V = v_{a,b,c}^{i,j,k} \in I_3 \cup J_3$ is

$$(6) \quad A_V(\rho, \xi) := A_V := A_{a,b,c}^{i,j,k} := \Omega(a^i \wedge b^j \wedge c^k) \neq 0,$$

where $a^1 = a_1$, $a^2 = a_1 \wedge a_2$, etc. Note that this is independent of the choice of bases.

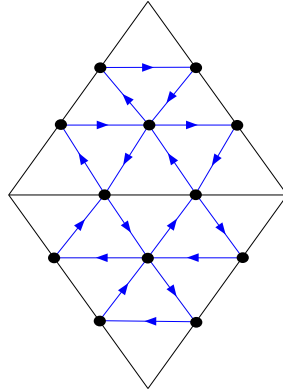


FIGURE 4. 3-triangulation.

We also put $A_{a,b,c}^{3,0,0} := \Omega(a^3) = \Omega(a_1 \wedge a_2 \wedge a_3) = 1$, which follows from the definition of the basis (a_1, a_2, a_3) of $\xi(a)$ with respect to Ω . Similarly $A_{a,b,c}^{0,3,0} = A_{a,b,c}^{0,0,3} = 1$. See also §2.3 below.

Given a quiver defined, as in Figure 4, with respect to the orientation of the surface, let

$$\varepsilon_{VW} = \#\{\text{arrows from } V \text{ to } W\} - \#\{\text{arrows from } W \text{ to } V\}.$$

The *Fock-Goncharov \mathcal{X} -coordinate* at V (defined for any $V \in I_3 \cup J_3$, $V \notin \partial \widehat{S}$) is

$$X_V(\rho, \xi) := X_V := \prod_{W \in I_3 \cup J_3} A_W^{\varepsilon_{VW}} \neq 0.$$

Remark 2.7. By [FG06, §10], the moduli space $\mathcal{A}_{\mathrm{SL}_3, \hat{S}}$ has a cluster algebraic structure [FZ02] described by quivers on the surface, such as that in Figure 4. In particular, each \mathcal{A} -coordinate transition map between different triangulations \mathcal{T} and \mathcal{T}' is positive rational.

2.2.2. Goncharov–Shen potential.

Definition 2.8 (Goncharov–Shen potential). Let

$$D := \{(2, 1, 0), (1, 2, 0), (1, 1, 1)\}.$$

Suppose the pointed ideal triangle (§2.1) $\Delta = (a, b, c)$ is counterclockwise oriented, as in Figure 5. For $(i, j, k) \in D$, the monomials

$$(7) \quad \alpha_{a;b,c}^{i,j,k} := \frac{A_{a,b,c}^{i-1,j,k+1} \cdot A_{a,b,c}^{i+1,j-1,k}}{A_{a,b,c}^{i,j,k} \cdot A_{a,b,c}^{i,j-1,k+1}} \quad (\text{recalling } A_{a,b,c}^{3,0,0} = 1),$$

introduced in [GS15, Lemma 3.1], correspond to the three rhombi in Figure 5. Define

$$P(\Delta) := P(a; b, c) := \alpha_{a;b,c}^{2,1,0} + \alpha_{a;b,c}^{1,2,0} + \alpha_{a;b,c}^{1,1,1}.$$

Let Θ be the collection of counterclockwise oriented pointed ideal triangles of \mathcal{T} . The *Goncharov–Shen potential* is

$$P = \sum_{\Delta \in \Theta} P(\Delta).$$

Thus, for a given ideal triangulation \mathcal{T} , the Goncharov–Shen potential is a positive Laurent polynomial in the \mathcal{A} -coordinates for $\mathcal{A}_{\mathrm{SL}_3, \hat{S}}$.

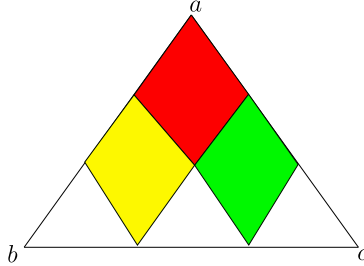


FIGURE 5. Red rhombus for $\alpha_{a;b,c}^{2,1,0}$, yellow rhombus for $\alpha_{a;b,c}^{1,2,0}$, and green rhombus for $\alpha_{a;b,c}^{1,1,1}$ in a pointed ideal triangle.

Remark 2.9. The Goncharov–Shen potential is mapping class group equivariant; in particular, it defines a rational positive function on the moduli space $\mathcal{A}_{\mathrm{SL}_3, \hat{S}}$. In [GS15] and [GHKK18], the GS potentials are understood as the mirror Landau–Ginzburg potentials. In [HS19, §4], the GS potentials are understood as generalized horocycle lengths.

2.2.3. Tropical points.

The moduli space $\mathcal{A}_{\mathrm{SL}_3, \hat{S}}$ is a positive space (Remark 2.7), so its points $\mathcal{A}_{\mathrm{SL}_3, \hat{S}}(\mathbb{P})$ are defined over any semifield \mathbb{P} . To each ideal triangulation \mathcal{T} there is associated a \mathcal{T} -chart $\mathcal{A}_{\mathrm{SL}_3, \hat{S}}(\mathbb{P})_{\mathcal{T}}$, determined by the \mathcal{A} -coordinates (§2.2.1), for the moduli space $\mathcal{A}_{\mathrm{SL}_3, \hat{S}}(\mathbb{P})$ over \mathbb{P} . In this paper, we will always be working in a \mathcal{T} -chart (see Definition 2.11 below).

The *higher decorated Teichmüller space* $\mathcal{A}_{\mathrm{SL}_3, \hat{S}}(\mathbb{R}_{>0})$ is the set of positive real points of $\mathcal{A}_{\mathrm{SL}_3, \hat{S}}$. By Remark 2.7, the cluster transformation between two triangulations \mathcal{T} and \mathcal{T}' sends

positive coordinates to positive coordinates. Hence, all the \mathcal{A} -coordinates of $\mathcal{A}_{\mathrm{SL}_3, \hat{S}}(\mathbb{R}_{>0})$ for any ideal triangulation are positive.

The *tropical semifield* $\mathbb{R}^t = (\mathbb{R}, \otimes, \oplus)$ is defined by $x \otimes y = x + y$ and $x \oplus y = \max\{x, y\}$. The isomorphism $x \rightarrow -x$ sends $(\mathbb{R}^t, +, \max)$ to $(\mathbb{R}^t, +, \min)$. In this section, we use $\mathbb{P} = \mathbb{R}^t = (\mathbb{R}^t, +, \min)$. The tropical semifields \mathbb{Z}^t and $\frac{1}{3}\mathbb{Z}^t$ are defined in the same way.

For the tropical semifield $\mathbb{P} = \mathbb{R}^t$, the \mathcal{T} -chart $\mathcal{A}_{\mathrm{SL}_3, \hat{S}}(\mathbb{R}^t)_{\mathcal{T}}$ is identified with \mathbb{R}^N . Here, N is the number of \mathcal{A} -coordinates, recalling Notation 2.1. Similarly, for the tropical semifields $\mathbb{P} = \mathbb{Z}^t, \frac{1}{3}\mathbb{Z}^t$ the \mathcal{T} -charts $\mathcal{A}_{\mathrm{SL}_3, \hat{S}}(\mathbb{Z}^t)_{\mathcal{T}}$ and $\mathcal{A}_{\mathrm{SL}_3, \hat{S}}(\frac{1}{3}\mathbb{Z}^t)_{\mathcal{T}}$ are identified with the lattices \mathbb{Z}^N and $(\frac{1}{3}\mathbb{Z})^N$, respectively.

The tropical \mathcal{A} -coordinates are denoted A_V^t for $V \in I_3 \cup J_3$; compare Definition 2.6.

The *tropicalization* f^t of a positive Laurent polynomial f is

$$f^t(x_1, \dots, x_k) = \lim_{C \rightarrow +\infty} \frac{\log f(e^{Cx_1}, \dots, e^{Cx_k})}{C}.$$

Tropicalizing the Goncharov-Shen potential P (§2.2.2), we have, by (7),

$$(8) \quad \left(\alpha_{a,b,c}^{i,j,k}\right)^t = \left(A_{a,b,c}^{i-1,j,k+1}\right)^t + \left(A_{a,b,c}^{i+1,j-1,k}\right)^t - \left(A_{a,b,c}^{i,j,k}\right)^t - \left(A_{a,b,c}^{i,j-1,k+1}\right)^t,$$

and

$$P^t = \min \left\{ \left(\alpha_{a,b,c}^{i,j,k}\right)^t \right\}_{\text{any } \alpha_{a,b,c}^{i,j,k} \text{ of } P}.$$

That is, the minimum is taken over all rhombi in all pointed ideal triangles of \mathcal{T} .

Note that, since $A_{a,b,c}^{3,0,0} = 1$ is constant (by the discussion after (6)), we have $(A_{a,b,c}^{3,0,0})^t = 0$.

Definition 2.10. The space of *positive real tropical points* is

$$\mathcal{A}_{\mathrm{SL}_3, \hat{S}}^+(\mathbb{R}^t) := \left\{ x \in \mathcal{A}_{\mathrm{SL}_3, \hat{S}}(\mathbb{R}^t) \mid P^t(x) \geq 0 \right\}.$$

Alternatively, in \mathcal{T} -charts,

$$\mathcal{A}_{\mathrm{SL}_3, \hat{S}}^+(\mathbb{R}^t)_{\mathcal{T}} := \left\{ x \in \mathcal{A}_{\mathrm{SL}_3, \hat{S}}(\mathbb{R}^t)_{\mathcal{T}} \cong \mathbb{R}^N \mid \left(\alpha_{a,b,c}^{i,j,k}\right)^t(x) \geq 0 \text{ for all } \alpha_{a,b,c}^{i,j,k} \text{ of } P^t \right\}.$$

The spaces $\mathcal{A}_{\mathrm{SL}_3, \hat{S}}^+(\mathbb{Z}^t)$ and $\mathcal{A}_{\mathrm{SL}_3, \hat{S}}^+(\frac{1}{3}\mathbb{Z}^t)$ are defined in the same way.

2.3. PGL_3 -decorated local systems.

We are interested in a closely related moduli space $\mathcal{A}_{\mathrm{PGL}_3, \hat{S}}$ defined similarly to $\mathcal{A}_{\mathrm{SL}_3, \hat{S}}$. As we will see, the \mathcal{A} -coordinates do not make sense for $\mathcal{A}_{\mathrm{PGL}_3, \hat{S}}$. Nevertheless, the Goncharov-Shen potential P is still well-defined. Following [GS15] (see the paragraph immediately following their Theorem 10.15), we can say that $\mathcal{A}_{\mathrm{PGL}_3, \hat{S}}$ is a positive space, so we can talk about its points $\mathcal{A}_{\mathrm{PGL}_3, \hat{S}}(\mathbb{P})$ over a semifield \mathbb{P} . In particular, we can talk about its positive tropical integer points $\mathcal{A}_{\mathrm{PGL}_3, \hat{S}}^+(\mathbb{Z}^t)$, which is our main object of study.

To define the space $\mathcal{A}_{\mathrm{PGL}_3, \hat{S}}$ it suffices to say what is the set of PGL_3 -decorated flags, denoted by $\mathcal{A}_{\mathrm{PGL}_3}$ (compare Definition 2.2); the rest of the definition then mimics that of $\mathcal{A}_{\mathrm{SL}_3, \hat{S}}$. Let $\mathcal{A}'_{\mathrm{PGL}_3}$ be the set of quadruples $(F, \check{f}_1, \check{f}_2, \check{f}_3)$ where F is a complete flag in E and \check{f}_i is a nonzero element of $F^{(i)}/F^{(i-1)}$ for $i = 1, 2, 3$. Then GL_3 acts transitively on $\mathcal{A}'_{\mathrm{PGL}_3}$ in the obvious way. If we view \mathbb{C}^* as the nonzero scalar matrices in GL_3 , then \mathbb{C}^* acts on $\mathcal{A}'_{\mathrm{PGL}_3}$ as well. We put $\mathcal{A}_{\mathrm{PGL}_3} := \mathcal{A}'_{\mathrm{PGL}_3}/\mathbb{C}^*$. The action of GL_3 descends to a transitive action of

PGL_3 on $\mathcal{A}_{\mathrm{PGL}_3}$. If U is any maximal unipotent subgroup of SL_3 (see §2.2.1), let U also denote its quotient in PGL_3 . We can then view $\mathcal{A}_{\mathrm{PGL}_3} \cong \mathrm{PGL}_3/U$ as a homogeneous set.

We denote elements of the resulting moduli space $\mathcal{A}_{\mathrm{PGL}_3, \hat{S}}$ by $(\rho, \xi + \mathbb{C}^*)$ where $\rho : \pi_1(\hat{S}) \rightarrow \mathrm{PGL}_3$ and $\xi + \mathbb{C}^* : m_b \cup m_p \rightarrow \mathcal{A}_{\mathrm{PGL}_3}$ (compare Definition 2.3).

By a *basis* of a PGL_3 -decorated flag $(F, \check{f}_1, \check{f}_2, \check{f}_3) + \mathbb{C}^*$ we mean a linear basis (g_1, g_2, g_3) of E adapted to the flag F and representing this projective class; that is, such that there exists some nonzero scalar λ so that $\lambda g_i + F^{(i-1)} = \check{f}_i \in F^{(i)}/F^{(i-1)}$ for all $i = 1, 2, 3$.

The Goncharov-Shen potential P is defined on the moduli space $\mathcal{A}_{\mathrm{PGL}_3, \hat{S}}$ as follows (compare §2.2.2). Make an arbitrary choice of a volume form Ω on E , as well as a basis (a_1, a_2, a_3) of the PGL_3 -decorated flag $(\xi + \mathbb{C}^*)(a) \in \mathcal{A}_{\mathrm{PGL}_3}$ for each marked point or puncture $a \in m_b \cup m_p$. With respect to these choices, define numbers $A_{a,b,c}^{i,j,k}$ by (6), and define the rhombus numbers $\alpha_{a,b,c}^{i,j,k}$ by (7); note that now $A_{a,b,c}^{3,0,0}$ need not be equal to 1. While the numbers $A_{a,b,c}^{i,j,k}$ depend on the choices we have made, one checks that the rhombus numbers $\alpha_{a,b,c}^{i,j,k}$ do not. Thus, the potential P is well-defined on $\mathcal{A}_{\mathrm{PGL}_3, \hat{S}}$.

We now turn to the tropical integer PGL_3 -points defined with respect to the Goncharov-Shen potential P . Note $\mathcal{A}_{\mathrm{PGL}_3, \hat{S}}(\mathbb{Z}^t) \subseteq \mathcal{A}_{\mathrm{SL}_3, \hat{S}}(\frac{1}{3}\mathbb{Z}^t)$. More precisely:

Definition 2.11. Let \mathcal{T} be an ideal triangulation of \hat{S} . In \mathcal{T} -charts (§2.2.3), we have the following notions.

The set of *lamination-tropical points* is

$$\mathcal{A}_{\mathrm{PGL}_3, \hat{S}}(\mathbb{Z}^t)_{\mathcal{T}} := \left\{ x \in \mathcal{A}_{\mathrm{SL}_3, \hat{S}}\left(\frac{1}{3}\mathbb{Z}^t\right)_{\mathcal{T}} \cong \left(\frac{1}{3}\mathbb{Z}\right)^N \mid \left(\alpha_{a,b,c}^{i,j,k}\right)^t(x) \in \mathbb{Z} \text{ for all } \alpha_{a,b,c}^{i,j,k} \text{ of } P^t \right\}.$$

Note this satisfies

$$\mathcal{A}_{\mathrm{SL}_3, \hat{S}}(\mathbb{Z}^t)_{\mathcal{T}} \subseteq \mathcal{A}_{\mathrm{PGL}_3, \hat{S}}(\mathbb{Z}^t)_{\mathcal{T}} \subseteq \mathcal{A}_{\mathrm{SL}_3, \hat{S}}\left(\frac{1}{3}\mathbb{Z}^t\right)_{\mathcal{T}}.$$

Similarly, the set of *web-tropical points* is

$$\mathcal{A}_{\mathrm{PGL}_3, \hat{S}}^+(\mathbb{Z}^t)_{\mathcal{T}} := \left\{ x \in \mathcal{A}_{\mathrm{SL}_3, \hat{S}}\left(\frac{1}{3}\mathbb{Z}^t\right)_{\mathcal{T}} \cong \left(\frac{1}{3}\mathbb{Z}\right)^N \mid \left(\alpha_{a,b,c}^{i,j,k}\right)^t(x) \in \mathbb{Z}_+ \text{ for all } \alpha_{a,b,c}^{i,j,k} \text{ of } P^t \right\}.$$

Note, by Definition 2.10, this satisfies

$$\mathcal{A}_{\mathrm{SL}_3, \hat{S}}^+(\mathbb{Z}^t)_{\mathcal{T}} \subseteq \mathcal{A}_{\mathrm{PGL}_3, \hat{S}}^+(\mathbb{Z}^t)_{\mathcal{T}} \subseteq \mathcal{A}_{\mathrm{SL}_3, \hat{S}}^+\left(\frac{1}{3}\mathbb{Z}^t\right)_{\mathcal{T}}.$$

We see then that we have the identities of tropical real points: $\mathcal{A}_{\mathrm{PGL}_3, \hat{S}}(\mathbb{R}^t) = \mathcal{A}_{\mathrm{SL}_3, \hat{S}}(\mathbb{R}^t)$ and $\mathcal{A}_{\mathrm{PGL}_3, \hat{S}}^+(\mathbb{R}^t) = \mathcal{A}_{\mathrm{SL}_3, \hat{S}}^+(\mathbb{R}^t)$.

From now on, we always view $\mathcal{A}_{\mathrm{PGL}_3, \hat{S}}(\mathbb{Z}^t) \subseteq \mathcal{A}_{\mathrm{SL}_3, \hat{S}}(\mathbb{R}^t)$ and $\mathcal{A}_{\mathrm{PGL}_3, \hat{S}}^+(\mathbb{Z}^t) \subseteq \mathcal{A}_{\mathrm{SL}_3, \hat{S}}^+(\mathbb{R}^t)$.

Remark 2.12.

- (1) It turns out (see [DS20, Remark 44]) that, in the expressions for $\mathcal{A}_{\mathrm{PGL}_3, \hat{S}}(\mathbb{Z}^t)$ and $\mathcal{A}_{\mathrm{PGL}_3, \hat{S}}^+(\mathbb{Z}^t)$ in Definition 2.11, we just as well could have assumed $x \in \mathcal{A}_{\mathrm{SL}_3, \hat{S}}(\mathbb{R}^t) \cong \mathbb{R}^N$. That is, all real solutions are, in fact, one third integer solutions. Moreover, in the case of $\mathcal{A}_{\mathrm{PGL}_3, \hat{S}}^+(\mathbb{Z}^t)$, these one third integer solutions are nonpositive (this is because the rhombus numbers (8) are opposite in sign to those appearing in [DS20]).

- (2) The set $\mathcal{A}_{\mathrm{PGL}_3, \widehat{S}}(\mathbb{Z}^t)$ of lamination-tropical points was called the set of *balanced points* in [Kim20].
- (3) By [GS15, §3], when \widehat{S} is a disk with three marked points on its boundary, the positive integer tropical points are canonically identified with the Knutson–Tao hive cone [KT99].
- (4) See also the Conceptual Remarks 3.4, 4.20, 6.15, and 7.37.

3. TROPICAL POINTS AND WEBS

We now introduce the main object of study, the Knutson–Tao–Goncharov–Shen cone $\mathcal{C}_{\mathcal{T}} \subseteq \mathbb{Z}_+^N$ associated to an ideal triangulation \mathcal{T} of a marked surface \widehat{S} , and we summarize the work of [DS20] relating tropical points to topological objects called webs.

3.1. The Knutson–Tao–Goncharov–Shen cone and reduced webs.

We recall only the topological and notational definitions of §2.1. Let \widehat{S} be a marked surface.

3.1.1. KTGS cone.

Given a pointed ideal triangle Δ in an ideal triangulation \mathcal{T} of \widehat{S} (§2.1), assume nonnegative integers (see also Remark 2.12(1)) $a, b, c, d \in \mathbb{Z}$ (resp. $a, b, c \in \mathbb{Z}$) are assigned to some interior (resp. corner) rhombus, where the numbers a, b are assigned to the two obtuse vertices, and the numbers c, d are assigned to the two acute vertices. To such an assigned rhombus, we associate a *Knutson–Tao rhombus inequality* $a + b - c - d \geq 0$ and a *modulo 3 congruence condition* $(a + b - c - d)/3 \in \mathbb{Z}$. Here, we set $d = 0$ if the rhombus is a corner rhombus, where then d corresponds to the corner vertex.

Definition 3.1. A *positive integer cone* \mathcal{C} is a submonoid of \mathbb{Z}_+^k (Notation 2.1) for some k . That is, \mathcal{C} is closed under addition and contains the zero vector.

Recall the definition (Notation 2.1) of the natural number N . This is the same as the number of non-ideal points of the 3-triangulation \mathcal{T}_3 . We order these N non-ideal points arbitrarily in the following definition (compare §4.3), so that to each such non-ideal point of \mathcal{T}_3 we associate a coordinate of \mathbb{Z}^N . In this way, a point of \mathbb{Z}^N assigns to each rhombus in a pointed ideal triangle Δ four numbers $a, b, c, d \in \mathbb{Z}$ as above.

Definition 3.2. Given an ideal triangulation \mathcal{T} of \widehat{S} , let the *Knutson–Tao–Goncharov–Shen cone* $\mathcal{C}_{\mathcal{T}} \subseteq \mathbb{Z}^N$, or just the *KTGS cone* for short, be the submonoid defined by the property that its points satisfy all of the Knutson–Tao rhombus inequalities and modulo 3 congruence conditions, varying over all rhombi of all pointed ideal triangles Δ of \mathcal{T} .

Proposition 3.3. The KTGS cone $\mathcal{C}_{\mathcal{T}} \subseteq \mathbb{Z}_+^N \subseteq \mathbb{Z}^N$ is a positive integer cone.

Proof. This is by [DS20, Corollary 46 and Definition 49]; see also Remark 2.12(1). ■

Conceptual Remark 3.4. We think of the KTGS cone $\mathcal{C}_{\mathcal{T}} \subseteq \mathbb{Z}_+^N$, defined above, as the isomorphic coordinate chart

$$\mathcal{C}_{\mathcal{T}} \cong -3\mathcal{A}_{\mathrm{PGL}_3, \widehat{S}}^+(\mathbb{Z}^t)_{\mathcal{T}}$$

where, in the theoretical language of §2.3, $\mathcal{A}_{\mathrm{PGL}_3, \widehat{S}}(\mathbb{Z}^t)_{\mathcal{T}} \subseteq (\frac{1}{3}\mathbb{Z})^N \cong \mathcal{A}_{\mathrm{SL}_3, \widehat{S}}(\frac{1}{3}\mathbb{Z}^t)_{\mathcal{T}}$ and $\mathcal{A}_{\mathrm{PGL}_3, \widehat{S}}^+(\mathbb{Z}^t)_{\mathcal{T}} \subseteq \mathcal{A}_{\mathrm{PGL}_3, \widehat{S}}(\mathbb{Z}^t)_{\mathcal{T}} \cap (-\frac{1}{3}\mathbb{Z}_+)^N$ as in Remark 2.12(1).

3.1.2. Reduced webs.

A *web* (possibly with boundary) W in \widehat{S} [DS20, §8.1] is an oriented trivalent graph embedded in \widehat{S} such that:

- the boundary $\partial W = W \cap (\partial \widehat{S} - m_b)$ of the web lies on the boundary of the surface (minus the marked points) and may be nonempty, in which case its boundary points are required to be monovalent vertices;
- the three edges of W at an internal vertex are either all oriented in or all oriented out;
- we allow that W have components homeomorphic to the circle, called *loops*, which do not contain any vertices;
- we allow that W have components homeomorphic to the closed interval, called *arcs*, which have exactly two vertices on $\partial \widehat{S} - m_b$ and do not have any internal vertices.

Webs are considered up to *parallel equivalence*, meaning related either by an ambient isotopy of $\widehat{S} - m_b$ or a homotopy in $\widehat{S} - m_b$ exchanging two “parallel” loop (resp. arc) components of W bounding an embedded annulus (resp. rectangle, two of whose sides are contained in $\partial \widehat{S} - m_b$, as in Figure 6).

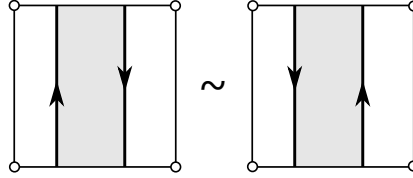


FIGURE 6. Boundary parallel move in the ideal square.

A *face* of a web W [DS20, §8.1] is a contractible component of the complement $W^c \subseteq \widehat{S}$. *Internal* (resp. *external*) faces are those not intersecting (resp. intersecting) the boundary $\widehat{S} - m_b$. A face with n sides (counted with multiplicity, and including sides on the boundary $\partial \widehat{S} - m_b$) is called a n -*face*. Internal faces always have an even number of sides. An *external H-4-face* is an external 4-face limiting to a single component of W (there is only one type of external 2- or 3-face).

A web W is *reduced* if each internal face has at least six sides, and there are no external 2-, 3-, or H-4-faces. (Reduced webs were called “rung-less essential webs” in [DS20, §8.2]; see also [FS22].) Denote by $\mathcal{W}_{\widehat{S}}$ the set of reduced webs up to parallel equivalence. (Note that $\mathcal{W}_{\widehat{S}}$ is what we called $\mathcal{W}_{3,\widehat{S}}$ in §1.)

3.2. Web tropical coordinate map.

In [DS20, §8.2], for any marked surface \widehat{S} and for each ideal triangulation \mathcal{T} of \widehat{S} , we defined a bijection of sets

$$\Phi_{\mathcal{T}} : \mathcal{W}_{\widehat{S}} \xrightarrow{\sim} \mathcal{C}_{\mathcal{T}}$$

from the set $\mathcal{W}_{\widehat{S}}$ of parallel equivalence classes of reduced webs to the KTGS cone $\mathcal{C}_{\mathcal{T}} \subseteq \mathbb{Z}_+^N$, called the *web tropical coordinate map*. We now recall the definition of this map.

3.2.1. Split ideal triangulations, good positions, and web schematics.

The *split ideal triangulation* associated to \mathcal{T} , which by abuse of notation we also denote by \mathcal{T} , is defined by splitting each ideal edge of \mathcal{T} (including boundary edges) into two disjoint ideal edges. In particular, the surface \widehat{S} is cut into ideal triangles and *bigons*, as shown in Figure 7. Note that although bigons do not admit ideal triangulations (in particular, they

do not satisfy the hypothesis $\chi < d/2$ of §2.1 since $d = 2$), we can still consider them as marked surfaces, where all the definitions for webs make sense.

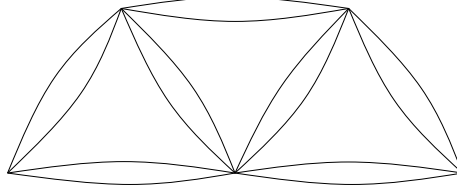


FIGURE 7. Split ideal triangulation.

As proved in [FS22] and [DS20, §8.2], by isotopy we can put any reduced web $W \in \mathcal{W}_{\hat{S}}$ into *good position* with respect to the split ideal triangulation \mathcal{T} , meaning (see below for more details):

- the restriction of the web W to any bigon of \mathcal{T} is a *ladder web* (see Figure 8(1));
- the restriction of the web W to any triangle of \mathcal{T} is a *honeycomb web*, namely an oriented honeycomb together with oriented corner arcs (see Figure 9(1)).

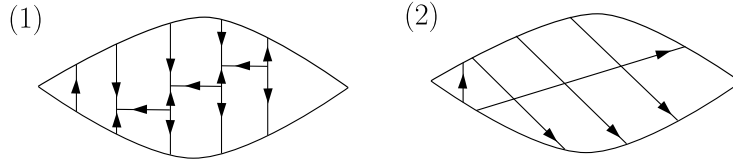


FIGURE 8. Ladder web in a bigon.

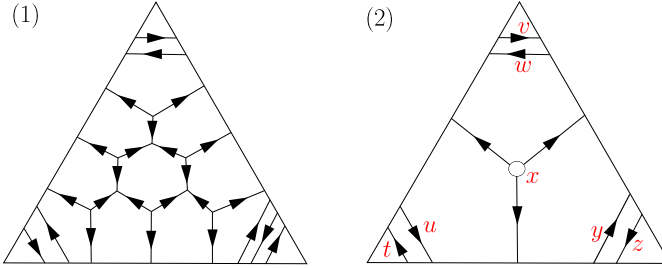


FIGURE 9. Honeycomb web in a triangle: $x = 3$, $y = 2$, and $z = t = u = v = w = 1$. Here the honeycomb is oriented outward (there may also be inward oriented honeycombs).

More precisely, the triangle condition (called “rung-less essential” in [DS20, §3.4]) is equivalent to saying that the restriction of W to the triangle is reduced. The bigon condition (called “essential” in [DS20, §3.4]) is equivalent to asking that (1) all internal faces have at least six sides; and (2) for each edge E of the bigon, and for every compact embedded arc α in the bigon such that $\partial\alpha = \alpha \cap E$ and such that α intersects W transversely, we have that the number of intersection points $W \cap \overline{E}$ does not exceed the number of intersection points $W \cap \alpha$; here, $\overline{E} \subseteq E$ is the segment in E between the two endpoints of α . Note this is a weaker condition than $W|_{\text{bigon}}$ being reduced, since, although it does not allow for external 2- or 3-faces, it does allow for external H-4-faces (also called “rungs” of the ladder web).

In particular, W has minimal geometric intersection with the split ideal triangulation \mathcal{T} .

Note that for a web W in good position: there are two types of honeycombs in triangles, *out-* and *in-honeycombs* (see Figure 9); there may or may not be a honeycomb in a given triangle; and, no conditions on the orientations of the corner arcs in a triangle are assumed.

Remark 3.5. For an earlier appearance of these honeycomb webs in ideal triangles, see [Kup96, pp. 140-141].

In Figure 8(2) we show the *bigon schematic diagram* for a ladder web in a bigon, where each “H” is replaced by a crossing.

In Figure 9(2) we show the *triangle schematic diagram* for a honeycomb web in a triangle. Here, the honeycomb component is completely determined by two pieces of information: its orientation (either all in or all out) and a nonnegative integer $x \in \mathbb{Z}_+$. Note that the schematic for corner arcs is not a “faithful” diagrammatic representation, in general, because it forgets the ordering of the oriented arcs on each corner; see Remark 3.6. However, as we will see, this schematic is sufficient to recover the web tropical coordinates.

Remark 3.6. As one last note about the schematic for corner arcs, if the surface \widehat{S} is an *ideal polygon* (a disk with marked points on its boundary), then the schematic is indeed faithful at the level of parallel equivalence classes of reduced webs. This is because, in this setting, permuting corner arcs preserves the equivalence class of the web; see §3.1. See Figure 6, showing a boundary parallel move in the ideal square.

Definition 3.7. Given the split ideal triangulation as in Figure 10, suppose we are given two oriented arcs intersecting in the bigon along the ideal edge between the two triangles. The intersection is called a

- (1) *non-admissible crossing* if the arcs go toward a common ideal triangle (Figure 10(1));
- (2) *admissible crossing* if the arcs go toward different ideal triangles (Figure 10(2)).

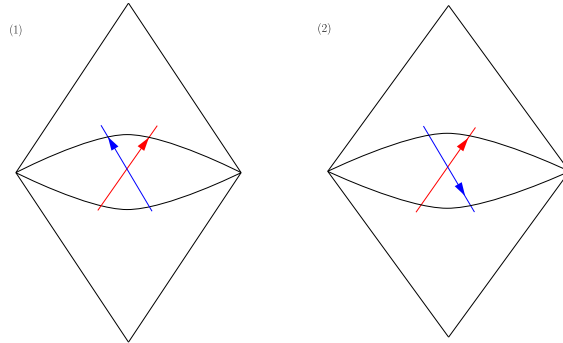


FIGURE 10. (1) Non-admissible crossing. (2) Admissible crossing.

The following fact is essentially by definition.

Observation 3.8. *For any reduced web W in good position with respect to the split ideal triangulation \mathcal{T} , the schematic diagram (Figure 8(2)) of any ladder web obtained by restricting W to a bigon has only admissible crossings.*

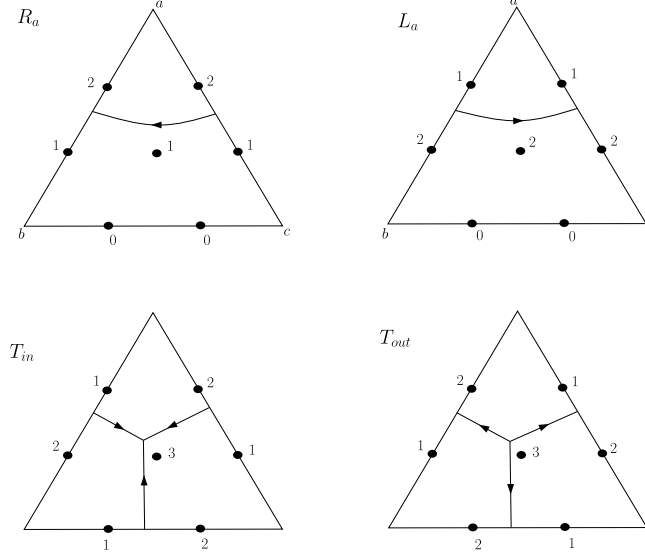


FIGURE 11. Tropical web coordinates for the eight “irreducible” reduced webs in the triangle. (The coordinates for the other four arcs R_b , L_b , R_c , L_c are obtained by triangular symmetry.)

3.2.2. Definition of the web tropical coordinates.

Another way to think of an ideal triangle Δ is as an ideal polygon (Remark 3.6) with three marked points (a, b, c) on its boundary, labeled counterclockwise say.

Let a reduced web W be in good position with respect to a split ideal triangulation \mathcal{T} of \widehat{S} . We start by defining the web tropical coordinates $\Phi(W|_{\Delta}) \in \mathcal{C}_{\Delta}$ “locally” for each restriction $W|_{\Delta}$ of W to an ideal triangle Δ of \mathcal{T} , as in Figure 9(1).

First, the images in $\mathcal{C}_{\Delta} \subseteq \mathbb{Z}_+^7$ under Φ of the eight “irreducible” (see §6 below) local reduced webs $R_a, L_a, R_b, L_b, R_c, L_c, T_{in}, T_{out}$ displayed in Figure 11 are defined as in that figure. One checks directly that these images satisfy the Knutson-Tao rhombus inequalities and the modulo 3 congruence conditions (§3.1).

Then, the image under Φ of the restriction $W|_{\Delta}$ is defined as follows. Let $T \in \{T_{in}, T_{out}\}$ be the oriented honeycomb appearing in $W|_{\Delta}$. Let the nonnegative integers $(x, w, v, u, t, y, z) \in \mathbb{Z}_+^7$ be defined by the schematic for $W|_{\Delta}$, as in Figure 9(2). Put

$$\Phi(W|_{\Delta}) := x\Phi(T) + v\Phi(L_a) + w\Phi(R_a) + t\Phi(L_b) + u\Phi(R_b) + z\Phi(L_c) + y\Phi(R_c) \in \mathcal{C}_{\Delta} \subseteq \mathbb{Z}_+^7.$$

Lastly, the web tropical coordinates $\Phi_{\mathcal{T}}(W) \in \mathcal{C}_{\mathcal{T}} \subseteq \mathbb{Z}_+^N$ for W are defined by “gluing together” the local coordinates $\Phi(W|_{\Delta})$ for the triangles Δ across the edges of \mathcal{T} . Note that the pair of coordinates of $\Phi(W|_{\Delta})$ along an edge E at the bigon interface between two triangles Δ and Δ' matches the corresponding pair of coordinates of $\Phi(W|_{\Delta'})$ along the other bigon edge E' , since these coordinates depend only on the number of oriented in- and out-strands crossing the bigon at either boundary edge E or E' . Thus, this gluing procedure is well-defined. In particular, in this way coordinates are assigned to the un-split ideal triangulation \mathcal{T} ; this is why, in practice, one can go back and forth between the split and un-split triangulation.

See Figure 12 for an example where \widehat{S} is the once punctured torus. As another example, the face coordinate (namely, the coordinate that is 3 for T_{in} and T_{out}) for the honeycomb

web W shown in Figure 9(1) is $3 \cdot 3 + 4 \cdot 1 + 3 \cdot 2 = 19$. There are plenty of examples of computing web coordinates throughout the paper; for instance, see §5.

In [DS20, §8.2] we showed $\Phi_{\mathcal{T}}(W) \in \mathcal{C}_{\mathcal{T}}$ is independent of the choice of good position of W with respect to the split ideal triangulation \mathcal{T} . Moreover, we proved the result mentioned at the beginning of this subsection:

Theorem 3.9 ([DS20, Theorem 80]). *For each ideal triangulation \mathcal{T} of the marked surface \widehat{S} , the web tropical coordinate map*

$$\Phi_{\mathcal{T}} : \mathcal{W}_{\widehat{S}} \xrightarrow{\sim} \mathcal{C}_{\mathcal{T}},$$

from the set $\mathcal{W}_{\widehat{S}}$ of parallel equivalence classes of reduced webs in \widehat{S} to the Knutson-Tao-Goncharov-Shen cone $\mathcal{C}_{\mathcal{T}} \subseteq \mathbb{Z}_{+}^N$, is a bijection of sets.

We will need the following fact, which is immediate from the definitions.

Observation 3.10. *For any disjoint reduced webs $W, W' \in \mathcal{W}_{\widehat{S}}$, we have $W \cup W' \in \mathcal{W}_{\widehat{S}}$ and*

$$\Phi_{\mathcal{T}}(W \cup W') = \Phi_{\mathcal{T}}(W) + \Phi_{\mathcal{T}}(W') \in \mathcal{C}_{\mathcal{T}}.$$

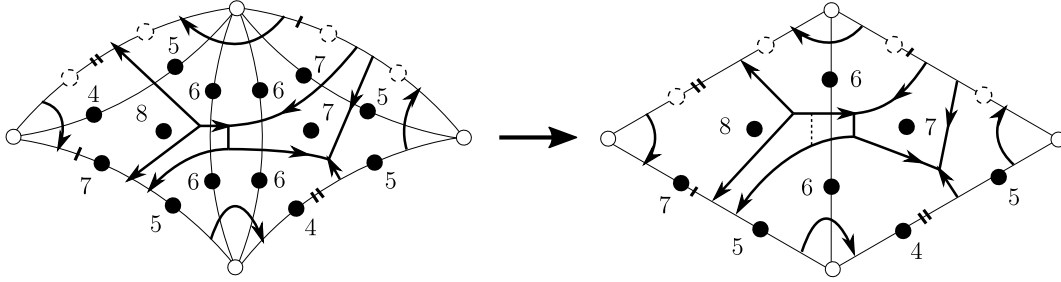


FIGURE 12. Gluing construction for the tropical coordinates for a reduced web in the once punctured torus.

4. NATURALITY OF THE WEB TROPICAL COORDINATES

In §3, we recalled the construction [DS20] of the web tropical coordinate map $\Phi_{\mathcal{T}} : \mathcal{W}_{\widehat{S}} \rightarrow \mathcal{C}_{\mathcal{T}} \subseteq \mathbb{Z}_{+}^N$, depending on a choice of ideal triangulation \mathcal{T} of the marked surface \widehat{S} . By Theorem 3.9, $\Phi_{\mathcal{T}}$ is a bijection.

In this section, we show that these coordinates are *natural* with respect to changing the triangulation $\mathcal{T} \rightarrow \mathcal{T}'$. That is, the induced coordinate change map $\mathcal{C}_{\mathcal{T}} \rightarrow \mathcal{C}_{\mathcal{T}'}$ is a tropical \mathcal{A} -coordinate cluster transformation, in the language of Fock-Goncharov [FG06].

Remark 4.1. See [SSW] for another proof of the main result of this section, Theorem 4.3.

4.1. Precise statement of naturality for the square.

Recall that an *ideal square* \square is a disk with four marked points on its boundary. (See also Remark 3.6.) An ideal triangulation of \square is a choice of diagonal of the square; there are two such triangulations, related by a *diagonal flip*.

Definition 4.2. Let \mathcal{T} and \mathcal{T}' be the two ideal triangulations of the square \square . The *tropical \mathcal{A} -coordinate cluster transformation for the square* is the piecewise-linear function

$$\mu_{\mathcal{T}', \mathcal{T}} : \mathbb{Z}^{12} \longrightarrow \mathbb{Z}^{12}$$

defined by

$$\mu_{\mathcal{T}', \mathcal{T}}(x_1, x_2, x_3, x_4, x_5, x_6, x_7, x_8, y_1, y_2, y_3, y_4) = (x'_1, x'_2, x'_3, x'_4, x'_5, x'_6, x'_7, x'_8, z_1, z_2, z_3, z_4),$$

where the right hand side of the equation is given by Equations (1), (2), (3), (4), (5). See also Figure 2. (Here, we think of the domain of $\mu_{\mathcal{T}', \mathcal{T}}$ as associated to \mathcal{T} , and the codomain to \mathcal{T}' .)

Note that Equations (4), (5) use Equations (1), (2), (3).

The main result of this paper is:

Theorem 4.3. *Let \mathcal{T} and \mathcal{T}' be the two ideal triangulations of the square \square , and let $\Phi_{\mathcal{T}} : \mathcal{W}_{\square} \rightarrow \mathcal{C}_{\mathcal{T}} \subseteq \mathbb{Z}_+^{12}$ and $\Phi_{\mathcal{T}'} : \mathcal{W}_{\square} \rightarrow \mathcal{C}_{\mathcal{T}'} \subseteq \mathbb{Z}_+^{12}$ be the associated web tropical coordinate maps. Then,*

$$\mu_{\mathcal{T}', \mathcal{T}}(c) = \Phi_{\mathcal{T}'} \circ \Phi_{\mathcal{T}}^{-1}(c) \in \mathcal{C}_{\mathcal{T}'} \quad (c \in \mathcal{C}_{\mathcal{T}}).$$

Remark 4.4. Note it is not even clear, a priori, from the definitions that $\mu_{\mathcal{T}', \mathcal{T}}(c) \geq 0$ for $c \in \mathcal{C}_{\mathcal{T}}$.

4.2. Proof of Theorem 4.3.

By definition of the tropical coordinates, and of good position of a reduced web W in \mathcal{W}_{\square} with respect to the triangulations \mathcal{T} and \mathcal{T}' , we immediately get:

Observation 4.5. *For all $W \in \mathcal{W}_{\square}$, the images $c = \Phi_{\mathcal{T}}(W) \in \mathcal{C}_{\mathcal{T}}$ and $\Phi_{\mathcal{T}'} \circ \Phi_{\mathcal{T}}^{-1}(c) \in \mathcal{C}_{\mathcal{T}'}$ satisfy Equation (1).*

Definition 4.6. Let the punctures of the square \square be labeled a, b, c, d as in Figure 22 (part 1) below. Also as in the figure, define the 8 oriented *corner arcs* $L_a, R_a, L_b, R_b, L_c, R_c, L_d, R_d$ in \mathcal{W}_{\square} . Their 12 coordinates are provided in the figure as well.

One checks by direct computation that:

Observation 4.7. *The images $c = \Phi_{\mathcal{T}}(W) \in \mathcal{C}_{\mathcal{T}}$, for $W = L_a, R_a, L_b, R_b, L_c, R_c, L_d, R_d$ any of the 8 corner arcs, satisfy Theorem 4.3.*

Definition 4.8. A given reduced web W in \mathcal{W}_{\square} is the disjoint union of (i) all its corner arc components, together called the *corner part* and denoted W_r ; and (ii) their complement $W_c := W - W_r$, which we call the *cornerless part* of the web W .

A reduced web W is *cornerless* if $W = W_c$. That is, W has no corner arcs.

Let $\mathcal{R} \subseteq \mathcal{W}_{\square}$ be the set of *corner webs*, that is, webs whose cornerless parts are empty: $W = W_r$. That is, an element of \mathcal{R} is a disjoint union of corner arcs.

Lemma 4.9. *For any disjoint reduced webs $W \in \mathcal{R}$ and $W' \in \mathcal{W}_{\square}$, we have $W \cup W' \in \mathcal{W}_{\square}$ and*

$$\mu_{\mathcal{T}', \mathcal{T}}(\Phi_{\mathcal{T}}(W)) + \mu_{\mathcal{T}', \mathcal{T}}(\Phi_{\mathcal{T}}(W')) = \mu_{\mathcal{T}', \mathcal{T}}(\Phi_{\mathcal{T}}(W \cup W')) \in \mathbb{Z}^{12}.$$

Proof. By Observation 3.10, we get

$$\Phi_{\mathcal{T}}(W) + \Phi_{\mathcal{T}}(W') = \Phi_{\mathcal{T}}(W \cup W') \in \mathcal{C}_{\mathcal{T}}.$$

For any corner arc in Figure 22(1)-(8), thus for any $W \in \mathcal{R}$ (again by Observation 3.10), the left hand sides of Equations (2), (3), (4), (5) are always of the form $\max\{u, u\} - v$. Since

$$(\max\{u, u\} - v) + (\max\{x, y\} - z) = \max\{u + x, u + y\} - (v + z) \in \mathbb{Z},$$

we obtain the desired equality. ■

Proof of Theorem 4.3.

Recall by Theorem 3.9 that any $c \in \mathcal{C}_{\mathcal{T}}$ is of the form $c = \Phi_{\mathcal{T}}(W)$ for some $W \in \mathcal{W}_{\square}$. For any reduced web $W \in \mathcal{W}_{\square}$, suppose that its coordinates via $\Phi_{\mathcal{T}}$ are labeled as in the left hand side of Figure 2, and via $\Phi_{\mathcal{T}'}$ as in the right hand side of Figure 2. By Observation 4.5, Equation (1) is satisfied for any web W in \mathcal{W}_{\square} . In addition, by Observation 4.7, the Equations (2), (3), (4), (5) are satisfied for any web W in \mathcal{R} , that is, W consisting only of corner arcs. By Lemma 4.9 together with another application of Observation 3.10 to \mathcal{T}' , we have thus reduced the problem to establishing Equations (2), (3), (4), (5) for any cornerless web $W = W_c$.

The main difficulty is that, for a given cornerless web $W = W_c$ in good position with respect to the ideal triangulation \mathcal{T} , after flipping the diagonal $\mathcal{T} \rightarrow \mathcal{T}'$ it is not obvious how W rearranges itself back into good position with respect to the new triangulation \mathcal{T}' . (See, however, §5 for examples of this rearranging into good position after the flip.)

We circumvent this difficulty by solving the problem “uniformly”, that is, without knowing how the new good position looks after the flip. The hypothesis that the web $W = W_c$ does not have any corner arcs will be important here.

To start, observe that it suffices to establish just Equation (2). Indeed, Equations (3), (4), (5) then immediately follow by 90 degree rotational symmetry. (Solve for y_1 and y_3 , respectively, in the last two equations.)

With this goal in mind, we argue

$$(*) \quad z_2 = x'_2 + x'_3 = x_2 + x_3 = \max(x_2 + y_3, x_3 + y_1) - y_2 \in \mathbb{Z}_+.$$

Throughout, consider Figure 13, recalling the notion of a web schematic; see §3.2.1 and Remark 3.6.

The second equation of $(*)$ has already been justified, by Observation 4.5.

Let us justify the first equation of $(*)$. There are two cases, namely when m' represents an out- or an in-honeycomb.

When m' is “out”, we compute:

$$x'_2 = b' + 2z' + m', \quad x'_3 = c' + 2y' + 2m', \quad z_2 = b' + c' + 2y' + 2z' + 3m'.$$

When m' is “in”, we compute:

$$x'_2 = b' + 2z' + 2m', \quad x'_3 = c' + 2y' + m', \quad z_2 = b' + c' + 2y' + 2z' + 3m'.$$

In both cases, the desired formula $z_2 = x'_2 + x'_3$ holds.

The justification of the third equation of $(*)$ is more involved. We begin with a topological consequence.

Claim 4.10. *Let $W = W_c$ be a cornerless reduced web in the square. Up to 180 degree rotational symmetry of the square, there are three cases:*

(1) *When the n and m honeycombs are both “out”: Then,*

$$a + n + x = b + y \quad \& \quad w + d = z + m + c.$$

Moreover, if $y \geq n + x$, then $b = 0$; and, if $y \leq n + x$, then $a = 0$.

(Note this is the case displayed in the left hand side of Figure 13.)

(2) *When the n honeycomb is “out”, and the m honeycomb is “in”: Then,*

$$a + n + x = b + y + m \quad \& \quad w + d = z + c.$$

Moreover, if $y + m \geq n + x$, then $b = 0$; and, if $y + m \leq n + x$, then $a = 0$.

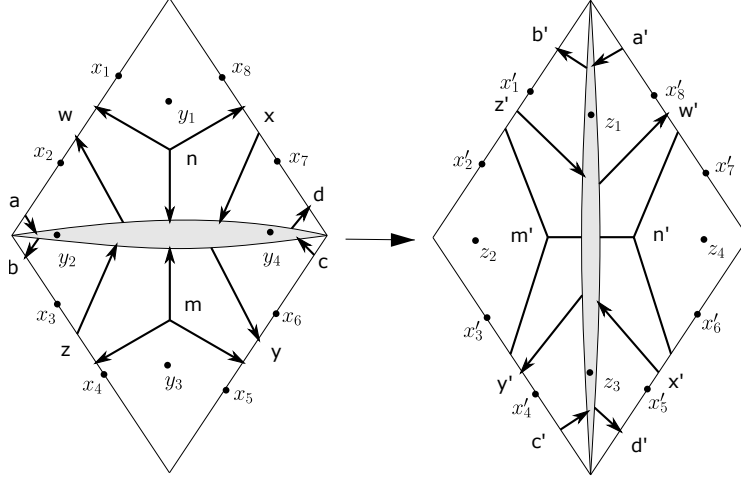


FIGURE 13. Schematic for the cornerless web $W = W_c$ in the square, before and after the flip. The variables $a, b, c, d, x, y, z, w, n, m$ are known, and can be read off from the good position of W with respect to \mathcal{T} . The primed variables a', b', \dots, m' are not assumed to be known. Because W has no corner arcs, there are no arcs at the top and bottom vertices before the flip, nor at the left and right vertices after the flip; it follows by Observation 3.8 that we cannot have a and b (or c and d) simultaneously nonzero. To be concrete, we have shown the case where the honeycombs labeled n and m are out-honeycombs; we will justify the other cases as well. Note that the orientations of the n' and m' honeycombs are not assumed to be known (and do not follow from the orientations of the n and m honeycombs).

(3) When the n and m honeycombs are both “in”: Then,

$$a + x = b + y + m \quad \& \quad w + d + n = z + c.$$

Moreover, if $y + m \geq x$, then $b = 0$; and, if $y + m \leq x$, then $a = 0$.

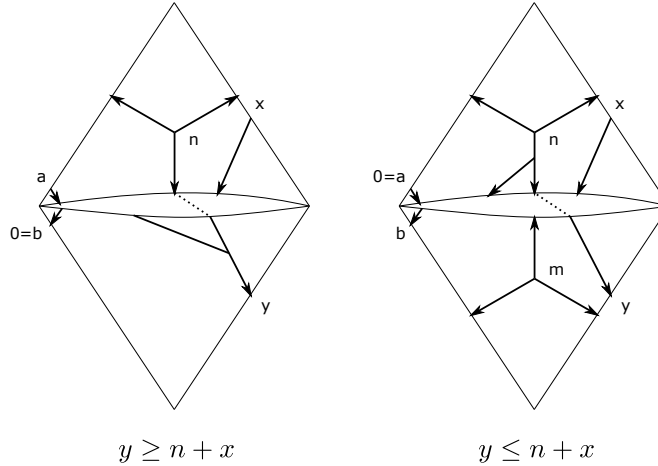


FIGURE 14. Proof of Claim 4.10. The web is assumed not to have any corner arcs. Shown is the case when the n and m honeycombs are both “out”.

The key topological property used to prove all three statements of the claim is the following: The number of “out” strands (resp. “in” strands) along one boundary edge of the bigon, as displayed on the left hand side of Figure 13, is equal to the number of “in” strands (resp. “out” strands) along the other boundary edge of the bigon.

We prove the first statement, (1), of the claim; the proofs of the second and third statements are similar. So assume the n and m honeycombs are both “out”.

By the above topological property, we have the desired two identities of the statement.

For the second part of the statement: When $y \geq n + x$, if b were nonzero, then a would have to be nonzero, since $b + y = a + n + x$. Then b would be attaching to a ; see the schematic shown in the left hand side of Figure 14 (see also the caption of Figure 13). But this contradicts the hypothesis that W has no corner arcs. Similarly, $a = 0$ when $y \leq n + x$; see the right hand side of Figure 14. This establishes the claim.

Claim 4.11. *Let $W = W_c$ be a cornerless reduced web in the square. Up to 180 degree rotational symmetry of the square, there are three cases:*

- (1) *When the n and m honeycombs are both “out”: Then, $x_2 + y_3 \geq x_3 + y_1$ if and only if $y \geq n + x$; conversely, $x_2 + y_3 \leq x_3 + y_1$ if and only if $y \leq n + x$.
(Note this is the case displayed in the left hand side of Figure 13.)*
- (2) *When the n honeycomb is “out”, and the m honeycomb is “in”: Then, $x_2 + y_3 \geq x_3 + y_1$ if and only if $y + m \geq n + x$; conversely, $x_2 + y_3 \leq x_3 + y_1$ if and only if $y + m \leq n + x$.*
- (3) *When the n and m honeycombs are both “in”: Then, $x_2 + y_3 \geq x_3 + y_1$ if and only if $y + m \geq x$; conversely, $x_2 + y_3 \leq x_3 + y_1$ if and only if $y + m \leq x$.*

We prove the first statement; the proofs of the second and third statements are similar. So assume the n and m honeycombs are both “out”. By Figure 13, we compute:

$$\begin{aligned} x_2 &= w + 2a + n, & y_3 &= b + c + 2y + 2z + 3m, \\ x_3 &= z + 2b + 2m, & y_1 &= a + d + 2x + 2w + 3n. \end{aligned}$$

Thus,

$$\begin{aligned} (x_2 + y_3) - (x_3 + y_1) &= -w + a - 2n - b + c + 2y + z + m - d - 2x \geq 0 \\ \iff a + c + 2y + z + m &\geq w + 2n + b + d + 2x. \end{aligned}$$

By applying the two identities of part (1) of Claim 4.10, the above inequality is equivalent to $3y \geq 3n + 3x$ as desired. Conversely, by reversing the direction of the inequality throughout the argument, we have $x_2 + y_3 \leq x_3 + y_1$ if and only if $y \leq n + x$. This establishes the claim.

We are now prepared to justify the third equation of (*), which we recall is

$$(**) \quad x_2 + x_3 = \max(x_2 + y_3, x_3 + y_1) - y_2.$$

First, let us assume the n and m honeycombs are both “out”, as in the left hand side of Figure 13. The values of x_2, y_3, x_3, y_1 were computed above, and we gather

$$\begin{aligned} x_2 + x_3 &= w + 2a + n + z + 2b + 2m, \\ x_2 + y_3 &= w + 2a + n + b + c + 2y + 2z + 3m, \\ x_3 + y_1 &= z + 2b + 2m + a + d + 2x + 2w + 3n. \end{aligned}$$

By Figure 13, there are two ways to express y_2 :

$$y_2 = w + d + 2a + 2n + 2x = z + m + c + 2b + 2y.$$

There are two cases to establish (**). In the case $x_2 + y_3 \geq x_3 + y_1$, we compute, using the second form of y_2 above:

$$\begin{aligned} \max(x_2 + y_3, x_3 + y_1) - y_2 &= (x_2 + y_3) - y_2 \\ &= w + 2a + n - b + z + 2m \stackrel{?}{=} x_2 + x_3 \iff b \stackrel{?}{=} 0. \end{aligned}$$

For this case, by part (1) of Claim 4.11, we have $y \geq n + x$. Thus, $b = 0$ by part (1) of Claim 4.10, as desired.

In the case $x_2 + y_3 \leq x_3 + y_1$, we compute, using the first form of y_2 above:

$$\begin{aligned} \max(x_2 + y_3, x_3 + y_1) - y_2 &= (x_3 + y_1) - y_2 \\ &= z + 2b + 2m - a + w + n \stackrel{?}{=} x_2 + x_3 \iff a \stackrel{?}{=} 0. \end{aligned}$$

For this case, by part (1) of Claim 4.11, we have $y \leq n + x$. Thus, $a = 0$ by part (1) of Claim 4.10, as desired.

This establishes (**) when both the honeycombs are “out”. When the n honeycomb is “out”, and the m honeycomb is “in”; or, when the n and m honeycombs are both “in”: By essentially the same calculation, one computes again that, in the case $x_2 + y_3 \geq x_3 + y_1$, then (**) is equivalent to $b = 0$, and in the case $x_2 + y_3 \leq x_3 + y_1$, then (**) is equivalent to $a = 0$. These are justified by parts (2) and (3), respectively, of Claims 4.11 and 4.10.

This completes the proof of the main result. ■

Remark 4.12. We emphasize that the above proof depended crucially on two topological properties (both used in the proof of Claim 4.10): (1) the *bigon property* about “in” and “out” strands; and, (2) the *cornerless property* saying that a and b cannot be simultaneously nonzero.

The trick was to use Lemma 4.9 to separate the corner arc case from the cornerless case, and then to use the fact that it is obvious that the boundary coordinates do not change after the flip. It is somewhat surprising that there is this relationship (*) between the internal and boundary coordinates; we do not know if such a relationship occurs in higher rank. In §7, we give another application of this “separating corner and cornerless webs” strategy.

4.3. Naturality for a marked surface.

Let \widehat{S} be a marked surface, let \mathcal{T} be an ideal triangulation, and let N denote the number of global tropical coordinates; see §2.1. In §3, we introduced the web tropical coordinate map $\Phi_{\mathcal{T}} : \mathcal{W}_{\widehat{S}} \rightarrow \mathcal{C}_{\mathcal{T}}$, where we implicitly assumed an inclusion $\mathcal{C}_{\mathcal{T}} \subseteq \mathbb{Z}_+^N$ of the KTGS cone of \mathcal{T} (any permutation of the coordinates of \mathbb{Z}_+^N determines a different inclusion). This choice played no role there, since we were only considering a single triangulation. We now consider multiple triangulations, where it becomes necessary to keep track of such choices.

4.3.1. Dotted triangulations.

More precisely, let $\mathcal{T} = \mathcal{T}_0$ be an initial choice of ideal triangulation, which we mark with N dots in the usual way (as for instance in Figure 4). Such a dotted initial triangulation $\mathcal{T} = \mathcal{T}_0$ is called a *base (dotted) triangulation*. Fix a labeling of the dots of \mathcal{T} from $1, 2, \dots, N$; we say that the base triangulation $\mathcal{T} = \mathcal{T}_0$ is *labeled*. This determines a bijection $\{1, 2, \dots, N\} \rightarrow \{\text{dots}\}$, hence also an inclusion $\mathcal{C}_{\mathcal{T}} \subseteq \mathbb{Z}_+^N$ (since a point in $\mathcal{C}_{\mathcal{T}}$ is, most precisely, a function $\{\text{dots}\} \rightarrow \mathbb{Z}_+$; see Figure 11 for instance).

Example (part 1). See the first diagram 0 in Figure 15.

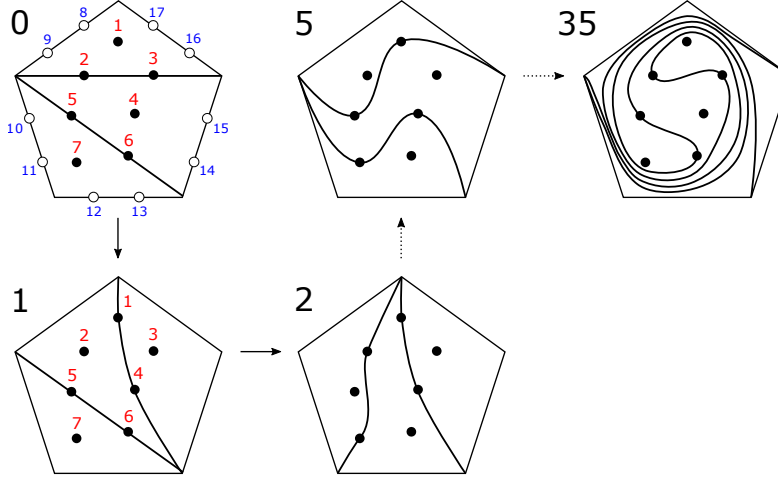


FIGURE 15. Pentagon Relation for SL_3 , namely the sequence of five diagonal flips from \mathcal{T}_0 to \mathcal{T}_5 . It takes 35 flips to come back to the original dotted triangulation. That is, as dotted triangulations, $\mathcal{T}_0 = \mathcal{T}_{35}$ and $\mathcal{T}_0 \neq \mathcal{T}_i$ for $i = 1, 2, \dots, 34$. The ten boundary coordinates (shown only in the first picture) are fixed, or “frozen”, by these flip mutations but still enter into the computations for the interior coordinates. See Remark 4.15 for a computation.

We now imagine forgetting $\mathcal{T} = \mathcal{T}_0$, but leaving the dots associated to \mathcal{T} where they were on the surface. Another triangulation \mathcal{T}' is *dotted* (with respect to the dotting of \mathcal{T}) if there are two dots (from \mathcal{T}) on each edge of \mathcal{T}' and one dot (from \mathcal{T}) in each face of \mathcal{T}' . Note that, using the labeling of the dots fixed along with the base triangulation $\mathcal{T} = \mathcal{T}_0$, each dotted triangulation \mathcal{T}' determines an inclusion $\mathcal{C}_{\mathcal{T}'} \subseteq \mathbb{Z}_+^N$ as above for $\mathcal{T} = \mathcal{T}_0$.

We refer to \mathcal{T}' without a dotting as the underlying *topological triangulation*.

Example (part 2). The triangulations $\mathcal{T}_1, \mathcal{T}_2, \mathcal{T}_5, \mathcal{T}_{35}$ shown in the last four diagrams 1, 2, 5, 35 in Figure 15 are dotted with respect to the dotted triangulation \mathcal{T}_0 in the first diagram 0. Note that, as triangulations, $\mathcal{T}_0 = \mathcal{T}_5 = \mathcal{T}_{35}$, but, as dotted triangulations, $\mathcal{T}_0 = \mathcal{T}_{35} \neq \mathcal{T}_5$.

4.3.2. Tropical \mathcal{A} -coordinate cluster transformation for a marked surface.

We pause our discussion of the topology and geometry of webs and cones, and turn to a purely algebraic result of Fomin-Zelevinsky and Fock-Goncharov (see Theorem 4.13 below).

There is a procedure to start from a base triangulation $\mathcal{T} = \mathcal{T}_0$ and generate new dotted triangulations in a controlled way, via diagonal flips. Indeed, if \mathcal{T}_i is dotted, and if $(\square, \mathcal{T}_i|_{\square})$ is a triangulated square in \mathcal{T}_i , the diagonal flip at \square induces a new dotted triangulation \mathcal{T}_{i+1} . (For simplicity, we always assume that \mathcal{T}_{i+1} is not self-folded; see §2.1.) Note that the induced embedding of \mathcal{T}_{i+1} in \hat{S} is well-defined up to isotopy in $\hat{S} - \{\text{dots}\}$, since the triangulated square $(\square, \mathcal{T}_i|_{\square})$ comes with a canonical foliation including the diagonal as a leaf. Observe that the sequence $\mathcal{T} = \mathcal{T}_0 \rightarrow \mathcal{T}_1 \rightarrow \mathcal{T}_2 \rightarrow \dots$ of dotted triangulations so-obtained depends on the chosen sequence of diagonal flips, so is not unique.

Example (part 3). See for instance the passage from the diagrams 0 to 1 or from the diagrams 1 to 2 in Figure 15.

Let $\mathcal{T} = \mathcal{T}_0$ be labeled as well, and let \mathcal{T}_i and \mathcal{T}_{i+1} be as above. Then their dottings induce a *flip mutation function*

$$\mu_{\mathcal{T}_{i+1}, \mathcal{T}_i} : \mathbb{Z}^N \longrightarrow \mathbb{Z}^N$$

defined in the square \square as in Definition 4.2 (that is, by the formulas (1), (2), (3), (4), (5) of Figure 2) and outside the square as the identity. (We remind that the domain is associated to \mathcal{T}_i and the codomain to \mathcal{T}_{i+1} .) In particular, the formulas are the same irrespective of whether the boundary of the square has any self-gluing. If

$$(\dagger) \quad \mathcal{T} = \mathcal{T}_0 \rightarrow \mathcal{T}_1 \rightarrow \mathcal{T}_2 \rightarrow \cdots \rightarrow \mathcal{T}_{m-1} \rightarrow \mathcal{T}_m = \mathcal{T}'$$

is a sequence of flips as above, ending at a dotted triangulation $\mathcal{T}_m = \mathcal{T}'$, define the associated *mutation function (for this sequence of flips)*

$$\mu_{\mathcal{T}_m, \mathcal{T}_0} : \mathbb{Z}^N \longrightarrow \mathbb{Z}^N$$

as the function composition

$$\mu_{\mathcal{T}_m, \mathcal{T}_0} := \mu_{\mathcal{T}_m, \mathcal{T}_{m-1}} \circ \cdots \circ \mu_{\mathcal{T}_2, \mathcal{T}_1} \circ \mu_{\mathcal{T}_1, \mathcal{T}_0}.$$

Here, we have used the standard convention that $(g \circ f)(x) := g(f(x))$.

Now, let in addition

$$(\dagger\dagger) \quad \mathcal{T} = \mathcal{T}_0 \rightarrow \tilde{\mathcal{T}}_1 \rightarrow \tilde{\mathcal{T}}_2 \rightarrow \cdots \rightarrow \tilde{\mathcal{T}}_{\tilde{m}-1} \rightarrow \tilde{\mathcal{T}}_{\tilde{m}} = \mathcal{T}'$$

be another sequence of diagonal flips starting at the same base triangulation $\mathcal{T} = \mathcal{T}_0$, and ending at the same topological triangulation \mathcal{T}' , but where the dottings of $\mathcal{T}_m = \mathcal{T}'$ and $\tilde{\mathcal{T}}_{\tilde{m}} = \mathcal{T}'$ are possibly different. Define the associated permutation linear map

$$\sigma_{\tilde{\mathcal{T}}_{\tilde{m}}, \mathcal{T}_m} : \mathbb{Z}^N \longrightarrow \mathbb{Z}^N$$

as follows: For $i \in \{1, 2, \dots, N\}$, if the i -labeled dot is on an edge (resp. face) of $\mathcal{T}_m = \mathcal{T}'$, and if the corresponding dot on the corresponding edge (resp. face) of $\tilde{\mathcal{T}}_{\tilde{m}} = \mathcal{T}'$ is labeled $\sigma(i)$, then $\sigma_{\tilde{\mathcal{T}}_{\tilde{m}}, \mathcal{T}_m}$ maps the i -th standard basis vector e_i of \mathbb{Z}^N to the $\sigma(i)$ -th standard basis vector $e_{\sigma(i)}$ of \mathbb{Z}^N .

Example (part 4). We could take $\mathcal{T}_i = \tilde{\mathcal{T}}_i$ in Figure 15 with $m = 5$ and $\tilde{m} = 35$. Then,

$$\sigma(1) = 3, \quad \sigma(2) = 1, \quad \sigma(3) = 4, \quad \sigma(4) = 6, \quad \sigma(5) = 2, \quad \sigma(6) = 7, \quad \sigma(7) = 5$$

and $\sigma(i) = i$ is the identity on all of the boundary coordinates ($i = 8, 9, \dots, 17$).

Theorem 4.13 ([FZ02, FG06]). *Let $\mathcal{T} = \mathcal{T}_0$ be a labeled base dotted triangulation. Given two flip sequences (\dagger) and $(\dagger\dagger)$ of dotted triangulations ending at the same topological triangulation \mathcal{T}' , the following diagram commutes:*

$$\begin{array}{ccc} \mathbb{Z}^N & \xrightarrow{\mu_{\mathcal{T}_m, \mathcal{T}_0}} & \mathbb{Z}^N \\ & \searrow \mu_{\tilde{\mathcal{T}}_{\tilde{m}}, \mathcal{T}_0} & \downarrow \sigma_{\tilde{\mathcal{T}}_{\tilde{m}}, \mathcal{T}_m} \\ & & \mathbb{Z}^N \end{array}$$

An immediate consequence of this theorem is:

Observation 4.14. *Using the notation of Theorem 4.13, (\dagger) and $(\dagger\dagger)$: For $\mathcal{T}' = \mathcal{T}$ and $m = 0$, we get $\mu_{\mathcal{T}_m, \mathcal{T}_0} = \mu_{\mathcal{T}_0, \mathcal{T}_0} = \text{identity}$, hence*

$$\mu_{\tilde{\mathcal{T}}_{\tilde{m}}, \mathcal{T}_0} = \sigma_{\tilde{\mathcal{T}}_{\tilde{m}}, \mathcal{T}_0} : \mathbb{Z}^N \longrightarrow \mathbb{Z}^N$$

is a permutation map.

Example (part 5). To get a feel for the content of Theorem 4.13, let us consider (similar to part 4 of this example) $\mathcal{T}_i = \tilde{\mathcal{T}}_i$ in Figure 15 with $m = 0$ and $\tilde{m} = 5$, where $\sigma_{\mathcal{T}_5, \mathcal{T}_0}$ is defined by

$$\sigma(1) = 2, \quad \sigma(2) = 5, \quad \sigma(3) = 1, \quad \sigma(4) = 3, \quad \sigma(5) = 7, \quad \sigma(6) = 4, \quad \sigma(7) = 6$$

and $\sigma(i) = i$ for $i = 8, 9, \dots, 17$.

Then Observation 4.14 says $\sigma_{\mathcal{T}_5, \mathcal{T}_0}^{-1} \circ \mu_{\mathcal{T}_5, \mathcal{T}_0}$ is the identity map $\mathbb{Z}^{17} \rightarrow \mathbb{Z}^{17}$. This is the so-called *Pentagon Relation* for SL_3 . By construction this is obvious for the 8-th through the 17-th coordinates, because these are the “frozen” coordinates on the boundary of the pentagon. So the heart of the statement is the validity of the seven identities:

$$f_i(x_1, x_2, \dots, x_{17}) = x_i \quad (i = 1, 2, \dots, 7; \quad x_j \in \mathbb{Z}; \quad j = 1, 2, \dots, 17)$$

where $f_i : \mathbb{Z}^{17} \rightarrow \mathbb{Z}$ is defined as the i -th component of $\sigma_{\mathcal{T}_5, \mathcal{T}_0}^{-1} \circ \mu_{\mathcal{T}_5, \mathcal{T}_0}$. In particular, f_i is a complicated piecewise-linear function built out of the operations $+$, $-$, and \max .

Remark 4.15. Of the seven identities $f_i(x_1, x_2, \dots, x_{17}) = x_i$ discussed in Example (part 5), the most nontrivial is the case $i = 5$. Appendix B at the end of this article contains a Mathematica notebook which provides the explicit expression for $f_5(x_1, x_2, \dots, x_{17})$.

To finish this digression, a well-known fact [Pen87] says that any two triangulations \mathcal{T} and \mathcal{T}' are related by a sequence of diagonal flips (\dagger) . By Theorem 4.13, we thus immediately obtain:

Corollary 4.16. *Let $\mathcal{T} = \mathcal{T}_0$ be a labeled base dotted triangulation. For any topological triangulation \mathcal{T}' , there is a function*

$$\mu_{\mathcal{T}', \mathcal{T}_0} : \mathbb{Z}^N \longrightarrow \mathbb{Z}^N,$$

defined only up to permutation of the coordinates of the codomain \mathbb{Z}^N , satisfying the property that if $\mathcal{T}_m = \mathcal{T}'$ is related to $\mathcal{T} = \mathcal{T}_0$ by a sequence of diagonal flips (\dagger) , then

$$\mu_{\mathcal{T}', \mathcal{T}_0} = \mu_{\mathcal{T}_m, \mathcal{T}_{m-1}} \circ \dots \circ \mu_{\mathcal{T}_2, \mathcal{T}_1} \circ \mu_{\mathcal{T}_1, \mathcal{T}_0}$$

where the $\mu_{\mathcal{T}_{i+1}, \mathcal{T}_i} : \mathbb{Z}^N \rightarrow \mathbb{Z}^N$ are the corresponding (well-defined) flip mutation functions. ■

Definition 4.17. The (pseudo-)function $\mu_{\mathcal{T}', \mathcal{T}_0} : \mathbb{Z}^N \rightarrow \mathbb{Z}^N$ from Corollary 4.16 is called the *tropical \mathcal{A} -coordinate cluster transformation* for the marked surface \hat{S} associated to the labeled base dotted triangulation $\mathcal{T} = \mathcal{T}_0$ and the topological triangulation \mathcal{T}' . Below, we will drop the subscript and just write $\mu_{\mathcal{T}', \mathcal{T}}$ for this function.

Remark 4.18.

- (1) Throughout this sub-subsection, there has been nothing special about the integers \mathbb{Z} compared to, say, the rational numbers \mathbb{Q} . In particular, Theorem 4.13 makes sense and is true with \mathbb{Z} replaced by \mathbb{Q} .

- (2) The Pentagon Relation for SL_3 (Figure 15), equivalent to the seven identities $f_i(x_1, x_2, \dots, x_{17}) = x_i$ for $i = 1, 2, \dots, 7$ discussed in Example (part 5) above is the main relation required to establish Theorem 4.13.

4.3.3. Naturality of the web tropical coordinate map.

We are now ready to generalize Theorem 4.3 to any marked surface \widehat{S} .

Let $\mathcal{T} = \mathcal{T}_0$ be a labeled base dotted triangulation, and let \mathcal{T}' be any topological triangulation; see §4.3.1. Associated to this topological data is the tropical \mathcal{A} -coordinate cluster transformation $\mu_{\mathcal{T}', \mathcal{T}} : \mathbb{Z}^N \rightarrow \mathbb{Z}^N$, which is only defined up to permutation of the coordinates of the codomain \mathbb{Z}^N ; see Definition 4.17.

Lastly, recall from §4.3.1 that the labels for the dots of $\mathcal{T} = \mathcal{T}_0$ determine an inclusion $\mathcal{C}_{\mathcal{T}} \subseteq \mathbb{Z}_+^N$ of its KTGS cone. Since \mathcal{T}' is not assumed to be dotted, the inclusion $\mathcal{C}_{\mathcal{T}'} \subseteq \mathbb{Z}_+^N$ of its KTGS cone is only defined up to permutation of the coordinates of \mathbb{Z}_+^N .

Theorem 4.19. *Let \mathcal{T} and \mathcal{T}' be triangulations, and let $\mu_{\mathcal{T}', \mathcal{T}} : \mathbb{Z}^N \rightarrow \mathbb{Z}^N$ be the corresponding tropical \mathcal{A} -coordinate cluster transformation, as just explained. For the associated web tropical coordinate maps $\Phi_{\mathcal{T}} : \mathcal{W}_{\widehat{S}} \rightarrow \mathcal{C}_{\mathcal{T}} \subseteq \mathbb{Z}_+^N$ and $\Phi_{\mathcal{T}'} : \mathcal{W}_{\widehat{S}} \rightarrow \mathcal{C}_{\mathcal{T}'} \subseteq \mathbb{Z}_+^N$, we have*

$$\mu_{\mathcal{T}', \mathcal{T}}(c) = \Phi_{\mathcal{T}'} \circ \Phi_{\mathcal{T}}^{-1}(c) \in \mathcal{C}_{\mathcal{T}'} \quad (c \in \mathcal{C}_{\mathcal{T}}),$$

where this equality is only defined up to permutation of the coordinates of $\mathcal{C}_{\mathcal{T}'} \subseteq \mathbb{Z}_+^N$.

Proof. This is essentially an immediate consequence of Theorem 4.3.

Indeed, consider a flip sequence (\dagger) of dotted triangulations \mathcal{T}_i , namely such that \mathcal{T}_{i+1} is related to \mathcal{T}_i by a single diagonal flip. Recall (§4.3.1) that the dotting of \mathcal{T}_i induces an inclusion $\mathcal{C}_{\mathcal{T}_i} \subseteq \mathbb{Z}_+^N$ of its KTGS cone, and recall (§4.3.2) that $\mu_{\mathcal{T}_{i+1}, \mathcal{T}_i} : \mathbb{Z}^N \rightarrow \mathbb{Z}^N$ is the corresponding (well-defined) flip mutation function.

By Theorem 4.3, for each $i = 0, 1, \dots, m-1$ we have

$$(\$) \quad \mu_{\mathcal{T}_{i+1}, \mathcal{T}_i}(c_i) = \Phi_{\mathcal{T}_{i+1}} \circ \Phi_{\mathcal{T}_i}^{-1}(c_i) \in \mathcal{C}_{\mathcal{T}_{i+1}} \quad (c_i \in \mathcal{C}_{\mathcal{T}_i}).$$

By iterating $(\$)$, for any $c_0 = c \in \mathcal{C}_{\mathcal{T}} = \mathcal{C}_{\mathcal{T}_0}$ we obtain

$$\begin{aligned} \mu_{\mathcal{T}_m, \mathcal{T}_0}(c) &= \mu_{\mathcal{T}_m, \mathcal{T}_{m-1}} \circ \dots \circ \mu_{\mathcal{T}_3, \mathcal{T}_2} \circ \mu_{\mathcal{T}_2, \mathcal{T}_1} \circ \mu_{\mathcal{T}_1, \mathcal{T}_0}(c_0) \\ &= \mu_{\mathcal{T}_m, \mathcal{T}_{m-1}} \circ \dots \circ \mu_{\mathcal{T}_3, \mathcal{T}_2} \circ \mu_{\mathcal{T}_2, \mathcal{T}_1} (\Phi_{\mathcal{T}_1} \circ \Phi_{\mathcal{T}_0}^{-1}(c_0)) \\ &= \mu_{\mathcal{T}_m, \mathcal{T}_{m-1}} \circ \dots \circ \mu_{\mathcal{T}_3, \mathcal{T}_2} (\Phi_{\mathcal{T}_2} \circ \Phi_{\mathcal{T}_1}^{-1} (\Phi_{\mathcal{T}_1} \circ \Phi_{\mathcal{T}_0}^{-1}(c_0))) \\ &= \mu_{\mathcal{T}_m, \mathcal{T}_{m-1}} (\Phi_{\mathcal{T}_{m-1}} \circ \Phi_{\mathcal{T}_0}^{-1}(c_0)) \\ &= \Phi_{\mathcal{T}_m} \circ \Phi_{\mathcal{T}_0}^{-1}(c) \in \mathcal{C}_{\mathcal{T}_m}. \end{aligned}$$

The result follows from the defining property of the function $\mu_{\mathcal{T}', \mathcal{T}}$ (Corollary 4.16 and Definition 4.17). ■

Conceptual Remark 4.20. Another way to express Theorem 4.19, common in the literature, is to say that the web tropical coordinates, determined by the maps $\{\Phi_{\mathcal{T}}\}_{\mathcal{T}}$, are equivariant with respect to the extended mapping class group of the marked surface \widehat{S} . Said another way, they form natural coordinates for the positive tropical integer PGL_3 -points $\mathcal{A}_{\mathrm{PGL}_3, \widehat{S}}^+(\mathbb{Z}^t)$, where a point in $\mathcal{A}_{\mathrm{PGL}_3, \widehat{S}}^+(\mathbb{Z}^t)$ is thought of concretely as a reduced web W in $\mathcal{W}_{\widehat{S}}$.

Application 4.21. Generalizing Fock-Goncharov's (bounded) SL_2 -laminations [FG06, §12], Kim [Kim20] considers the space $\widehat{\mathcal{W}}_{\widehat{S}}$ of (bounded) SL_3 -laminations (he denotes this space

by $\mathcal{A}_L(S, \mathbb{Z})$, which extends the space $\mathcal{W}_{\hat{S}}$ of reduced webs by allowing for negative integer weights around the peripheral loops and arcs. He also extends the web tropical coordinate map $\Phi_{\mathcal{T}} : \mathcal{W}_{\hat{S}} \rightarrow \mathcal{C}_{\mathcal{T}} \subseteq \mathbb{Z}_+^N$ of Theorem 3.9 to an injective map $\tilde{\Phi}_{\mathcal{T}} : \tilde{\mathcal{W}}_{\hat{S}} \rightarrow \mathbb{Z}^N$, and characterizes the image as an integer lattice defined by certain *balancedness* conditions; it turns out that these conditions are equivalent to the modulo 3 congruence conditions of Definition 3.2. That is, whereas the reduced webs $\mathcal{W}_{\hat{S}}$ correspond to solutions of both the modulo 3 congruence conditions and the Knutson-Tao inequalities, the SL_3 -laminations $\tilde{\mathcal{W}}_{\hat{S}} \supseteq \mathcal{W}_{\hat{S}}$ correspond to solutions of only the modulo 3 congruence conditions.

By [Kim20, Proposition 3.35], which generalizes Theorem 4.19, the lamination tropical coordinates $\{\tilde{\Phi}_{\mathcal{T}}\}_{\mathcal{T}}$ are also natural, thereby constituting an explicit model for the tropical integer PGL_3 -points $\mathcal{A}_{\mathrm{PGL}_3, \hat{S}}(\mathbb{Z}^t)$; compare Remark 4.20 and see also Remark 2.12(2).

Kim's proof of [Kim20, Proposition 3.35] uses Theorem 4.19. One way to think about upgrading the naturality statement from webs to laminations is in terms of the proof strategy of Theorem 4.3; see §4.2, in particular Remark 4.12. Indeed, since Lemma 4.9 works as well for corner arcs with integer coefficients, the proof of Theorem 4.3 works more generally for the laminations $\tilde{\mathcal{W}}_{\hat{S}}$.

Application 4.22. The same strategy used in the proof of Theorem 4.19 provides an alternative, geometric topological proof of Theorem 4.13 (see also Remark 4.18(1)), but only valid on the restricted cone domain $\mathcal{C}_{\mathcal{T}_0} \subseteq \mathbb{Z}_+^N \subseteq \mathbb{Q}^N$ (or, by applying Kim's result for SL_3 -laminations $\tilde{\mathcal{W}}_{\hat{S}}$ from Application 4.21, on the restricted lattice domain $\tilde{\Phi}_{\mathcal{T}}(\tilde{\mathcal{W}}_{\hat{S}}) \subseteq \mathbb{Z}^N \subseteq \mathbb{Q}^N$).

5. WEB FAMILIES AND FLIP EXAMPLES IN THE SQUARE

In §4, we proved the naturality of the web tropical coordinates without having to see what the new good position of a web in the square looks like after flipping the diagonal, which is topologically nontrivial. In this section, we give some examples of seeing the good position after the flip. This gives us another way to check the formulas of Theorem 4.3; see also Remark 4.1 at the beginning of §4. These topological developments (in particular, Proposition 5.1) will also be applied in §7 in order to study the structure of the Knutson-Tao-Goncharov-Shen cone of the triangulated square.

5.1. Web families.

Recall the notion of a web schematic; see §3.2.1 and Remark 3.6. Recall also Definitions 4.6 and 4.8, for the notions of corner webs $W = W_r \in \mathcal{R}$ and cornerless webs $W = W_c$.

Proposition 5.1. *We can write the reduced webs in the square as a union*

$$\mathcal{W}_{\square} = \bigcup_{i=1}^{42} \mathcal{W}_i$$

of 42 families $\mathcal{W}_i \subseteq \mathcal{W}_{\square}$ of reduced webs, where by definition $W \in \mathcal{W}_i$ if its cornerless part W_c can be represented by the i -th cornerless schematic, 9 of which are shown in Figure 16 below; in fact, up to rotation, reflection, and orientation-reversing symmetry (see the caption of Figure 16), every family \mathcal{W}_i falls into one of these 9 cases.

Proof. This is a direct combinatorial count, done by hand. We note that the number of possibilities is restricted by the topology of web good positions; see Observation 3.8. \blacksquare

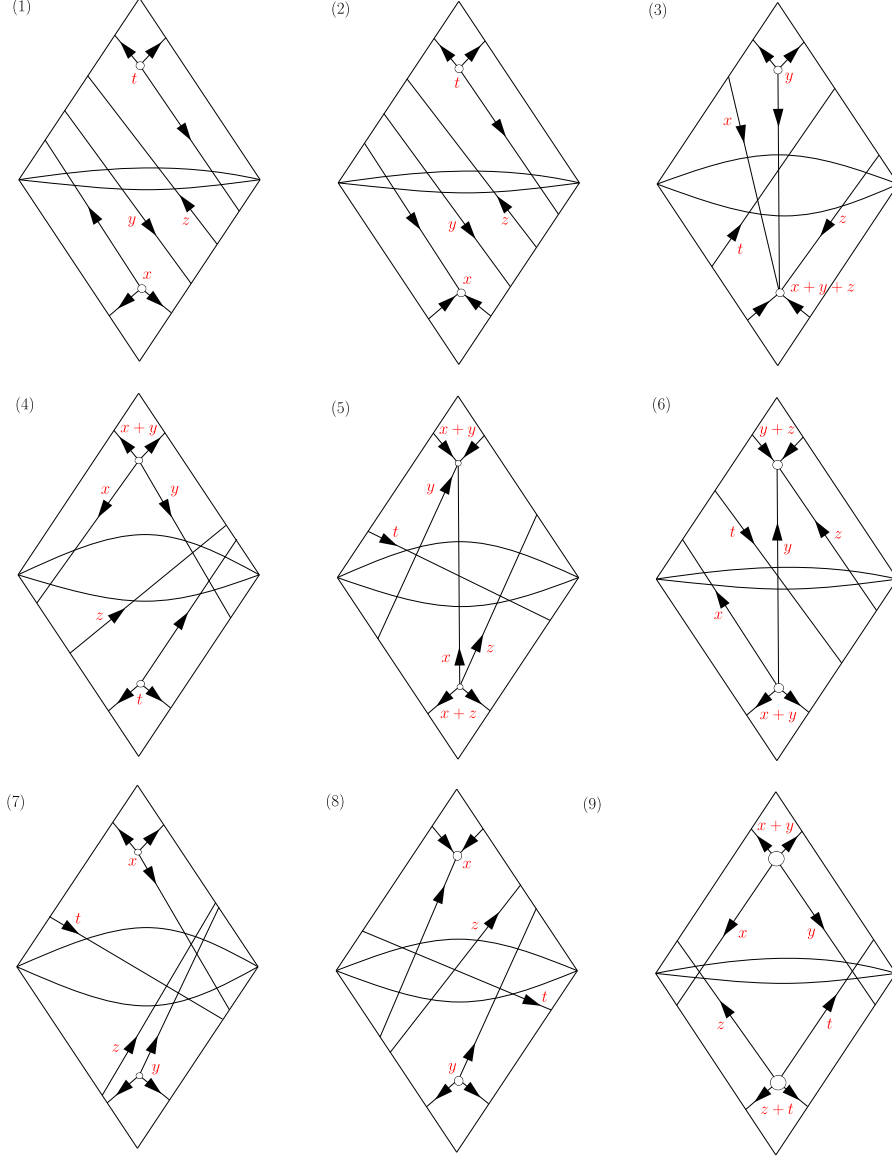


FIGURE 16. **Families (1)-(9).** Schematics for cornerless webs $W = W_c$. There are 9 reduced web families up to rotation, reflection, and orientation-reversing symmetry. (Note that orientation-reversing symmetry means simultaneously reversing the orientations of all components of the web.)

Notation 5.2. Completely arbitrarily, the index i_j for the family \mathcal{W}_{i_j} whose cornerless schematic is labeled (j) in Figure 16 ($j = 1, 2, \dots, 9$) is

$$i_1 = 29, \quad i_2 = 30, \quad i_3 = 42, \quad i_4 = 17, \quad i_5 = 5, \quad i_6 = 6, \quad i_7 = 2, \quad i_8 = 1, \quad i_9 = 33.$$

See also Remark 5.3 just below.

As we will see in §7, the family \mathcal{W}_i corresponds to the i -th sector shown in Figure 3.

Remark 5.3. If we define an equivalence relation on the 42 families \mathcal{W}_i by rotation, reflection, and orientation-reversing symmetry, then (using Notation 5.2 just above):

- (1) The symmetry class of \mathcal{W}_{i_1} has four members: $\mathcal{W}_{i_1} = \mathcal{W}_{29}; \mathcal{W}_{21}, \mathcal{W}_{24}, \mathcal{W}_{32}$.

- (2) The symmetry class of \mathcal{W}_{i_2} has four members: $\mathcal{W}_{i_2} = \mathcal{W}_{30}; \mathcal{W}_{23}, \mathcal{W}_{22}, \mathcal{W}_{31}$.
- (3) The symmetry class of \mathcal{W}_{i_3} has eight members: $\mathcal{W}_{i_3} = \mathcal{W}_{42}; \mathcal{W}_{36}, \mathcal{W}_{37}, \mathcal{W}_{38}, \mathcal{W}_{39}, \mathcal{W}_{40}, \mathcal{W}_{41}, \mathcal{W}_{35}$.
- (4) The symmetry class of \mathcal{W}_{i_4} has eight members: $\mathcal{W}_{i_4} = \mathcal{W}_{17}; \mathcal{W}_{18}, \mathcal{W}_{19}, \mathcal{W}_{20}, \mathcal{W}_{25}, \mathcal{W}_{26}, \mathcal{W}_{27}, \mathcal{W}_{28}$.
- (5) The symmetry class of \mathcal{W}_{i_5} has four members: $\mathcal{W}_{i_5} = \mathcal{W}_5; \mathcal{W}_8, \mathcal{W}_{13}, \mathcal{W}_{16}$.
- (6) The symmetry class of \mathcal{W}_{i_6} has four members: $\mathcal{W}_{i_6} = \mathcal{W}_6; \mathcal{W}_7, \mathcal{W}_{14}, \mathcal{W}_{15}$.
- (7) The symmetry class of \mathcal{W}_{i_7} has four members: $\mathcal{W}_{i_7} = \mathcal{W}_2; \mathcal{W}_3, \mathcal{W}_{10}, \mathcal{W}_{11}$.
- (8) The symmetry class of \mathcal{W}_{i_8} has four members: $\mathcal{W}_{i_8} = \mathcal{W}_1; \mathcal{W}_4, \mathcal{W}_9, \mathcal{W}_{12}$.
- (9) The symmetry class of \mathcal{W}_{i_9} has two members: $\mathcal{W}_{i_9} = \mathcal{W}_{33}; \mathcal{W}_{34}$.

We emphasize that each schematic in Figure 16 represents a subset $\mathcal{W}_i \subseteq \mathcal{W}_\square$ of reduced webs in the square. Note these subsets are not disjoint. Indeed, each intersection $\mathcal{W}_i \cap \mathcal{W}_j$ is at least “8-dimensional”, in an appropriate sense (see §7), since the set of corner webs \mathcal{R} is contained in each family \mathcal{W}_i . This intersection can contain more than just the corner webs. For instance, the intersection $\mathcal{W}_{29} \cap \mathcal{W}_{30}$, corresponding to schematics (1) and (2) in Figure 16, is “11-dimensional” (thus, in Figure 3, sectors 29 and 30 are separated by a wall); the last, 12-th, dimension comes from the source or sink labeled with the weight $x \in \mathbb{Z}_+$ in schematics (1) and (2). As another example, $\mathcal{W}_{29} \cap \mathcal{W}_{33}$, corresponding to schematics (1) and (9) in Figure 16, is “10-dimensional” (thus, in Figure 3, sectors 29 and 33 are not separated by a wall). In fact, each family \mathcal{W}_i is “12-dimensional” (intuitively, this is because the square has 12 Fock-Goncharov coordinates): 8 dimensions come from the corner part W_r , and 4 dimensions come from the cornerless part W_c . Correspondingly, each cornerless schematic in Figure 16 has four weights $x, y, z, t \in \mathbb{Z}_+$.

We remind (Remark 3.6) that, in schematics (1) and (2) in Figure 16, we could have reversed the orientations of the two arc components, without changing the class of the web in \mathcal{W}_\square . On the other hand, the orientation of the weight x component distinguishes schematic (1) from (2); note the caption of Figure 16. Also by Remark 3.6, the t and z strands in schematic (3), for example, do not cross in the upper triangle, for otherwise the web would have an external H-4-face (§3.2.1) on the boundary.

5.2. Flip examples.

The 9 symmetry classes of web families (see Figure 16 and Remark 5.3) fall into roughly three types. Let us study the flip a bit more intensively for one example of each type.

For the remainder of this section, let $W = W_c \in \mathcal{W}_\square$ be a cornerless web in the square and belonging to the family $\mathcal{W}_{i_j} \subseteq \mathcal{W}_\square$, where the value of i_j depends on which of the 9 cases we are considering ($j = 1, 2, \dots, 9$); see Notation 5.2.

Recall that \mathcal{T} (resp. \mathcal{T}') is the triangulation shown in the left hand side (resp. right hand side) of Figure 2. Consider the web tropical coordinate maps $\Phi_{\mathcal{T}} : \mathcal{W}_\square \rightarrow \mathcal{C}_{\mathcal{T}}$ and $\Phi_{\mathcal{T}'} : \mathcal{W}_\square \rightarrow \mathcal{C}_{\mathcal{T}'}$ (see §3). Denote $c = \Phi_{\mathcal{T}}(W) \in \mathcal{C}_{\mathcal{T}} \subseteq \mathbb{Z}_+^{12}$ by

$$c = (c_j)_{j=1,2,\dots,12} = (x_1, x_2, x_3, x_4, x_5, x_6, x_7, x_8, y_1, y_2, y_3, y_4),$$

and $c' = \Phi_{\mathcal{T}'} \circ \Phi_{\mathcal{T}}^{-1}(c) \in \mathcal{C}_{\mathcal{T}'} \subseteq \mathbb{Z}_+^{12}$ by

$$c' = (c'_j)_{j=1,2,\dots,12} = (x'_1, x'_2, x'_3, x'_4, x'_5, x'_6, x'_7, x'_8, z_1, z_2, z_3, z_4);$$

compare Definition 4.2 and Figure 2. We know right away that $x_i = x'_i$ for $i = 1, 2, \dots, 8$.

Our goal is to check that Equations (2), (3), (4), (5) are satisfied, by presenting the explicit good position of the family \mathcal{W}_{i_j} after the flip, allowing us to calculate the coordinates directly. We do this in the three example cases $j = 1, 3, 7$.

Recall in particular $x, y, z, t \in \mathbb{Z}_+$ in Figure 16.

Family (1). The simplest cases are given by schematics (1) and (2) of Figure 16. We verify case (1) here. The other case is similar. We compute the c_j 's and c'_j 's via Figure 11 below; see also §3.2.2.

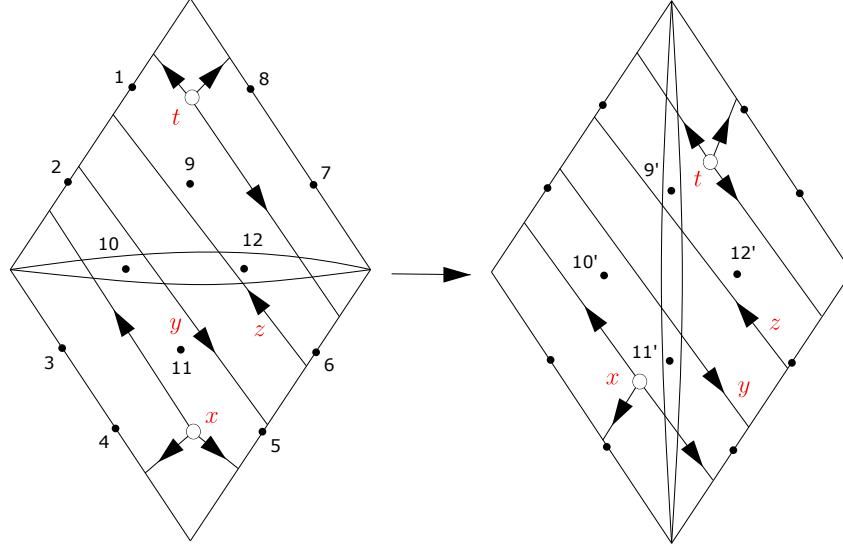


FIGURE 17. Family (1).

Notice in this case it is obvious that the web on the right hand side of Figure 17 is in good position with respect to the flipped triangulation.

Left hand side of Figure 17, coordinates c_j ($j = 1, 2, \dots, 12$):

(1)	$2x + y + 2z + 2t$	(2)	$x + 2y + z + t$
(3)	$2x$	(4)	x
(5)	$2x + 2y + z + 2t$	(6)	$x + y + 2z + t$
(7)	$2t$	(8)	t
(9)	$2x + y + 2z + 3t$	(10)	$x + 2y + z + 2t$
(11)	$3x + 2y + z + 2t$	(12)	$2x + y + 2z + t$

Right hand side of Figure 17, coordinates c'_j ($j = 9, \dots, 12$):

(9')	$x + y + 2z + 2t$	(10')	$3x + 2y + z + t$
(11')	$2x + 2y + z + t$	(12')	$x + y + 2z + 3t$

The following computations verify Equations (2), (3), (4), (5) in this case.

$$\text{Eq. (2): } \max\{(x + 2y + z + t) + (3x + 2y + z + 2t), (2x + y + 2z + 3t) + 2x\} - (x + 2y + z + 2t) = \max\{4x + 4y + 2z + 3t, 4x + y + 2z + 3t\} - (x + 2y + z + 2t) = 3x + 2y + z + t.$$

$$\text{Eq. (3): } \max\{(2x + y + 2z + 3t) + (x + y + 2z + t), 2t + (3x + 2y + z + 2t)\} - (2x + y + 2z + t) = \max\{3x + 2y + 4z + 4t, 3x + 2y + z + 4t\} - (2x + y + 2z + t) = x + y + 2z + 3t.$$

$$\text{Eq. (4): } \max\{(2x + y + 2z + 2t) + (x + y + 2z + 3t), t + (3x + 2y + z + t)\} - (2x + y + 2z + 3t) = \max\{3x + 2y + 4z + 5t, 3x + 2y + z + 2t\} - (2x + y + 2z + 3t) = x + y + 2z + 2t.$$

$$\text{Eq. (5): } \max\{(3x + 2y + z + t) + (2x + 2y + z + 2t), (x + y + 2z + 3t) + x\} - (3x + 2y + z + 2t) = \max\{5x + 4y + 2z + 3t, 2x + y + 2z + 3t\} - (3x + 2y + z + 2t) = 2x + 2y + z + t.$$

Family (3). The next simplest cases are given by schematics (3), (4), (5), (6), and (9) of Figure 16. We verify case (3) here. The other four cases are similar. We compute the c_j 's and c'_j 's via Figure 11 below; see also §3.2.2.

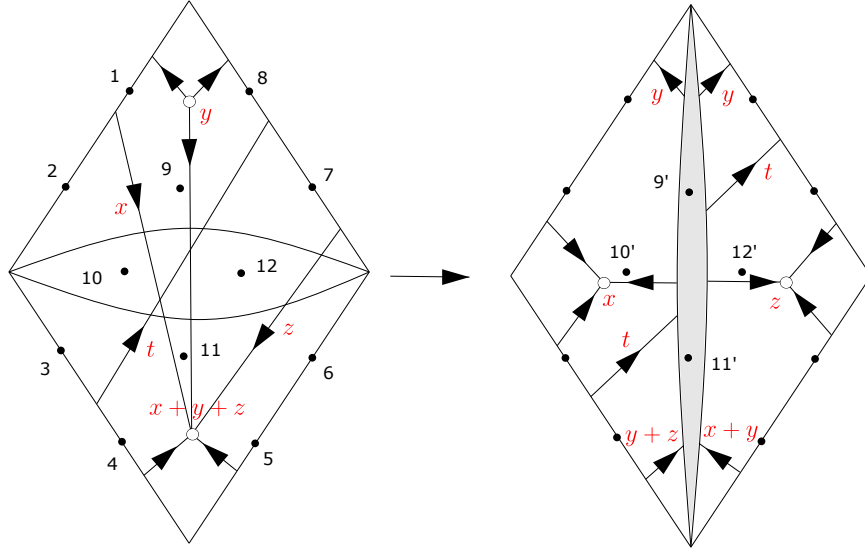


FIGURE 18. Family (3).

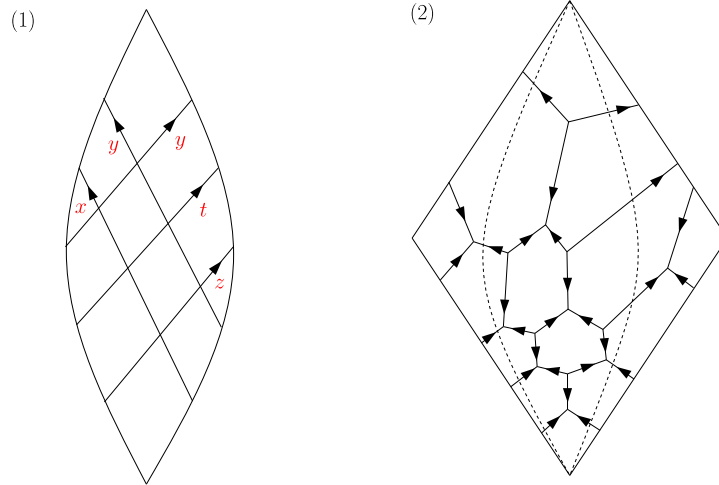


FIGURE 19. (1) Bigon schematic after the flip. (2) An example of the web in good position after the flip: $x = y = z = t = 1$.

Unlike in the previous example, it is less obvious that the schematic appearing on the right hand side of Figure 18 faithfully displays how the good position looks after the flip. That this is indeed the case is a bit subtle topologically, however can be verified by an explicit procedure that draws the desired flipped bigon on top of the starting web as represented by the left hand side of Figure 18. We demonstrate this bigon drawing procedure in Figure 24 in Appendix A at the end of this article.

The schematic diagram of the web in good position restricted to the flipped bigon in the right hand side of Figure 18 is shown in Figure 19(1). It is an enjoyable exercise to check that this bigon schematic agrees with the web example schematically shown in Figure 24.

Another guiding example showing the web in good position after the flip (without using schematics), is provided in Figure 19(2).

Left hand side of Figure 18, coordinates c_j ($j = 1, 2, \dots, 12$):

(1) $x + 2y$	(2) $2x + y$
(3) $x + y + z + t$	(4) $2x + 2y + 2z + 2t$
(5) $x + y + z$	(6) $2x + 2y + 2z$
(7) $2y + z + 2t$	(8) $y + 2z + t$
(9) $x + 3y + 2z + t$	(10) $2x + 2y + 2z + t$
(11) $3x + 3y + 3z + 2t$	(12) $x + y + z + 2t$.

Right hand side of Figure 18, coordinates c'_j ($j = 9, \dots, 12$):

(9') $2x + 3y + z + t$	(10') $3x + 2y + z + t$
(11') $x + 3y + 2z + 2t$	(12') $2x + 4y + 3z + 2t$.

The following computations verify Equations (2), (3), (4), (5) in this case.

Eq. (2): $\max\{(2x+y)+(3x+3y+3z+2t), (x+3y+2z+t)+(x+y+z+t)\} - (2x+2y+2z+t) = \max\{5x+4y+3z+2t, 2x+4y+3z+2t\} - (2x+2y+2z+t) = 3x+2y+z+t$.

Eq. (3): $\max\{(x+3y+2z+t)+(2x+2y+2z), (2y+z+2t)+(3x+3y+3z+2t)\} - (x+y+z+2t) = \max\{3x+5y+4z+t, 3x+5y+4z+4t\} - (x+y+z+2t) = 2x+4y+3z+2t$.

Eq. (4): $\max\{(x+2y)+(2x+4y+3z+2t), (y+2z+t)+(3x+2y+z+t)\} - (x+3y+2z+t) = \max\{3x+6y+3z+2t, 3x+3y+3z+2t\} - (x+3y+2z+t) = 2x+3y+z+t$.

Eq. (5): $\max\{(3x+2y+z+t)+(x+y+z), (2x+4y+3z+2t)+(2x+2y+2z+2t)\} - (3x+3y+3z+2t) = \max\{4x+3y+2z+t, 4x+6y+5z+4t\} - (3x+3y+3z+2t) = x+3y+2z+2t$.

Family (7). The last group of cases are given by schematics (7) and (8) of Figure 16. We verify case (7) here. The other case is similar. We compute the c_j 's and c'_j 's via Figure 11 below; see also §3.2.2.

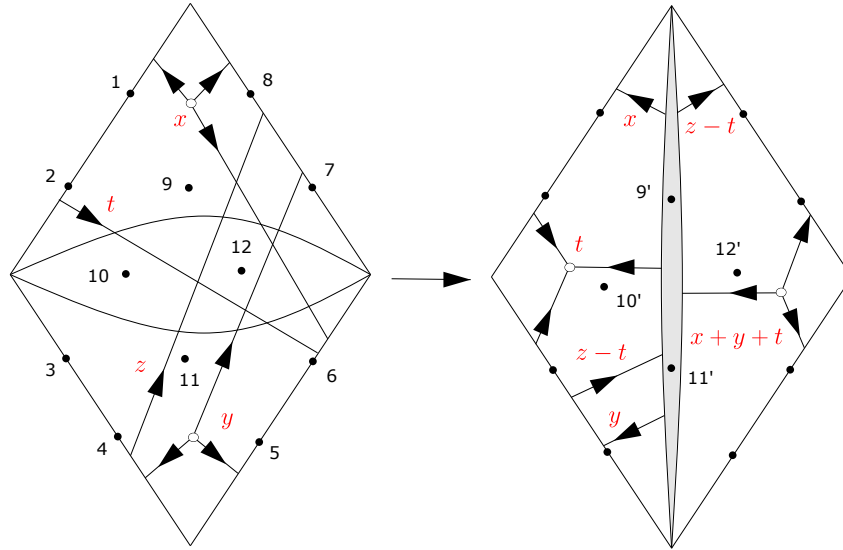


FIGURE 20. Family (7), shown when $z \geq t$.

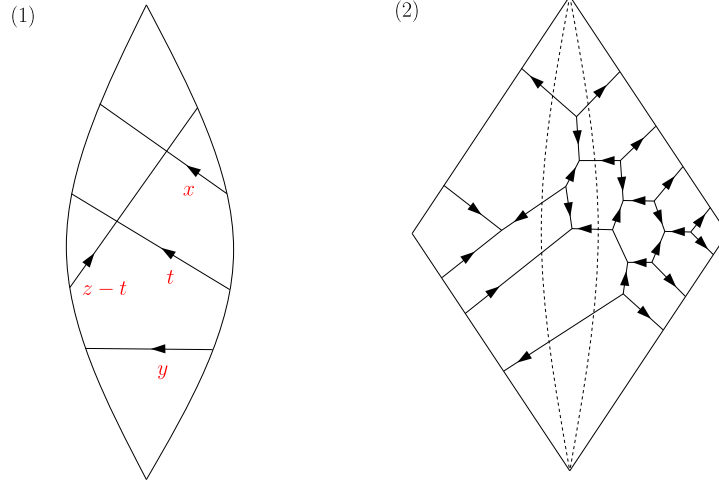


FIGURE 21. (1) Bigon schematic after the flip. (2) An example of the web in good position after the flip: $x = y = t = 1$ and $z = 2$.

Note that, unlike for the previous two examples, in this case there are two possibilities: $z \geq t$ and $z \leq t$. In Figure 20, we display the case when $z \geq t$ (the $z \leq t$ case is similar).

As for the previous example, it is not immediately obvious that the schematic appearing on the right hand side of Figure 20 displays the correct good position. We again verify this by explicitly drawing the flipped bigon, as shown in Figure 25 in Appendix A at the end of this article.

The schematic diagram of the web in good position restricted to the flipped bigon in the right hand side of Figure 20 is shown in Figure 21(1). It is an enjoyable exercise to check that this bigon schematic agrees with the web example schematically shown in Figure 25.

Another guiding example showing the web in good position after the flip (without using schematics), is provided in Figure 21(2).

We demonstrate the calculation when $z \geq t$ (the case $z \leq t$ is similar).

Left hand side of Figure 20, coordinates c_j ($j = 1, 2, \dots, 12$):

<p>(1) $2x + t$</p> <p>(3) $2y + z$</p> <p>(5) $2x + 2y + 2t$</p> <p>(7) $2x + 2y + 2z$</p> <p>(9) $3x + y + z + t$</p> <p>(11) $2x + 3y + 2z + 2t$</p>	<p>(2) $x + 2t$</p> <p>(4) $y + 2z$</p> <p>(6) $x + y + t$</p> <p>(8) $x + y + z$</p> <p>(10) $2x + y + z + 2t$</p> <p>(12) $x + 2y + 2z + t$</p>
---	---

Right hand side of Figure 20, coordinates c'_j ($j = 9, \dots, 12$):

<p>(9') $2x + 2y + z + t$</p> <p>(11') $x + y + 2z - t$</p>	<p>(10') $x + 2y + z + 2t$</p> <p>(12') $3x + 3y + 2z + t$</p>
---	--

The following computations verify Equations (2), (3), (4), (5) in this case. Note that the last equation uses the assumption $z \geq t$.

Eq. (2): $\max\{(x + 2t) + (2x + 3y + 2z + 2t), (3x + y + z + t) + (2y + z)\} - (2x + y + z + 2t) =$
 $\max\{3x + 3y + 2z + 4t, 3x + 3y + 2z + t\} - (2x + y + z + 2t) = x + 2y + z + 2t.$

$$\begin{aligned}
 \text{Eq. (3): } & \max\{(3x+y+z+t)+(x+y+t), (2x+2y+2z)+(2x+3y+2z+2t)\} - (x+2y+2z+t) = \\
 & \max\{4x+2y+z+2t, 4x+5y+4z+2t\} - (x+2y+2z+t) = 3x+3y+2z+t. \\
 \text{Eq. (4): } & \max\{(2x+t)+(3x+3y+2z+t), (x+y+z)+(x+2y+z+2t)\} - (3x+y+z+t) = \\
 & \max\{5x+3y+2z+2t, 2x+3y+2z+2t\} - (3x+y+z+t) = 2x+2y+z+t. \\
 \text{Eq. (5): } & \max\{(x+2y+z+2t)+(2x+2y+2t), (3x+3y+2z+t)+(y+2z)\} - (2x+3y+2z+2t) = \\
 & \max\{3x+4y+z+4t, 3x+4y+4z+t\} - (2x+3y+2z+2t) = (3x+4y+4z+t) - \\
 & (2x+3y+2z+2t) = x+y+2z-t.
 \end{aligned}$$

6. KTGS CONE FOR THE SQUARE: HILBERT BASIS

In the remaining two sections, we study the structure of the Knutson-Tao-Goncharov-Shen cone $\mathcal{C}_{\mathcal{T}} \subseteq \mathbb{Z}_+^N$ associated to an ideal triangulation \mathcal{T} of a marked surface \widehat{S} (Definition 3.2 and Proposition 3.3) when $\widehat{S} = \square$ is an ideal square. In this case, an ideal triangulation \mathcal{T} is simply a choice of a diagonal of \square .

6.1. Positive integer cones and Hilbert bases.

Recall from §2.1 that \mathbb{Z}_+ denotes the set of nonnegative integers. Recall also from §3.1:

Definition 6.1. A subset $\mathcal{M} \subseteq \mathbb{Z}^k$ (or $\subseteq \mathbb{R}^k$) is a *submonoid* if \mathcal{M} is closed under addition and contains 0.

Definition 6.2. Let $\mathcal{M} \subseteq \mathbb{Z}^k$ (or $\subseteq \mathbb{R}^k$) be a submonoid. An element $x \in \mathcal{M}$ is *irreducible* if x is nonzero, and x cannot be written as the sum of two nonzero elements of \mathcal{M} .

We denote by $\mathcal{H} \subseteq \mathcal{M}$ the set of irreducible elements of \mathcal{M} .

A subset $\mathcal{D} \subseteq \mathcal{M}$ is:

- \mathbb{Z}_+ -*spanning* if every $x \in \mathcal{M}$ is of the form $x = \lambda_1 x_1 + \lambda_2 x_2 + \cdots + \lambda_m x_m$ for some $x_i \in \mathcal{D}$ and $\lambda_i \in \mathbb{Z}_+$, in which case we write $x \in \text{span}_{\mathbb{Z}_+}(\mathcal{D})$;
- a *minimum* \mathbb{Z}_+ -spanning set if, in addition, for every \mathbb{Z}_+ -spanning set $\mathcal{D}' \subseteq \mathcal{M}$ we have $\mathcal{D} \subseteq \mathcal{D}'$.

Note that a minimum \mathbb{Z}_+ -spanning set is unique if it exists.

Recall (Definition 3.1) that a positive integer cone $\mathcal{C} \subseteq \mathbb{Z}_+^k$ is a submonoid of \mathbb{Z}_+^k .

Proposition 6.3. *The subset $\mathcal{H} \subseteq \mathcal{C} \subseteq \mathbb{Z}_+^k$ of irreducible elements of a positive integer cone $\mathcal{C} \subseteq \mathbb{Z}_+^k$ is the unique minimum \mathbb{Z}_+ -spanning subset of \mathcal{C} .*

Proof. If x is irreducible and is in the \mathbb{Z}_+ -span of x'_1, x'_2, \dots, x'_m for $x'_i \in \mathcal{C}$, then $x = x'_{i_0}$ for some i_0 by the irreducibility property. Thus \mathcal{H} is contained in any \mathbb{Z}_+ -spanning set \mathcal{D} .

It remains to show that every element x of \mathcal{C} is in the \mathbb{Z}_+ -span of \mathcal{H} . We argue by induction on the sum $\Sigma(x) \in \mathbb{Z}_+$ of the coordinates of $x \in \mathbb{Z}_+^k$; that is, on the quantity $\Sigma(x) := \sum_{i=1}^k n_i$ where $x = (n_1, n_2, \dots, n_k) \in \mathcal{C} \subseteq \mathbb{Z}_+^k$. This is true if $x = 0$, where $\Sigma(x) = 0$. So assume that x is nonzero, and that x' is in the \mathbb{Z}_+ -span of \mathcal{H} whenever $\Sigma(x') < \Sigma(x)$. If x is irreducible, we are done. Else, $x = y + z$ with both $y, z \in \mathcal{C} \subseteq \mathbb{Z}_+^k$ nonzero. So $\Sigma(y) < \Sigma(x)$ and $\Sigma(z) < \Sigma(x)$. Thus, y and z are in the \mathbb{Z}_+ -span of \mathcal{H} by hypothesis, so x is as well. ■

Remark 6.4. Note that the \mathbb{Z}_+ -spanning property of \mathcal{H} in Proposition 6.3 is not true if we had only assumed that $\mathcal{C} = \mathcal{M}$ is a submonoid of \mathbb{Z}^k . For example, the submonoid $\mathcal{M} = \mathbb{Z}^k$ has no irreducible elements.

In the following sections, we will take $\mathcal{C} = \mathcal{C}_{\mathcal{T}} \subseteq \mathbb{Z}_+^N$ to be the KTGS positive integer cone associated to an ideal triangulation \mathcal{T} of a marked surface \widehat{S} . It seems to be a significant

property that the KTGS cone $\mathcal{C}_{\mathcal{T}}$ comes naturally as a subset of a single orthant of \mathbb{Z}^N ; see Proposition 3.3 and Remarks 2.12(1), 3.4.

Definition 6.5. Let $\mathcal{H} \subseteq \mathcal{C} \subseteq \mathbb{Z}_+^k$ be as in Proposition 6.3. If \mathcal{H} is a finite set, then it is called the *Hilbert basis* of the positive integer cone $\mathcal{C} \subseteq \mathbb{Z}_+^k$.

Example 6.6.

- (1) The standard basis of \mathbb{Z}^k is the Hilbert basis \mathcal{H} of the positive integer cone $\mathcal{C} = \mathbb{Z}_+^k$.
- (2) By Proposition 6.3, the set $\mathcal{H} = \{(1, 0), (1, 1), (0, 2)\}$ is the Hilbert basis of the positive integer cone $\mathcal{C} = \mathbb{Z}_+(1, 0) + \mathbb{Z}_+(1, 1) + \mathbb{Z}_+(0, 2) \subseteq \mathbb{Z}_+^2$.
- (3) Similarly, again by Proposition 6.3, the set $\mathcal{H} = \{(0, 1, 0), (1, 1, 0), (1, 0, 1), (0, 1, 1)\}$ is the Hilbert basis of the positive integer cone $\mathcal{C} = \text{span}_{\mathbb{Z}_+}(\mathcal{H}) \subseteq \mathbb{Z}_+^3$.

Remark 6.7. Hilbert bases [Hil90, Sch81] are important objects in linear algebra and linear programming, and are defined for more general cones than what we have discussed here. Some of our terminology might be non-standard, adapted for the purposes of this paper.

6.2. Hilbert basis of the KTGS cone for the triangle and the square.

6.2.1. Hilbert basis for the triangle.

We begin by recalling from [DS20, §5] the case of a single ideal triangle $\widehat{S} = \mathcal{T} = \Delta$. Let $\mathcal{C}_{\Delta} \subseteq \mathbb{Z}_+^7$ be the corresponding KTGS positive integer cone.

Recall the eight “irreducible” webs $L_a, R_a, L_b, R_b, L_c, R_c, T_{in}, T_{out}$ in \mathcal{W}_{Δ} defined in §3.2.2. For each such web W^H , its 7 tropical coordinates $\Phi_{\Delta}(W^H) \in \mathcal{C}_{\Delta} \subseteq \mathbb{Z}_+^7$ are provided in Figure 11.

Proposition 6.8. *The 8-element subset*

$$\mathcal{H}_{\Delta} = \{\Phi_{\Delta}(W^H); \quad W^H = L_a, R_a, L_b, R_b, L_c, R_c, T_{in}, T_{out}\} \subseteq \mathcal{C}_{\Delta}$$

is the Hilbert basis of the KTGS cone $\mathcal{C}_{\Delta} \subseteq \mathbb{Z}_+^7$ for the triangle.

Proof. This is a consequence [DS20, Proposition 45] and its proof.

Indeed, we need to show that \mathcal{H}_{Δ} is the set of irreducible elements. To start, any such $\Phi_{\Delta}(W^H)$ is nonzero. By the last sentence of [DS20, Proposition 45], we have that \mathcal{H}_{Δ} is a \mathbb{Z}_+ -spanning set for \mathcal{C}_{Δ} . One checks by hand that no single element of \mathcal{H}_{Δ} can be written as a \mathbb{Z}_+ -linear combination of other elements of \mathcal{H}_{Δ} . (This last property is particularly clear when viewed in the isomorphic cone $\mathcal{C} \subseteq \mathbb{Z}_+^6 \times \mathbb{Z} \subseteq \mathbb{Z}^7$, namely the image of \mathcal{C}_{Δ} under a certain linear isomorphism $\mathbb{R}^7 \rightarrow \mathbb{R}^7$ of geometric origin; for details, see the proof of [DS20, Proposition 45]. In §7, we generalize this linear isomorphism to the square case.)

The result follows by Proposition 6.3. ■

Remark 6.9. As a word of caution, [DS20, Proposition 45] does not imply that an element of \mathcal{C}_{Δ} has a unique decomposition as a sum of Hilbert basis elements. Indeed, in \mathcal{C}_{Δ} , we have the relation $\Phi_{\Delta}(T_{in}) + \Phi_{\Delta}(T_{out}) = \Phi_{\Delta}(L_a) + \Phi_{\Delta}(L_b) + \Phi_{\Delta}(L_c)$. See also §6.3 below.

It is also not true that if $\Phi_{\Delta}(W') \leq \Phi_{\Delta}(W) \in \mathcal{C}_{\Delta} \subseteq \mathbb{Z}_+^7$, in the sense that the inequality holds for each coordinate, then W' is topologically “contained in” W . Indeed, in the above example, we have $\Phi_{\Delta}(T_{in})$ or $\Phi_{\Delta}(T_{out}) \leq \Phi_{\Delta}(L_a) + \Phi_{\Delta}(L_b) + \Phi_{\Delta}(L_c)$ in \mathcal{C}_{Δ} . An even simpler example is $\Phi_{\Delta}(L_a) \leq \Phi_{\Delta}(R_b) + \Phi_{\Delta}(R_c)$.

6.2.2. Hilbert basis for the square.

We turn to the square \square , which for the rest of this section is equipped with an ideal triangulation \mathcal{T} , namely a choice of diagonal of \square .

Recall the 8 oriented corner arcs in the square \square (Definition 4.6); these are the “irreducible” webs (1)-(8) in \mathcal{W}_\square depicted in Figure 22 (part 1). The triangulation \mathcal{T} determines 14 more “irreducible” webs in \square , namely the webs (9)-(22) in \mathcal{W}_\square depicted in Figure 22 (part 2). The bracket notation used in Figure 22 (part 2) is explained in the caption of the figure. In sum, let us denote these 22 “irreducible” webs by $W_i^H \in \mathcal{W}_\square$ for $i = 1, 2, \dots, 22$.

Let $\Phi_{\mathcal{T}} : \mathcal{W}_\square \rightarrow \mathcal{C}_{\mathcal{T}}$ be the associated web tropical coordinate map. For each web W_i^H , its 12 tropical coordinates $\Phi_{\mathcal{T}}(W_i^H) \in \mathcal{C}_{\mathcal{T}} \subseteq \mathbb{Z}_+^{12}$ are also provided in Figure 22 (part 2).

Theorem 6.10. *For the webs $\{W_i^H\}_{i=1,2,\dots,22}$ in \mathcal{W}_\square displayed in Figure 22, the subset*

$$\mathcal{H}_{(\square, \mathcal{T})} = \{\Phi_{\mathcal{T}}(W_i^H); \quad i = 1, 2, \dots, 22\} \subseteq \mathcal{C}_{\mathcal{T}}$$

is the Hilbert basis of the KTGS cone $\mathcal{C}_{\mathcal{T}} \subseteq \mathbb{Z}_+^{12}$ for the triangulated square (\square, \mathcal{T}) .

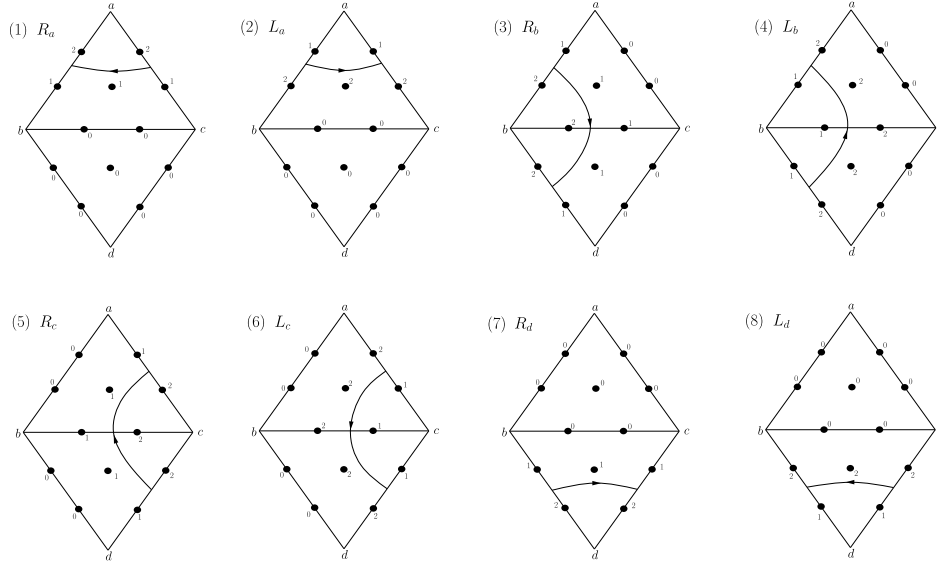


FIGURE 22. (Part 1 of 2; see below.) The first 8 elements of the 22 element Hilbert basis for the KTGS cone $\mathcal{C}_{\mathcal{T}}$ of the triangulated square (\square, \mathcal{T}) , pictured via the corresponding “irreducible” reduced webs $\{W_i^H\}_{i=1,2,\dots,22}$.

Remark 6.11. Note that if the other triangulation \mathcal{T}' of \square had been chosen, then only the webs W_1^H, \dots, W_8^H and $W_{19}^H, \dots, W_{22}^H$ would appear among the 22 “irreducible” webs W_i^H corresponding to \mathcal{T}' . In other words, the set of webs corresponding to the Hilbert basis $\mathcal{H}_{(\square, \mathcal{T})}$ of $\mathcal{C}_{\mathcal{T}}$ depends on which triangulation \mathcal{T} of the square is chosen.

We will need a little bit of preparation before proving the theorem.

Let Δ and Δ' be the two triangles appearing in the split triangulation \mathcal{T} of \square (§3.2.1). Say, Δ is the top triangle on the left hand side of Figure 2, and Δ' is the bottom triangle. In particular, neither Δ nor Δ' include the intermediate bigon. If W is a reduced web in \square in good position with respect to the split ideal triangulation \mathcal{T} , then the restrictions $W|_\Delta$ and $W|_{\Delta'}$ are in good position in their respective triangles (by definition of good position of W

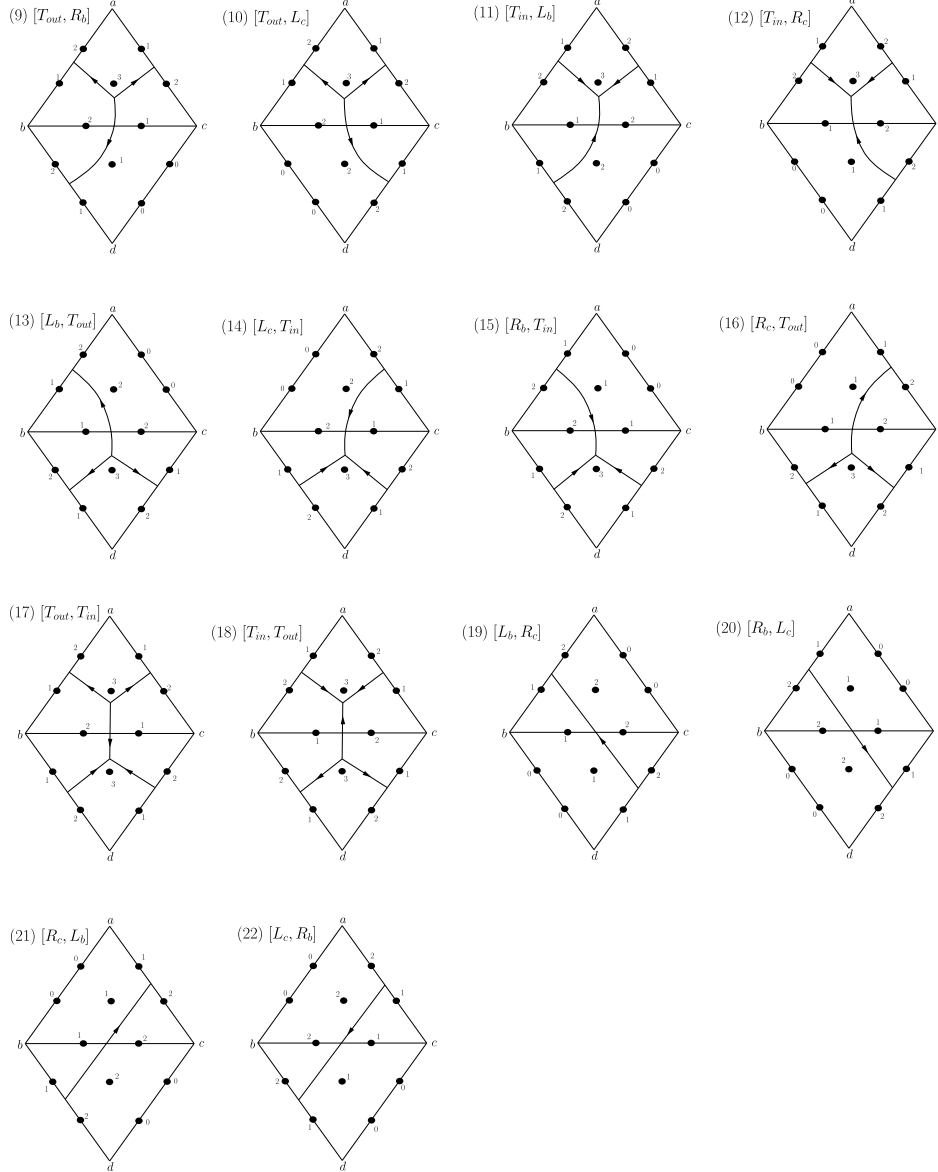


FIGURE 22. (Part 2 of 2; see above.) The last 14 elements of the 22 element Hilbert basis for the KTGS cone $\mathcal{C}_{\mathcal{T}}$ of the triangulated square (\square, \mathcal{T}) , pictured via the corresponding “irreducible” reduced webs $\{W_i^H\}_{i=1,2,\dots,22}$. The square bracket is a purely notational device for webs (9)-(22); the first entry of $[\cdot, \cdot]$ corresponds to the top triangle, and the second entry to the bottom triangle.

with respect to \mathcal{T}). At the level of coordinates, this induces two projections $\pi_{\Delta} : \mathcal{C}_{\mathcal{T}} \rightarrow \mathcal{C}_{\Delta}$ and $\pi_{\Delta'} : \mathcal{C}_{\mathcal{T}} \rightarrow \mathcal{C}_{\Delta'}$ defined by $\pi_{\Delta}(\Phi_{\mathcal{T}}(W)) = \Phi_{\Delta}(W|_{\Delta})$ and $\pi_{\Delta'}(\Phi_{\mathcal{T}}(W)) = \Phi_{\Delta'}(W|_{\Delta'})$. Compare Figure 12.

Lemma 6.12. *For a reduced web W in \mathcal{W}_{\square} , suppose its image $\Phi_{\mathcal{T}}(W)$ is an irreducible element of $\mathcal{C}_{\mathcal{T}}$. Then, the projections $\pi_{\Delta}(\Phi_{\mathcal{T}}(W))$ and $\pi_{\Delta'}(\Phi_{\mathcal{T}}(W))$ are, respectively, in the Hilbert bases \mathcal{H}_{Δ} and $\mathcal{H}_{\Delta'}$ of the cones \mathcal{C}_{Δ} and $\mathcal{C}_{\Delta'}$.*

Consequently, the set of irreducible elements of $\mathcal{C}_{\mathcal{T}}$ is finite (thus forming a Hilbert basis) and is a subset of $\mathcal{H}_{(\square, \mathcal{T})}$, as defined in Theorem 6.10.

Proof. Assuming the first statement, the second statement immediately follows by Definition 6.5, Proposition 6.8, and the construction of the 22 element set $\mathcal{H}_{(\square, \mathcal{T})} \subseteq \mathcal{C}_{\mathcal{T}}$.

To establish the first statement, assume W is in good position with respect to \mathcal{T} . It suffices to show that if $\pi_{\Delta}(\Phi_{\mathcal{T}}(W)) = \Phi_{\Delta}(W|_{\Delta}) \in \mathcal{C}_{\Delta}$ is reducible, then $\Phi_{\mathcal{T}}(W) \in \mathcal{C}_{\mathcal{T}}$ is reducible. So assume that there are nonempty reduced webs A_1 and A_2 in \mathcal{W}_{Δ} such that $\Phi_{\Delta}(W|_{\Delta}) = \Phi_{\Delta}(A_1) + \Phi_{\Delta}(A_2)$ in \mathcal{C}_{Δ} . (At this point, one should be mindful of Remark 6.9.) We explicitly construct nonempty reduced webs W_1 and W_2 in \mathcal{W}_{\square} such that

$$(*) \quad \Phi_{\mathcal{T}}(W) = \Phi_{\mathcal{T}}(W_1) + \Phi_{\mathcal{T}}(W_2) \in \mathcal{C}_{\mathcal{T}}.$$

Let E (resp. E') denote the bigon edge intersecting Δ (resp. Δ'). Let n and m (resp. n_i and m_i for $i = 1, 2$) be, respectively, the number of out- and in-strand-ends of $W|_{\Delta}$ (resp. A_i) on E ; similarly, let n' and m' be, respectively, the number of out- and in-strand-ends of $W|_{\Delta'}$ on E' . Note $n' = m$ and $m' = n$.

By [DS20, Definition 35, property (2)], which says that the two edge coordinates on E uniquely determine the number of out- and in-strand-ends on E (this is a simple linear algebra calculation), we must have $n = n_1 + n_2$ and $m = m_1 + m_2$. We gather $n' = m_1 + m_2$ and $m' = n_1 + n_2$.

Now, for each $i = 1, 2$, arbitrarily choose m_i out-strand-ends and n_i in-strand-ends of $W|_{\Delta'}$ on E' , which we call i -strand-ends of $W|_{\Delta'}$. Let us say that a component C' of $W|_{\Delta'}$ is A_i -connecting if at least one of its strand-ends on E' is an i -strand-end; note that (1) a corner arc C' is A_i -connecting for at most one i (possibly none, when C' is on the corner opposite E'), and (2) a honeycomb C' is A_i -connecting for at least one i , and may be both A_1 - and A_2 -connecting.

Let $h' \in \mathbb{Z}_+$ be the size of the honeycomb H' of $W|_{\Delta'}$, and let $h'^{(i)}$ be the number of i -strand-ends of H' ; note that $h' = h'^{(1)} + h'^{(2)}$. For each $i = 1, 2$, define A'_i to be the reduced web in $\mathcal{W}_{\Delta'}$ consisting of the A_i -connecting corner arc components C' of $W|_{\Delta'}$ together with a honeycomb of size $h'^{(i)}$ oriented as H' (and we can include the non- A_i -connecting components C' into A'_i , say); note in particular that $\Phi_{\Delta'}(W|_{\Delta'}) = \Phi_{\Delta'}(A'_1) + \Phi_{\Delta'}(A'_2) \in \mathcal{C}_{\Delta'}$.

Lastly, for each $i = 1, 2$, define W_i in \mathcal{W}_{\square} to be the unique nonempty reduced web in the square obtained from the triangle webs $A_i \in \mathcal{W}_{\Delta}$ and $A'_i \in \mathcal{W}_{\Delta'}$ by gluing across the bigon in the usual way (as in Figure 8). (Technically, it is the class of W_i in \mathcal{W}_{\square} that is unique, and W_i is determined up to corner arc permutations). By construction, $(*)$ holds. ■

Proof of Theorem 6.10.

By Lemma 6.12, it remains to show that each element of $\mathcal{H}_{(\square, \mathcal{T})}$ is irreducible in $\mathcal{C}_{\mathcal{T}}$. This property can be checked by hand. (The irreducibility becomes clearer in light of the linear map $\theta_{\mathcal{T}} : \mathbb{R}^{12} \rightarrow \mathbb{R}^{18}$ of §6.2.3 below, where the image $\theta_{\mathcal{T}}(\mathcal{H}_{(\square, \mathcal{T})}) \subseteq \mathbb{Z}_+^{18}$ is written explicitly). ■

6.2.3. Two linear isomorphisms: first isomorphism $\theta_{\mathcal{T}}$ by rhombus numbers.

Recall (Definition 3.2) that the KTGS cone $\mathcal{C}_{\mathcal{T}}$ for any triangulated marked surface $(\widehat{S}, \mathcal{T})$ is defined as the points in \mathbb{Z}^N satisfying two conditions per rhombus, where there are three rhombi per pointed ideal triangle Δ of \mathcal{T} (§2.1). Both conditions involve the quantity $a + b - c - d$ associated to the rhombus; the first being that $3\beta := a + b - c - d \geq 0$, and the

second that $\beta = (a + b - c - d)/3 \in \mathbb{Z}$ is an integer. (Recall $d = 0$ if the rhombus is a corner rhombus; §2.1.) Let $\{\beta_i\}_i$ denote these *rhombus numbers*, varying over all the rhombi of \mathcal{T} .

It will be convenient in the remainder of the paper to talk about real vector spaces \mathbb{R}^N , which we think of as containing \mathbb{Z}^N , in particular the KTGS cone $\mathcal{C}_{\mathcal{T}}$, as a subset.

In this sub-subsection, for the triangulated ideal square (\square, \mathcal{T}) we define a linear isomorphism $\theta_{\mathcal{T}}$ of real 12-dimensional vector spaces, which is used in the proof of Theorem 6.10 and in §7. Here, 12 is the number of tropical coordinates for the square. Note that the triangulated square has 18 rhombi $\{\beta_i\}_{i=1,2,\dots,18}$, as displayed in Figure 23 below in §7.

Definition 6.13. Let (\square, \mathcal{T}) be the triangulated square, whose coordinates are labeled as in the left hand side of Figure 2. Define a linear map

$$\theta_{\mathcal{T}} : \mathbb{R}^{12} \longrightarrow \mathbb{R}^{18}$$

by the formula

$$\theta_{\mathcal{T}}(x_1, x_2, \dots, x_8, y_1, \dots, y_4) = (\beta_1, \beta_2, \beta_3, \beta_4, \beta_5, \beta_6, \beta_7, \beta_8, \beta_9, \beta_{10}, \beta_{11}, \beta_{12}, \beta_{13}, \beta_{14}, \beta_{15}, \beta_{16}, \beta_{17}, \beta_{18}),$$

where the $\{\beta_i\}_{i=1,2,\dots,18}$ are the 18 rhombus numbers defined above.

For example, the images under $\theta_{\mathcal{T}}$ of the 22-element Hilbert basis $\mathcal{H}_{(\square, \mathcal{T})} \subseteq \mathcal{C}_{\mathcal{T}}$ of Theorem 6.10 are calculated from Figures 22 and 23 to be:

- (1) $\theta_{\mathcal{T}}(\Phi_{\mathcal{T}}([R_a])) = (1, 0, 0, 0, 0, 0, 0, 0, 0, 0, 0, 0, 0, 0, 0, 0, 0, 0)$
- (2) $\theta_{\mathcal{T}}(\Phi_{\mathcal{T}}([L_a])) = (0, 1, 1, 0, 0, 0, 0, 0, 0, 0, 0, 0, 0, 0, 0, 0, 0, 0)$
- (3) $\theta_{\mathcal{T}}(\Phi_{\mathcal{T}}([R_b])) = (0, 0, 0, 1, 0, 0, 0, 0, 0, 0, 0, 0, 1, 0, 0, 0, 0, 0)$
- (4) $\theta_{\mathcal{T}}(\Phi_{\mathcal{T}}([L_b])) = (0, 0, 0, 0, 1, 1, 0, 0, 0, 0, 0, 0, 0, 1, 1, 0, 0, 0)$
- (5) $\theta_{\mathcal{T}}(\Phi_{\mathcal{T}}([R_c])) = (0, 0, 0, 0, 0, 0, 1, 0, 0, 0, 0, 0, 0, 0, 0, 1, 0, 0)$
- (6) $\theta_{\mathcal{T}}(\Phi_{\mathcal{T}}([L_c])) = (0, 0, 0, 0, 0, 0, 0, 1, 1, 0, 0, 0, 0, 0, 0, 0, 1, 1)$
- (7) $\theta_{\mathcal{T}}(\Phi_{\mathcal{T}}([R_d])) = (0, 0, 0, 0, 0, 0, 0, 0, 0, 1, 0, 0, 0, 0, 0, 0, 0, 0)$
- (8) $\theta_{\mathcal{T}}(\Phi_{\mathcal{T}}([L_d])) = (0, 0, 0, 0, 0, 0, 0, 0, 0, 0, 1, 1, 0, 0, 0, 0, 0, 0)$
- (9) $\theta_{\mathcal{T}}(\Phi_{\mathcal{T}}([T_{out}, R_b])) = (0, 0, 1, 0, 0, 1, 0, 0, 1, 0, 0, 0, 1, 0, 0, 0, 0, 0)$
- (10) $\theta_{\mathcal{T}}(\Phi_{\mathcal{T}}([T_{out}, L_c])) = (0, 0, 1, 0, 0, 1, 0, 0, 1, 0, 0, 0, 0, 0, 0, 0, 1, 1)$
- (11) $\theta_{\mathcal{T}}(\Phi_{\mathcal{T}}([T_{in}, L_b])) = (0, 1, 0, 0, 1, 0, 0, 1, 0, 0, 0, 0, 0, 1, 1, 0, 0, 0)$
- (12) $\theta_{\mathcal{T}}(\Phi_{\mathcal{T}}([T_{in}, R_c])) = (0, 1, 0, 0, 1, 0, 0, 1, 0, 0, 0, 0, 0, 0, 0, 0, 1, 0, 0)$
- (13) $\theta_{\mathcal{T}}(\Phi_{\mathcal{T}}([L_b, T_{out}])) = (0, 0, 0, 0, 1, 1, 0, 0, 0, 0, 0, 1, 0, 0, 1, 0, 0, 1)$
- (14) $\theta_{\mathcal{T}}(\Phi_{\mathcal{T}}([L_c, T_{in}])) = (0, 0, 0, 0, 0, 0, 1, 1, 0, 1, 0, 0, 1, 0, 0, 1, 0, 0)$
- (15) $\theta_{\mathcal{T}}(\Phi_{\mathcal{T}}([R_b, T_{in}])) = (0, 0, 0, 1, 0, 0, 0, 0, 0, 0, 1, 0, 0, 1, 0, 0, 1, 0)$
- (16) $\theta_{\mathcal{T}}(\Phi_{\mathcal{T}}([R_c, T_{out}])) = (0, 0, 0, 0, 0, 0, 1, 0, 0, 0, 0, 1, 0, 0, 1, 0, 0, 1)$
- (17) $\theta_{\mathcal{T}}(\Phi_{\mathcal{T}}([T_{out}, T_{in}])) = (0, 0, 1, 0, 0, 1, 0, 0, 1, 0, 1, 0, 0, 1, 0, 0, 1, 0)$
- (18) $\theta_{\mathcal{T}}(\Phi_{\mathcal{T}}([T_{in}, T_{out}])) = (0, 1, 0, 0, 1, 0, 0, 1, 0, 0, 0, 1, 0, 0, 1, 0, 0, 1)$
- (19) $\theta_{\mathcal{T}}(\Phi_{\mathcal{T}}([L_b, R_c])) = (0, 0, 0, 0, 1, 1, 0, 0, 0, 0, 0, 0, 0, 0, 0, 1, 0, 0)$
- (20) $\theta_{\mathcal{T}}(\Phi_{\mathcal{T}}([R_b, L_c])) = (0, 0, 0, 1, 0, 0, 0, 0, 0, 0, 0, 0, 0, 0, 0, 0, 1, 1)$
- (21) $\theta_{\mathcal{T}}(\Phi_{\mathcal{T}}([R_c, L_b])) = (0, 0, 0, 0, 0, 0, 1, 0, 0, 0, 0, 0, 0, 1, 1, 0, 0, 0)$

$$(22) \quad \theta_{\mathcal{T}}(\Phi_{\mathcal{T}}([L_c, R_b])) = (0, 0, 0, 0, 0, 0, 0, 1, 1, 0, 0, 0, 1, 0, 0, 0, 0, 0).$$

When there is no confusion, we also let β_i denote the general i -th coordinate of \mathbb{R}^{18} . Consider the subspace $V_{\mathcal{T}} \subseteq \mathbb{R}^{18}$ defined by

$$(\dagger) \quad V_{\mathcal{T}} = \{(\beta_i)_i \in \mathbb{R}^{18}; \quad X_1 := \beta_3 - \beta_2 = \beta_6 - \beta_5 = \beta_9 - \beta_8, \quad X_2 := \beta_4 - \beta_{13} = \beta_{17} - \beta_9, \\ X_3 := \beta_{12} - \beta_{11} = \beta_{15} - \beta_{14} = \beta_{18} - \beta_{17}, \quad X_4 := \beta_{16} - \beta_7 = \beta_5 - \beta_{15}\}.$$

See §7.3.1 for a discussion of the geometric meaning of the subspace $V_{\mathcal{T}}$ and the quantities X_i .

Proposition 6.14. *The linear map $\theta_{\mathcal{T}} : \mathbb{R}^{12} \rightarrow \mathbb{R}^{18}$ is an isomorphism of \mathbb{R}^{12} onto $V_{\mathcal{T}}$. That is, $\theta_{\mathcal{T}}$ is injective, and the image of $\theta_{\mathcal{T}}$ is equal to $V_{\mathcal{T}}$. In particular, $V_{\mathcal{T}}$ is 12-dimensional.*

Proof. By elementary linear algebra, the above 22 images $\{\theta_{\mathcal{T}}(\Phi_{\mathcal{T}}(W_i^H))\}_{i=1,2,\dots,22} \subseteq \mathbb{Z}_+^{18}$ span a 12 dimensional subspace of \mathbb{R}^{18} . So $\theta_{\mathcal{T}}$ is injective.

That $\theta_{\mathcal{T}}(\mathbb{R}^{12}) \subseteq V_{\mathcal{T}}$ follows from the definition of the rhombus numbers $\{\beta_i\}_{i=1,2,\dots,18}$; compare Figure 23.

That $V_{\mathcal{T}} \subseteq \mathbb{R}^{18}$ is 12-dimensional follows from a computation showing that the linear map $f : \mathbb{R}^{18} \rightarrow \mathbb{R}^6$ defined by

$$f(\beta_1, \beta_2, \dots, \beta_{18}) = (\beta_3 - \beta_2 + \beta_5 - \beta_6, \quad \beta_6 - \beta_5 + \beta_8 - \beta_9, \quad \beta_4 - \beta_{13} + \beta_9 - \beta_{17}, \\ \beta_{12} - \beta_{11} + \beta_{14} - \beta_{15}, \quad \beta_{15} - \beta_{14} + \beta_{17} - \beta_{18}, \quad \beta_{16} - \beta_7 + \beta_{15} - \beta_5)$$

has rank 6 (note $V_{\mathcal{T}}$ is the kernel of f). ■

Conceptual Remark 6.15. Recall (§2.3) $\mathcal{A}_{\text{PGL}_3, \square}(\mathbb{R}^t) = \mathcal{A}_{\text{SL}_3, \square}(\mathbb{R}^t)$. Recall also from Remark 3.4 that we view the positive integer cone $\mathcal{C}_{\mathcal{T}} \cong -3\mathcal{A}_{\text{PGL}_3, \square}^+(\mathbb{Z}^t)_{\mathcal{T}}$ as a \mathcal{T} -chart for the positive tropical integer points $\mathcal{A}_{\text{PGL}_3, \square}^+(\mathbb{Z}^t) \subseteq \mathcal{A}_{\text{SL}_3, \square}(\mathbb{R}^t)$.

We think of $\mathbb{R}^{12} \cong \mathcal{A}_{\text{SL}_3, \square}(\mathbb{R}^t)_{\mathcal{T}}$ as the coordinate chart of $\mathcal{A}_{\text{SL}_3, \square}(\mathbb{R}^t)$ associated to the ideal triangulation \mathcal{T} , with one tropical \mathcal{A} -coordinate $-3(A_{a;b,c}^{i,j,k})^t$ per dot of \mathcal{T} (§2.2).

We view the rhombus numbers $\{\beta_i\}_{i=1,2,\dots,18}$ as the tropicalizations $(\alpha_{a;b,c}^{i,j,k})^t$ of the rhombus functions $\alpha_{a;b,c}^{i,j,k}$ on the moduli space $\mathcal{A}_{\text{PGL}_3, \square}$ (§2.3).

By Proposition 6.14, we can also think of the rhombus numbers $\{\beta_i\}_i \in V_{\mathcal{T}} \subseteq \mathbb{R}^{18}$ as coordinates for $\mathcal{A}_{\text{PGL}_3, \square}(\mathbb{R}^t)$ via the isomorphism $\theta_{\mathcal{T}}$, that is:

$$\mathcal{A}_{\text{PGL}_3, \square}(\mathbb{R}^t)_{\mathcal{T}} \cong V_{\mathcal{T}} \xrightarrow{\theta_{\mathcal{T}}} \mathbb{R}^{12} \cong \mathcal{A}_{\text{SL}_3, \square}(\mathbb{R}^t)_{\mathcal{T}}.$$

6.3. Tropical skein relations in the KTGS cone for the square.

We end this section with a noteworthy observation, which will not be needed later.

We saw in Remark 6.9 that there are interesting relations even in the KTGS cone $\mathcal{C}_{\Delta} \subseteq \mathbb{Z}_+^7$ for the triangle. In fact, this is the only relation (in the sense analogous to Proposition 6.16 below). The intuitive reason there is only 1 relation for the triangle is because the Hilbert basis for \mathcal{C}_{Δ} has 8 elements, whereas there are only 7 Fock-Goncharov coordinates.

We now describe all of the relations in the KTGS cone $\mathcal{C}_{\mathcal{T}} \subseteq \mathbb{Z}_+^{12}$ for the square. Intuitively, there are 10 relations because the Hilbert basis for $\mathcal{C}_{\mathcal{T}}$ has 22 elements, whereas there are only 12 Fock-Goncharov coordinates.

Proposition 6.16. *The following 10 linear relations are independent and complete among the 22 elements of the Hilbert basis $\mathcal{H}_{(\square, \mathcal{T})} \subseteq \mathcal{C}_{\mathcal{T}}$ for the KTGS cone for the square:*

$$(1) \quad \Phi_{\mathcal{T}}([T_{in}, L_b]) + \Phi_{\mathcal{T}}([T_{out}, L_c]) = \Phi_{\mathcal{T}}([L_a]) + \Phi_{\mathcal{T}}([L_b]) + \Phi_{\mathcal{T}}([L_c])$$

- (2) $\Phi_{\mathcal{T}}([T_{out}, L_c]) + \Phi_{\mathcal{T}}([T_{in}, R_c]) = \Phi_{\mathcal{T}}([L_a]) + \Phi_{\mathcal{T}}([L_c]) + \Phi_{\mathcal{T}}([L_b, R_c])$
- (3) $\Phi_{\mathcal{T}}([L_c, T_{in}]) + \Phi_{\mathcal{T}}([L_b, T_{out}]) = \Phi_{\mathcal{T}}([L_b]) + \Phi_{\mathcal{T}}([L_c]) + \Phi_{\mathcal{T}}([L_d])$
- (4) $\Phi_{\mathcal{T}}([L_b, T_{out}]) + \Phi_{\mathcal{T}}([R_b, T_{in}]) + \Phi_{\mathcal{T}}([T_{out}, R_b]) = \Phi_{\mathcal{T}}([L_b]) + \Phi_{\mathcal{T}}([R_b]) + \Phi_{\mathcal{T}}([L_d]) + \Phi_{\mathcal{T}}([T_{out}, L_c])$
- (5) $\Phi_{\mathcal{T}}([R_c, T_{out}]) + \Phi_{\mathcal{T}}([L_b, R_c]) = \Phi_{\mathcal{T}}([L_b, T_{out}]) + \Phi_{\mathcal{T}}([R_c])$
- (6) $\Phi_{\mathcal{T}}([T_{out}, T_{in}]) + \Phi_{\mathcal{T}}([L_b, T_{out}]) = \Phi_{\mathcal{T}}([L_b]) + \Phi_{\mathcal{T}}([L_d]) + \Phi_{\mathcal{T}}([T_{out}, L_c])$
- (7) $\Phi_{\mathcal{T}}([T_{in}, T_{out}]) + \Phi_{\mathcal{T}}([T_{out}, L_c]) = \Phi_{\mathcal{T}}([L_a]) + \Phi_{\mathcal{T}}([L_c]) + \Phi_{\mathcal{T}}([L_b, T_{out}])$
- (8) $\Phi_{\mathcal{T}}([T_{out}, R_b]) + \Phi_{\mathcal{T}}([R_b, L_c]) = \Phi_{\mathcal{T}}([R_b]) + \Phi_{\mathcal{T}}([T_{out}, L_c])$
- (9) $\Phi_{\mathcal{T}}([L_b, R_c]) + \Phi_{\mathcal{T}}([R_c, L_b]) = \Phi_{\mathcal{T}}([L_b]) + \Phi_{\mathcal{T}}([R_c])$
- (10) $\Phi_{\mathcal{T}}([T_{out}, L_c]) + \Phi_{\mathcal{T}}([L_c, R_b]) = \Phi_{\mathcal{T}}([T_{out}, R_b]) + \Phi_{\mathcal{T}}([L_c]).$

Proof. More precisely, what is meant by the statement of the proposition is the following. Let $f : \mathbb{R}^{22} \rightarrow \mathbb{R}^{12}$ be the linear map

$$f(\lambda_1, \lambda_2, \dots, \lambda_{22}) = \sum_{i=1}^{22} \lambda_i \Phi_{\mathcal{T}}(W_i^H) \in \mathbb{R}^{12},$$

where the webs W_i^H are as in Theorem 6.10. As in the proof of Proposition 6.14, each of the 10 relations above determines an element r_j of \mathbb{R}^{22} . Let $V \subseteq \mathbb{R}^{22}$ be the kernel of f . The claim is that the elements $\{r_j\}_{j=1,2,\dots,10}$ form a basis of V ; in particular, V is 10-dimensional.

By Figure 22, one checks that the 10 relations are satisfied, so $r_j \in V$. By elementary linear algebra, the 10 elements $\{r_j\}_j \subseteq V$ are linearly independent. It remains to show that the linear map $f : \mathbb{R}^{22} \rightarrow \mathbb{R}^{12}$ has rank 12, for which it suffices to show that the 22 elements $\{\Phi_{\mathcal{T}}(W_i^H)\}_i \subseteq \mathbb{Z}_+^{12} \subseteq \mathbb{R}^{12}$ span \mathbb{R}^{12} . This is true because, by the proof of Proposition 6.14, the images of these 22 elements under the linear map $\theta_{\mathcal{T}} : \mathbb{R}^{12} \rightarrow \mathbb{R}^{18}$ span the 12 dimensional subspace $V_{\mathcal{T}} \subseteq \mathbb{R}^{18}$. \blacksquare

Remark 6.17. The relations of Proposition 6.16 can be viewed as *tropical SL_3 skein relations*. Indeed, they can be “predicted” as the result of resolving the overlapping webs in the square (corresponding to a given relation in the cone) by one of the two Kuperberg SL_3 skein relations [Kup96, §4, $q = 1$] (one resolution per crossing in the picture). See also [Xie13].

7. KTGS CONE FOR THE SQUARE: SECTOR DECOMPOSITION

In §6, we saw that the Knutson-Tao-Goncharov-Shen cone $\mathcal{C}_{\mathcal{T}} \subseteq \mathbb{Z}_+^{12}$ for the triangulated square (\square, \mathcal{T}) has a Hilbert basis $\mathcal{H}_{(\square, \mathcal{T})} \subseteq \mathcal{C}_{\mathcal{T}}$ consisting of 22 elements (Figure 22). There are many linear dependence relations in \mathbb{R}^{12} among these Hilbert basis elements; see Proposition 6.16. In this last section, we study certain linearly independent subsets of the Hilbert basis $\mathcal{H}_{(\square, \mathcal{T})}$ that have topological interpretations in terms of webs.

More specifically, we show that each of the 42 web families $\mathcal{W}_i \subseteq \mathcal{W}_{\square}$ (Proposition 5.1 and Figure 16) corresponds to a 12-dimensional subcone $\mathcal{C}_{\mathcal{T}}^i \subseteq \mathcal{C}_{\mathcal{T}}$ (called a sector) generated by 12 Hilbert basis elements. Moreover, every point in the KTGS cone $\mathcal{C}_{\mathcal{T}}$ lies in such a sector $\mathcal{C}_{\mathcal{T}}^i$. These sectors have a geometric description in terms of tropical integer \mathcal{X} -coordinates (Figure 23) for reduced webs $W \in \mathcal{W}_{\square}$, which are functions of the corresponding positive tropical integer \mathcal{A} -coordinates (Figure 12); we already encountered some of these ideas in §6.2.3.

In summary, this analysis gives us a deeper understanding of the combinatorial, geometric, and topological properties of the KTGS cone $\mathcal{C}_{\mathcal{T}} \subseteq \mathbb{Z}_+^{12}$ for the square; see Figure 3.

7.1. Cones over the real numbers.

Recall that \mathbb{R}_+ (resp. \mathbb{R}_-) denotes the set of nonnegative (nonpositive) real numbers.

Remark 7.1. Some of our terminology might be non-standard, adapted for the purposes of this paper; compare Remark 6.7.

7.1.1. Cones and sector decompositions.

Definition 7.2.

- A (real) cone $C \subseteq \mathbb{R}^k$ is a subset of \mathbb{R}^k such that

$$C = \left\{ \sum_{i=1}^m \lambda_i c_i; \quad \lambda_i \in \mathbb{R}_+ \right\}$$

for some finite set $\{c_i\}_{i=1,2,\dots,m} \subseteq \mathbb{R}^k$, called a *generating set* of C .

We also write $C = \text{span}_{\mathbb{R}_+}(c_1, c_2, \dots, c_m)$ for the above equation.

- The minimum number of elements of a generating set is called the *rank* of the cone C . A generating set $\{c_i\}_i$ of minimum size is called a *basis* of C .
- The subspace $\tilde{C} \subseteq \mathbb{R}^k$ defined by

$$\tilde{C} = \left\{ \sum_i \tilde{\lambda}_i c_i; \quad \tilde{\lambda}_i \in \mathbb{R} \right\}$$

is independent of the choice of generating set $\{c_i\}_i$, and its dimension is called the *dimension* of the cone C . Note $\dim(C) \leq \text{rank}(C) < \infty$.

- A cone C is a *sector* if $\dim(C) = \text{rank}(C)$.
- A cone $C \subseteq \mathbb{R}^k$ is *full* if $\dim(C) = k$.

Example 7.3.

- (1) $C = \mathbb{R}$ is a full cone with basis $\{1, -1\}$. Its rank is 2, and its dimension is 1, so it is not a sector.
- (2) $C = \mathbb{R}^2$ is a full cone with basis $\{e_1, e_2, -e_1 - e_2\}$. Its rank is 3, and its dimension is 2, so it is not a sector. Here, e_i is the i -th standard basis element.
The subcone $C' = \mathbb{R}e_1 \subseteq C$ is not full and is not a sector.
- (3) One checks that the full cone $C = \mathbb{R}^k$ has rank $k+1$, by taking as a basis the vertices of the k -dimensional simplex centered at the origin.
- (4) For $j = 1, 2, \dots, k$, the cone $C^{(j)} = \sum_{i=1}^j \mathbb{R}_+ e_i \subseteq \mathbb{R}^k$ is a sector of rank j . It is full only for $j = k$, namely when $C^{(j)} = C^{(k)} = \mathbb{R}_+^k$ is the positive orthant.

Remark 7.4. Note that if a cone C has rank r and if $\{c_i\}_i$ is a generating set for C , there does not necessarily exist a subset $\{c_{i_j}\}_{j=1,2,\dots,r}$ that is a basis. For example, take $C = \mathbb{R}^2$ with generating set $\{e_1, -e_1, e_2, -e_2\}$.

Definition 7.5.

- A *sector decomposition* of a full cone $C \subseteq \mathbb{R}^k$ is a finite collection $\{C_i\}_{i=1,2,\dots,p}$ of subcones $C_i \subseteq C$ satisfying:
 - each C_i is a full sector;
 - $C = C_1 \cup C_2 \cup \dots \cup C_p$ is the union of the sectors C_i ;
 - For each distinct $i, j \in \{1, 2, \dots, p\}$, the intersection $C_i \cap C_j \subseteq \mathbb{R}^k$ has empty interior (namely, this intersection does not contain an open subset of \mathbb{R}^k).

- If C and C' are two full cones in \mathbb{R}^k , then the intersection $C \cap C'$ is a *wall* if $C \cap C'$ is a cone of dimension $k - 1$.

Example 7.6.

- (1) In Example 7.3(1), putting $C_1 = \mathbb{R}_+$ and $C_2 = \mathbb{R}_-$ yields a sector decomposition of the cone $C = \mathbb{R}$. The intersection $C_1 \cap C_2 = \{0\}$ is a wall.
- (2) In Example 7.3(2), putting $C_1 = \mathbb{R}_+e_1 + \mathbb{R}_+e_2$, $C_2 = \mathbb{R}_+e_2 + \mathbb{R}_+(-e_1 - e_2)$, and $C_3 = \mathbb{R}_+(-e_1 - e_2) + \mathbb{R}_+e_1$ yields a sector decomposition of $C = \mathbb{R}^2$. Each sector faces two walls, and each pairwise-distinct intersection $C_i \cap C_j$ is a wall.
- (3) Again in Example 7.3(2), alternatively putting $C_1 = \text{span}_{\mathbb{R}_+}(e_1, e_2)$, $C_2 = \text{span}_{\mathbb{R}_+}(e_2, -e_1)$, $C_3 = \text{span}_{\mathbb{R}_+}(-e_1, -e_2)$, and $C_4 = \text{span}_{\mathbb{R}_+}(-e_2, e_1)$ yields a sector decomposition of $C = \mathbb{R}^2$. Each sector faces two walls, the intersections $C_i \cap C_{i+1}$ are walls, but the intersections $C_1 \cap C_3 = C_2 \cap C_4 = \{0\}$ are not walls.
- (4) In Example 7.3(4), putting $C_1 = C^{(k)} = \mathbb{R}_+^k$ yields a sector decomposition with a single sector.

Observation 7.7. *If $\{C_i\}_{i=1,2,\dots,p}$ is a sector decomposition of a full cone $C \subseteq \mathbb{R}^k$, and if $W = C_i \cap C_\ell$ is a wall, then there is no other pair of sectors giving this wall: $W = C_{i'} \cap C_{\ell'}$ if and only if $\{i, \ell\} = \{i', \ell'\}$.*

This essentially follows since walls have codimension 1 in \mathbb{R}^k . We give a proof here for completeness.

Proof of Observation 7.7. Let the $k - 1$ dimensional subcone $W \subseteq C$ be generated by $\{w_j\}_{j=1,2,\dots,m}$. Let v_i in the k dimensional cone C_i be linearly independent from $\{w_j\}_j$.

Let w be a fixed point in the interior of W , namely $w = \sum_{j=1}^m \lambda_j w_j$ for some $\lambda_j > 0$. Then there is $\epsilon_i > 0$ such that

$$(\$) \quad \left\{ w + \lambda^{(i)} v_i + \sum_{j=1}^m \tilde{\lambda}_j w_j; \quad 0 \leq \lambda^{(i)} < \epsilon_i \quad \text{and} \quad \lambda_j - \epsilon_i < \tilde{\lambda}_j < \lambda_j + \epsilon_i \right\} \subseteq C_i.$$

Let $v_i^\perp \in \widetilde{W}^\perp - \{0\} \subseteq \mathbb{R}^k$ be the nonzero component of v_i perpendicular to the subspace \widetilde{W} (with respect to the standard inner product, say); note v_i^\perp is not necessarily in C_i . By shrinking ϵ_i , we can arrange that $(\$)$ holds with v_i replaced by v_i^\perp ; denote the resulting subset $(\$)$ by $\overline{U}_i \subseteq C_i$. Similarly, define a subset $\overline{U}_\ell \subseteq C_\ell$ depending on some $v_\ell^\perp \neq 0 \in \widetilde{W}^\perp$ and $\epsilon_\ell > 0$. By further shrinking, let us arrange that $\epsilon_i = \epsilon_\ell$.

So far, we have not used the assumption that k is the dimension of the ambient space \mathbb{R}^k . We now use this assumption, to note that $\widetilde{W}^\perp \subseteq \mathbb{R}^k$ is 1 dimensional, and that \overline{U}_i and \overline{U}_ℓ have nonempty interiors in \mathbb{R}^k .

Without loss of generality, assume $|v_i^\perp| \leq |v_\ell^\perp|$. If v_ℓ^\perp pointed in the same direction as v_i^\perp , then by construction $C_i \cap C_\ell \supseteq \overline{U}_i \cap \overline{U}_\ell = \overline{U}_i$ would have nonempty interior, violating the hypothesis that C_i and C_ℓ are part of a sector decomposition of the full cone $C \subseteq \mathbb{R}^k$. Thus, v_ℓ^\perp points in the opposite direction as v_i^\perp .

Now, assume $C_{i'} \cap C_{\ell'} = W$ as well; define $\overline{U}_{i'} \subseteq C_{i'}$ and $\overline{U}_{\ell'} \subseteq C_{\ell'}$ as above. After possibly swapping indices, we have that v_i^\perp and $v_{i'}^\perp$ (resp. v_ℓ^\perp and $v_{\ell'}^\perp$) point in the same direction. Arguing as above, it follows that $\overline{U}_i \cap \overline{U}_{i'} \subseteq C_i \cap C_{i'}$ and $\overline{U}_\ell \cap \overline{U}_{\ell'} \subseteq C_\ell \cap C_{\ell'}$ have nonempty interiors. Therefore, $i = i'$ and $\ell = \ell'$. ■

Remark 7.8. Observation 7.7 is false for higher codimension intersections. For instance, in Example 7.6(3), we have $C_1 \cap C_3 = C_2 \cap C_4 = \{0\}$.

7.1.2. *Some technical statements about cones of the form $C \subseteq \mathbb{R}_+^k \times \mathbb{R}^n$.*

This sub-subsection can be skipped until §7.3.3.

Lemma 7.9. *Let $C \subseteq \mathbb{R}_+^k \times \mathbb{R}^n$ be a cone satisfying the following properties:*

- $e_i \in C$ for $i = 1, 2, \dots, k$, where e_i is the i -th standard basis element of $\mathbb{R}^k \times \mathbb{R}^n$;
- $\pi_n(C) = \mathbb{R}^n$, where $\pi_n : \mathbb{R}^k \times \mathbb{R}^n \rightarrow \mathbb{R}^n$ is the natural projection.

Then, $\dim(C) = k + n$. Namely, C is full.

Example (part 1). The rank of such a cone C as in Lemma 7.9 can equal the dimension or be strictly greater. For example, $C = \mathbb{R}_+ \times \mathbb{R}$ has rank 3, whereas $C' = \text{span}_{\mathbb{R}_+}(\{(1; 1), (0; -1)\}) \subseteq \mathbb{R}_+ \times \mathbb{R}$ has rank 2.

Proof of Lemma 7.9. Note $\mathbb{R}_+^k \times \{0\} \subseteq C$, so $\mathbb{R}^k \times \{0\} \subseteq \tilde{C}$; see Definition 7.2. The hypothesis $\pi_n(C) = \mathbb{R}^n$ thus implies $\{0\} \times \mathbb{R}^n \subseteq \tilde{C}$. It follows that $\tilde{C} = \mathbb{R}^k \times \mathbb{R}^n$. ■

Lemma 7.10. *Consider a full cone $C \subseteq \mathbb{R}_+^k \times \mathbb{R}^n$ as in Lemma 7.9. Let $\{x_j\}_{j=1,2,\dots,m}$ be a finite subset of C with $m \geq n$, and let $\{J_i\}_{i=1,2,\dots,p}$ for some p be a collection of index sets $J_i = \{j_1^{(i)}, j_2^{(i)}, \dots, j_n^{(i)}\} \subseteq \{1, 2, \dots, m\}$ of constant size n .*

Assume in addition:

- $C = \cup_{i=1}^p C_i$ is the union of the subcones

$$C_i = \text{span}_{\mathbb{R}_+}(\{e_1, e_2, \dots, e_k\} \cup \{x_j; \quad j \in J_i\}) \subseteq C \subseteq \mathbb{R}_+^k \times \mathbb{R}^n \quad (i = 1, 2, \dots, p);$$

- the subcones

$$D_i = \text{span}_{\mathbb{R}_+}(\{\pi_n(x_j); \quad j \in J_i\}) \subseteq \mathbb{R}^n \quad (i = 1, 2, \dots, p)$$

are full sectors forming a sector decomposition $\{D_i\}_{i=1,2,\dots,p}$ of \mathbb{R}^n (Definition 7.5).

Then, the subcones $C_i \subseteq C$ are full sectors forming a sector decomposition $\{C_i\}_{i=1,2,\dots,p}$ of C .

Also, the sector C_i projects via π_n to the sector D_i . Moreover, $\pi_n(C_i \cap C_\ell) = D_i \cap D_\ell$ for all pairwise distinct i, ℓ .

Example (part 2). For $C \subseteq \mathbb{R}_+ \times \mathbb{R}$ as in part 1, put $x_1 = (0; 1)$ and $x_2 = (0; -1)$. For $C' \subseteq \mathbb{R}_+ \times \mathbb{R}$ as in part 1, put $x'_1 = (1; 1)$ and $x'_2 = (0; -1)$. In both cases, put $J_1 = J'_1 = \{1\}$ and $J_2 = J'_2 = \{2\}$.

Then, in both cases, $D_1 = D'_1 = \mathbb{R}_+$ and $D_2 = D'_2 = \mathbb{R}_-$. For C , we have $C_1 = \mathbb{R}_+ \times \mathbb{R}_+$ and $C_2 = \mathbb{R}_+ \times \mathbb{R}_-$. For C' , we have $C'_1 = \text{span}_{\mathbb{R}_+}(\{(1; 0), (1; 1)\})$ and $C'_2 = \mathbb{R}_+ \times \mathbb{R}_-$.

Lastly, $C_1 \cap C_2 = C'_1 \cap C'_2 = \mathbb{R}_+ \times \{0\}$, which projects by π_1 to $\{0\} = D_1 \cap D_2 = D'_1 \cap D'_2$.

Proof of Lemma 7.10. By construction $\pi_n(C_i) = D_i$, so $\pi_n(C_i \cap C_\ell) \subseteq D_i \cap D_\ell$. To see that the reverse inclusion holds requires a little argument. Consider a general element

$$y = \pi_n \left(\sum_{j \in J_i} \lambda_j x_j \right) = \pi_n \left(\sum_{j \in J_\ell} \lambda'_j x_j \right) \in D_i \cap D_\ell \subseteq \mathbb{R}^n \quad (\lambda_j, \lambda'_j \in \mathbb{R}_+).$$

For $k^* = 1, 2, \dots, k$, the k^* -coordinate of $v_i := \sum_{j \in J_i} \lambda_j x_j \in C_i$ is either \leq or \geq the k^* -coordinate of $v_\ell := \sum_{j \in J_\ell} \lambda'_j x_j \in C_\ell$; without loss of generality, assume it is \leq . Putting $\alpha \geq 0$ to be the difference of these k^* -coordinates, we have that $v_i^* := v_i + \alpha e_{k^*} \in C_i$ has

the same k^* -coordinate as v_ℓ and still satisfies $\pi_n(v_i^*) = y = \pi_n(v_\ell) \in D_i \cap D_\ell$. We then put v_i^* to be the new v_i , and reiterate this procedure for each k^* , updating v_i or v_ℓ at each step. The end result is that $v_i = v_\ell \in C_i \cap C_\ell$ and $\pi_n(v_i) = y = \pi_n(v_\ell)$ as desired.

We move on to establishing that $\{C_i\}_i$ is a sector decomposition of C .

To see that $C_i \subseteq \mathbb{R}^k \times \mathbb{R}^n$ is a full cone, use the hypothesis that D_i is open in \mathbb{R}^n , and proceed as in the proof of Lemma 7.9. By definition, C_i has a generating set consisting of $k + n$ elements. Thus, $k + n = \dim(C_i) \leq \text{rank}(C_i) \leq k + n$, so C_i is a sector.

That $C = \cup_i C_i$ is by hypothesis.

It remains to show that $C_i \cap C_\ell$ has empty interior for all pairwise-distinct i, ℓ . Suppose otherwise, so that there is a nonempty open subset $U \subseteq \mathbb{R}^k \times \mathbb{R}^n$ such that $U \subseteq C_i \cap C_\ell$. Since projections are open maps, $\pi_n(U)$ is a nonempty open subset of \mathbb{R}^n contained in $D_i \cap D_\ell$, contradicting that $\{D_i\}_i$ is a sector decomposition. \blacksquare

Lemma 7.11. *Let the full cone $C \subseteq \mathbb{R}_+^k \times \mathbb{R}^n$, the sector decomposition $\{D_i\}_{i=1,2,\dots,p}$ of \mathbb{R}^n , and the sector decomposition $\{C_i\}_{i=1,2,\dots,p}$ of C be as in Lemma 7.10.*

Assume in addition:

- *for each i, ℓ such that $D_i \cap D_\ell$ is a wall in \mathbb{R}^n (Definition 7.5), we have more specifically that the intersection $J_i \cap J_\ell \subseteq \{1, 2, \dots, m\}$ of index sets has $n - 1$ elements, and*

$$D_i \cap D_\ell = \text{span}_{\mathbb{R}_+}(\{\pi_n(x_j); j \in J_i \cap J_\ell\}) \subseteq \mathbb{R}^n.$$

Then, for any i, ℓ , we have that $C_i \cap C_\ell \subseteq \mathbb{R}_+^k \times \mathbb{R}^n$ is a wall in C if and only if $D_i \cap D_\ell \subseteq \mathbb{R}^n$ is a wall in \mathbb{R}^n . In particular, if this is the case for a given i, ℓ , then

$$(\%) \quad C_i \cap C_\ell = \text{span}_{\mathbb{R}_+}(\{e_1, e_2, \dots, e_k\} \cup \{x_j; j \in J_i \cap J_\ell\}) \subseteq \mathbb{R}_+^k \times \mathbb{R}^n.$$

This furnishes a one-to-one correspondence {walls of $\{D_i\}_i$ in \mathbb{R}^n } \leftrightarrow {walls of $\{C_i\}_i$ in C }.

Example (part 3). For $C, C' \subseteq \mathbb{R}_+ \times \mathbb{R}$ as in part 2, the sole wall in \mathbb{R} is $\{0\}$, corresponding to the sole wall $\mathbb{R}_+ \times \{0\}$ in C, C' .

As a non-example, where the hypothesis and part of the conclusion, (%), fail: In $\mathbb{R}_+ \times \mathbb{R}^2$ let $x_1 = (0; 0, 1)$, $x_2 = (1; 1, 0)$, $x_3 = (0; 0, -1)$, $x_4 = (2; 1, 0)$, $x_5 = (0; -1, 0)$. Put $J_1 = \{1, 2\}$, $J_2 = \{3, 4\}$, $J_3 = \{1, 5\}$, $J_4 = \{3, 5\}$. Put $C = \cup_{i=1}^4 C_i$. Then $D_1 \cap D_2 = \mathbb{R}_+ \times \{0\} \subseteq \mathbb{R}^2$ is a wall, but $J_1 \cap J_2 = \emptyset$ and $C_1 \cap C_2 = \text{span}_{\mathbb{R}_+}(\{e_1, x_4\}) \supsetneq \text{span}_{\mathbb{R}_+}(\{e_1\})$. Note that $x_2 \in \pi_2^{-1}(D_1 \cap D_2) - (C_1 \cap C_2)$. On the other hand, $D_3 \cap D_4 = \mathbb{R}_- \times \{0\}$, $J_3 \cap J_4 = \{5\}$, and $C_3 \cap C_4 = \mathbb{R}_+ \times \mathbb{R}_- \times \{0\} = \text{span}_{\mathbb{R}_+}(\{e_1, x_5\})$. Moreover, $\pi_2^{-1}(D_3 \cap D_4) = C_3 \cap C_4$.

Proof of Lemma 7.11. Assume first that $C_i \cap C_\ell$ is a wall in C . By Lemma 7.10, $\pi_n(C_i \cap C_\ell) = D_i \cap D_\ell$. Thus, since $C_i \cap C_\ell$ is a cone, we have that $D_i \cap D_\ell$ is a cone. It follows that the subspace $\widetilde{D}_{i\ell} := \widetilde{D_i \cap D_\ell} \subseteq \mathbb{R}^n$ is equal to the projection under π_n of the subspace $\widetilde{C}_{i\ell} := \widetilde{C_i \cap C_\ell} \subseteq \mathbb{R}^k \times \mathbb{R}^n$ (Definition 7.2), the latter which is $k + n - 1$ dimensional by assumption. By definition of C_i and C_ℓ , we have $\mathbb{R}^k \times \{0\} \subseteq \widetilde{C}_{i\ell}$. Thus $\widetilde{C}_{i\ell} = \mathbb{R}^k \times \pi_n(\widetilde{C}_{i\ell}) = \mathbb{R}^k \times \widetilde{D}_{i\ell}$. Hence $\widetilde{D}_{i\ell}$ is $n - 1$ dimensional, as desired.

Conversely, assume $D_i \cap D_\ell$ is a wall in \mathbb{R}^n . Let j_i (resp. j_ℓ) be the unique index in $J_i - (J_i \cap J_\ell)$ (resp. $J_\ell - (J_i \cap J_\ell)$). Since D_i (resp. D_ℓ) has dimension n , the set of vectors $\{\pi_n(x_j); j \in J_i\}$ (resp. $\{\pi_n(x_j); j \in J_\ell\}$) in \mathbb{R}^n is linearly independent. Since $D_i \cap D_\ell \subseteq$ (in fact, equals) $\text{span}_{\mathbb{R}_+}(\{\pi_n(x_j); j \in J_i \cap J_\ell\})$ by hypothesis, it follows that any expression

in \mathbb{R}^n of the form

$$\lambda_{j_i} \pi_n(x_{j_i}) + \sum_{j \in J_i \cap J_\ell} \lambda_j \pi_n(x_j) \in D_i \cap D_\ell \quad \text{or} \quad \lambda'_{j_\ell} \pi_n(x_{j_\ell}) + \sum_{j \in J_i \cap J_\ell} \lambda'_j \pi_n(x_j) \in D_i \cap D_\ell$$

must imply $\lambda_{j_i} = 0$ or $\lambda_{j_\ell} = 0$, respectively.

Consequently, since $\pi_n(C_i \cap C_\ell) \subseteq D_i \cap D_\ell$ (in fact, this is an equality by Lemma 7.10), any expression in $C \subseteq \mathbb{R}_+^k \times \mathbb{R}^n$ of the form

$$\sum_{r=1}^k \eta_r e_r + \lambda_{j_i} x_{j_i} + \sum_{j \in J_i \cap J_\ell} \lambda_j x_j = \sum_{r=1}^k \eta'_r e_r + \lambda'_{j_\ell} x_{j_\ell} + \sum_{j \in J_i \cap J_\ell} \lambda'_j x_j \in C_i \cap C_\ell \quad (\eta_r, \lambda_{j_i}, \lambda_j, \eta'_r, \lambda'_{j_\ell}, \lambda'_j \in \mathbb{R}_+)$$

implies, by applying π_n , that $\lambda_{j_i} = \lambda'_{j_\ell} = 0$. We gather that the \subseteq inclusion of (%) is true. Since the reverse inclusion holds by the definitions of C_i and C_ℓ , we have that (%) is true. In particular, $C_i \cap C_\ell$ is a cone.

To finish, we show $C_i \cap C_\ell$ is $k + n - 1$ dimensional. By the same argument as in the first paragraph of this proof, we have $\tilde{C}_{i\ell} = \mathbb{R}^k \times \tilde{D}_{i\ell}$. Since $\tilde{D}_{i\ell}$ is $n - 1$ dimensional by hypothesis, the claim is true.

It remains to construct the desired bijection $f : \{\text{walls of } \{D_i\}_i \text{ in } \mathbb{R}^n\} \rightarrow \{\text{walls of } \{C_i\}_i \text{ in } C\}$. Indeed, let $W = D_i \cap D_\ell$ be a wall in \mathbb{R}^n . Put $f(W)$ to be the wall $C_i \cap C_\ell$ in C . By Observation 7.7, the choice of $\{i, \ell\}$ such that $W = D_i \cap D_\ell$ is unique, so f is well-defined. Conversely, if $W' \subseteq \mathbb{R}_+^k \times \mathbb{R}^n$ is a wall of $\{C_i\}_i$ in C , put $g(W') = \pi_n(W') \subseteq \mathbb{R}^n$. Since $W' = C_i \cap C_\ell$ for some i, ℓ by definition, we have that $g(W') = \pi_n(C_i \cap C_\ell) = D_i \cap D_\ell$ is a wall in \mathbb{R}^n . Thus, we have defined a function $g : \{\text{walls of } \{C_i\}_i \text{ in } C\} \rightarrow \{\text{walls of } \{D_i\}_i \text{ in } \mathbb{R}^n\}$ (note we did not need to use Observation 7.7 for this direction). It is immediate from the construction that f and g are inverses of each other. \blacksquare

7.1.3. Cone completions.

Unlike §7.1.2, this sub-subsection will be used in §7.2.

Definition 7.12. Let $\mathcal{M} \subseteq \mathbb{R}^k$ be a submonoid (Definition 6.1) having a finite \mathbb{Z}_+ -spanning set $\{c_i\}_{i=1,2,\dots,m}$ (we say \mathcal{M} is *finitely generated*). Then, its *completion* $\overline{\mathcal{M}} \subseteq \mathbb{R}^k$ is the corresponding real cone with the same generating set $\{c_i\}_i$ (this is independent of the choice of generating set).

By Proposition 6.3, we immediately have:

Observation 7.13. Let $\mathcal{C} \subseteq \mathbb{Z}_+^k$ be a positive integer cone (Definition 3.1) admitting a Hilbert basis $\mathcal{H} \subseteq \mathcal{C}$ (Definition 6.5). Then, the rank of its completion $\overline{\mathcal{C}} \subseteq \mathbb{R}^k$ is less than or equal to the number of elements of the Hilbert basis \mathcal{H} .

Example 7.14.

- (1) In Example 6.6(1), we see $\overline{\mathcal{C}} = \mathbb{R}_+^k$ and $\dim(\overline{\mathcal{C}}) = \text{rank}(\overline{\mathcal{C}}) = k = |\mathcal{H}|$.
- (2) In Example 6.6(2), we see that $\overline{\mathcal{C}} = \mathbb{R}_+^2$ and $\dim(\overline{\mathcal{C}}) = \text{rank}(\overline{\mathcal{C}}) = 2 < 3 = |\mathcal{H}|$.
- (3) In Example 6.6(3), we have that $\overline{\mathcal{C}} = \text{span}_{\mathbb{R}_+}(\mathcal{H}) \subseteq \mathbb{R}_+^3$ and one checks that $\dim(\overline{\mathcal{C}}) = 3 < 4 = \text{rank}(\overline{\mathcal{C}}) = |\mathcal{H}|$, as no point of \mathcal{H} lies in the \mathbb{R}_+ -span of the other three points.

Lemma 7.15. Let $\mathcal{M} \subseteq \mathbb{R}^k$ be a finitely generated monoid. Assume there are finitely generated submonoids $\mathcal{M}_1, \mathcal{M}_2, \dots, \mathcal{M}_p \subseteq \mathcal{M}$ such that $\mathcal{M} = \cup_{i=1}^p \mathcal{M}_i$. Then, $\overline{\mathcal{M}} = \cup_{i=1}^p \overline{\mathcal{M}_i}$.

Proof. The inclusion \supseteq is by definition. Let $\{c_j\}_{j=1,2,\dots,m}$ be a finite generating set for \mathcal{M} . Put $C = \sum_{j=1}^m |c_j|$, where $|c_j|$ is the Euclidean length in \mathbb{R}^k . Then for each $x \in \overline{\mathcal{M}}$, there exists some $y \in \mathcal{M}$ such that $|x - y| \leq C$. Indeed, writing $x = \sum_{j=1}^m \lambda_j c_j$, put $y = \sum_{j=1}^m n_j c_j \in \mathcal{M}$ where $n_j \geq 0$ is the largest integer less than or equal to λ_j . We have that

$$|x - y| = \left| \sum_{j=1}^m (\lambda_j - n_j) c_j \right| \leq \sum_{j=1}^m (\lambda_j - n_j) |c_j| \leq C.$$

We now argue by contradiction. Put $A = \cup_{i=1}^p \overline{\mathcal{M}}_i$ and suppose there is $x \in \overline{\mathcal{M}} - A$. Note $x \neq 0$. Let $\pi : \mathbb{R}^k - \{0\} \rightarrow S^{k-1}$ be the natural projection onto the unit sphere. It suffices to show there exists an open ball $B \subseteq \mathbb{R}^k$ such that $\pi(x) \in B \cap S^{k-1}$ and such that $\pi(A - \{0\})$ does not intersect $B \cap S^{k-1}$. Indeed, since $\mathcal{M} \subseteq A$ by hypothesis, this would contradict that there is some point of \mathcal{M} in $\pi^{-1}(B \cap S^{k-1}) \subseteq \mathbb{R}^k$ at distance at most C from a point in the ray $\mathbb{R}_{>0}x \subseteq \overline{\mathcal{M}} \cap \pi^{-1}(B \cap S^{k-1})$.

Suppose such a B does not exist. Then, there is a sequence (a_n) in $A - \{0\}$ such that $\lim_{n \rightarrow \infty} \pi(a_n) = \pi(x)$ in S^{k-1} . Since the subcones $\overline{\mathcal{M}}_i$ are finitely generated, they are closed subsets of \mathbb{R}^k ; thus, A is closed as well. It follows that the intersection

$$A^c = A \cap \left\{ z \in \mathbb{R}^k; \quad \frac{1}{2} \leq |z| \leq \frac{3}{2} \right\}$$

is compact; thus, $\pi(A^c) \subseteq S^{k-1}$ is compact as well. We gather $\pi(A^c)$ is closed in S^{k-1} .

Now, since the ray through any point of A intersects A^c , we have $\pi(a_n) \in \pi(A^c)$ for all n . It follows by the closedness of $\pi(A^c)$ that $\pi(x) \in \pi(A^c)$; in particular, the ray through x intersects $A = \cup_{i=1}^p \overline{\mathcal{M}}_i$. But this ray cannot intersect any subcone $\overline{\mathcal{M}}_i$, as $\overline{\mathcal{M}}_i$ is closed under scaling by \mathbb{R}_+ and $x \notin A$ by assumption. This is a contradiction. \blacksquare

7.2. Sector decomposition of the KTGS cone for the triangle and the square.

Recall the notion of a sector decomposition $\{C_i\}_i$ of a full cone $C \subseteq \mathbb{R}^k$, and of a wall between two full cones; see Definition 7.5.

Definition 7.16. Let \widehat{S} be a marked surface, and let \mathcal{T} be an ideal triangulation of \widehat{S} . The *completed Knutson-Tao-Goncharov-Shen cone* $C_{\mathcal{T}}$ is the completion $C_{\mathcal{T}} = \overline{\mathcal{C}}_{\mathcal{T}} \subseteq \mathbb{R}_+^N$ of the KTGS cone $\mathcal{C}_{\mathcal{T}} \subseteq \mathbb{Z}_+^N$; see Definitions 7.12, 3.2 and Proposition 3.3.

7.2.1. Sector decomposition for the triangle.

Let $S = \Delta$ be the ideal triangle. We will use the notation of §6.2.1.

Proposition 7.17. *The completed KTGS cone $C_{\Delta} \subseteq \mathbb{R}_+^7$ is 7-dimensional. Putting*

$$\begin{aligned} C_{\Delta}^{\text{out}} &= \text{span}_{\mathbb{Z}_+} \left(\{ \Phi_{\Delta}(W^H); \quad W^H = L_a, R_a, L_b, R_b, L_c, R_c, T_{\text{out}} \} \right) \subseteq \mathcal{C}_{\Delta} \subseteq \mathbb{Z}_+^7, \\ C_{\Delta}^{\text{in}} &= \text{span}_{\mathbb{Z}_+} \left(\{ \Phi_{\Delta}(W^H); \quad W^H = L_a, R_a, L_b, R_b, L_c, R_c, T_{\text{in}} \} \right) \subseteq \mathcal{C}_{\Delta} \subseteq \mathbb{Z}_+^7, \\ C_{\Delta}^{\text{out}} &= \overline{\mathcal{C}}_{\Delta}^{\text{out}}, \quad C_{\Delta}^{\text{in}} = \overline{\mathcal{C}}_{\Delta}^{\text{in}} \subseteq C_{\Delta} \subseteq \mathbb{R}_+^7, \end{aligned}$$

yields a sector decomposition $\{C_{\Delta}^{\text{out}}, C_{\Delta}^{\text{in}}\}$ of C_{Δ} . Moreover, $C_{\Delta}^{\text{out}} \cap C_{\Delta}^{\text{in}}$ is a 6-dimensional wall, generated by the cone points $\Phi_{\Delta}(W^H)$ corresponding to the 6 corner arcs in \mathcal{W}_{Δ} .

Proof. This is a consequence of [DS20, Proposition 45] and its proof.

Indeed, by [DS20, Proposition 45] we have that $\mathcal{C}_\Delta = \mathcal{C}_\Delta^{\text{out}} \cup \mathcal{C}_\Delta^{\text{in}}$. Thus, $C_\Delta = C_\Delta^{\text{out}} \cup C_\Delta^{\text{in}}$ by Lemma 7.15. Also, again by [DS20, Proposition 45] (or elementary linear algebra), the cones C_Δ , C_Δ^{out} , $C_\Delta^{\text{in}} \subseteq \mathbb{R}_+^7$ are full; in particular, C_Δ^{out} and C_Δ^{in} are sectors.

As mentioned in passing during the proof of Proposition 6.8, by the proof of [DS20, Proposition 45] there is a linear isomorphism $f : \mathbb{R}^7 \rightarrow \mathbb{R}^7$ satisfying:

- $f(C_\Delta) \subseteq \mathbb{R}_+^6 \times \mathbb{R}$;
- f sends the corner arcs points $\Phi_\Delta(W^H)$ for $W^H = L_a, R_a, L_b, R_b, L_c, R_c$ to the first six standard basis elements e_i of $\mathbb{R}^6 \times \mathbb{R}$ for $i = 1, 2, \dots, 6$;
- $f(\Phi_\Delta(T_{\text{in}})) = (0, 0, 0, 0, 0, 0; 1)$ and $f(\Phi_\Delta(T_{\text{out}})) = (0, 1, 0, 1, 0, 1; -1)$.

It follows that $f(C_\Delta^{\text{out}}) \cap f(C_\Delta^{\text{in}}) = \mathbb{R}_+^6 \times \{0\}$ has empty interior; moreover, it is a 6-dimensional wall. As these properties are preserved by isomorphisms of \mathbb{R}^7 , we conclude the result. ■

Corollary 7.18. *The rank (Definition 7.2) of the completed KTGS cone $C_\Delta \subseteq \mathbb{R}_+^7$ is 8.*

Proof. By Proposition 6.8, the Hilbert basis \mathcal{H}_Δ of the positive integer cone $\mathcal{C}_\Delta \subseteq \mathbb{Z}_+^7$ has 8 elements. It follows by Observation 7.13 that $\text{rank}(C_\Delta) \leq 8$.

By Proposition 7.17, $\text{rank}(C_\Delta) \geq 7$. We show there is no generating set with 7 elements.

We again work in the isomorphic cone $C := f(C_\Delta) \subseteq \mathbb{R}_+^6 \times \mathbb{R}$ from the proof of Proposition 7.17. Suppose $\{c_i\}_{i=1,2,\dots,7}$ is a generating set of C . Let $\pi_6 : \mathbb{R}^6 \times \mathbb{R} \rightarrow \mathbb{R}^6$ be the natural projection. Since the standard basis element e_i is in C for $i = 1, 2, \dots, 6$, and since $\pi_6(C) \subseteq$ (in fact, equals) \mathbb{R}_+^6 , after possibly changing indices we can assume, for $i = 1, 2, \dots, 6$, that $c_i = (e_i^{(6)}; \alpha_i)$ where $e_i^{(6)}$ is the i -th standard basis element of \mathbb{R}^6 and $\alpha_i \in \mathbb{R}$.

Since, by above, C has a generating set where just the one generator $(0, 1, 0, 1, 0, 1; -1)$ has a negative last coordinate, it follows that any point of C with a negative last coordinate has positive second, fourth, and sixth coordinates. Thus, $\alpha_i \geq 0$ for $i = 1, 2, \dots, 6$.

The remaining generator c_7 must therefore have a negative last coordinate. We conclude $(0, 0, 0, 0, 0, 0; 1) \in C$ cannot be generated with $\{c_i\}_{i=1,2,\dots,7}$. ■

7.2.2. Sector decomposition for the square.

Let $S = \square$ be the ideal square, equipped with an ideal triangulation \mathcal{T} , namely a choice of diagonal. We will use the notation of §6.2.2. In particular, recall the 22 Hilbert basis webs W_j^H in \mathcal{W}_\square ($j = 1, 2, \dots, 22$); see Figure 22.

We define 42 subcones $C_{\mathcal{T}}^i \subseteq C_{\mathcal{T}}$ ($i = 1, 2, \dots, 42$) of the completed KTGS cone $C_{\mathcal{T}} \subseteq \mathbb{R}_+^{12}$ as follows. First, define 42 web subsets $\mathcal{Q}_i \subseteq \mathcal{W}_\square$ ($i = 1, 2, \dots, 42$), each containing quatre Hilbert basis webs W^H , by:

$$\begin{aligned}
\mathcal{Q}_1 &= \{[T_{\text{in}}, L_b], [R_c, T_{\text{out}}], [R_c, L_b], [R_b, L_c]\} & \mathcal{Q}_2 &= \{[T_{\text{out}}, L_c], [R_c, T_{\text{out}}], [R_c, L_b], [R_b, L_c]\} \\
\mathcal{Q}_3 &= \{[T_{\text{in}}, L_b], [R_b, L_c], [R_b, T_{\text{in}}], [R_c, L_b]\} & \mathcal{Q}_4 &= \{[T_{\text{out}}, L_c], [R_b, L_c], [R_b, T_{\text{in}}], [R_c, L_b]\} \\
\mathcal{Q}_5 &= \{[T_{\text{in}}, T_{\text{out}}], [T_{\text{in}}, L_b], [R_c, T_{\text{out}}], [R_b, L_c]\} & \mathcal{Q}_6 &= \{[L_b, T_{\text{out}}], [T_{\text{in}}, T_{\text{out}}], [T_{\text{in}}, R_c], [R_b, L_c]\} \\
\mathcal{Q}_7 &= \{[T_{\text{in}}, L_b], [L_c, R_b], [T_{\text{in}}, T_{\text{out}}], [R_c, T_{\text{out}}]\} & \mathcal{Q}_8 &= \{[T_{\text{in}}, T_{\text{out}}], [L_c, R_b], [L_b, T_{\text{out}}], [T_{\text{in}}, R_c]\} \\
\mathcal{Q}_9 &= \{[T_{\text{out}}, R_b], [L_c, R_b], [L_c, T_{\text{in}}], [L_b, R_c]\} & \mathcal{Q}_{10} &= \{[T_{\text{in}}, R_c], [L_c, R_b], [L_c, T_{\text{in}}], [L_b, R_c]\} \\
\mathcal{Q}_{11} &= \{[T_{\text{out}}, R_b], [L_c, R_b], [L_b, T_{\text{out}}], [L_b, R_c]\} & \mathcal{Q}_{12} &= \{[T_{\text{in}}, R_c], [L_c, R_b], [L_b, T_{\text{out}}], [L_b, R_c]\} \\
\mathcal{Q}_{13} &= \{[T_{\text{out}}, T_{\text{in}}], [T_{\text{out}}, R_b], [L_c, T_{\text{in}}], [L_b, R_c]\} & \mathcal{Q}_{14} &= \{[T_{\text{out}}, L_c], [R_b, T_{\text{in}}], [T_{\text{out}}, T_{\text{in}}], [L_b, R_c]\} \\
\mathcal{Q}_{15} &= \{[T_{\text{out}}, T_{\text{in}}], [T_{\text{out}}, R_b], [L_c, T_{\text{in}}], [R_c, L_b]\} & \mathcal{Q}_{16} &= \{[T_{\text{out}}, L_c], [R_b, T_{\text{in}}], [T_{\text{out}}, T_{\text{in}}], [R_c, L_b]\} \\
\mathcal{Q}_{17} &= \{[T_{\text{out}}, R_b], [T_{\text{out}}, L_c], [R_c, L_b], [R_c, T_{\text{out}}]\} & \mathcal{Q}_{18} &= \{[T_{\text{in}}, L_b], [R_b, T_{\text{in}}], [L_c, T_{\text{in}}], [R_c, L_b]\}
\end{aligned}$$

$$\begin{aligned}
\mathcal{Q}_{19} &= \{[T_{in}, L_b], [L_c, R_b], [L_c, T_{in}], [T_{in}, R_c]\} & \mathcal{Q}_{20} &= \{[T_{out}, R_b], [L_c, R_b], [L_b, T_{out}], [R_c, T_{out}]\} \\
\mathcal{Q}_{21} &= \{[T_{out}, R_b], [L_c, R_b], [R_c, T_{out}], [R_c, L_b]\} & \mathcal{Q}_{22} &= \{[T_{out}, R_b], [L_c, R_b], [L_c, T_{in}], [R_c, L_b]\} \\
\mathcal{Q}_{23} &= \{[T_{in}, L_b], [L_c, R_b], [R_c, T_{out}], [R_c, L_b]\} & \mathcal{Q}_{24} &= \{[T_{in}, L_b], [L_c, R_b], [L_c, T_{in}], [R_c, L_b]\} \\
\mathcal{Q}_{25} &= \{[T_{out}, L_c], [T_{out}, R_b], [L_b, T_{out}], [L_b, R_c]\} & \mathcal{Q}_{26} &= \{[T_{in}, R_c], [R_b, T_{in}], [L_c, T_{in}], [L_b, R_c]\} \\
\mathcal{Q}_{27} &= \{[T_{in}, L_b], [R_b, L_c], [R_b, T_{in}], [T_{in}, R_c]\} & \mathcal{Q}_{28} &= \{[T_{out}, L_c], [R_b, L_c], [L_b, T_{out}], [R_c, T_{out}]\} \\
\mathcal{Q}_{29} &= \{[L_b, T_{out}], [R_b, L_c], [L_b, R_c], [T_{out}, L_c]\} & \mathcal{Q}_{30} &= \{[R_b, T_{in}], [R_b, L_c], [L_b, R_c], [T_{out}, L_c]\} \\
\mathcal{Q}_{31} &= \{[T_{in}, R_c], [R_b, L_c], [L_b, T_{out}], [L_b, R_c]\} & \mathcal{Q}_{32} &= \{[T_{in}, R_c], [R_b, L_c], [R_b, T_{in}], [L_b, R_c]\} \\
\mathcal{Q}_{33} &= \{[T_{out}, R_b], [T_{out}, L_c], [L_b, T_{out}], [R_c, T_{out}]\} & \mathcal{Q}_{34} &= \{[T_{in}, L_b], [R_b, T_{in}], [L_c, T_{in}], [T_{in}, R_c]\} \\
\mathcal{Q}_{35} &= \{[T_{in}, T_{out}], [T_{in}, L_b], [T_{in}, R_c], [R_b, L_c]\} & \mathcal{Q}_{36} &= \{[T_{in}, T_{out}], [R_b, L_c], [L_b, T_{out}], [R_c, T_{out}]\} \\
\mathcal{Q}_{37} &= \{[T_{in}, L_b], [L_c, R_b], [T_{in}, T_{out}], [T_{in}, R_c]\} & \mathcal{Q}_{38} &= \{[T_{in}, T_{out}], [L_c, R_b], [L_b, T_{out}], [R_c, T_{out}]\} \\
\mathcal{Q}_{39} &= \{[T_{out}, L_c], [T_{out}, R_b], [T_{out}, T_{in}], [L_b, R_c]\} & \mathcal{Q}_{40} &= \{[T_{out}, T_{in}], [R_b, T_{in}], [L_c, T_{in}], [L_b, R_c]\} \\
\mathcal{Q}_{41} &= \{[T_{out}, L_c], [T_{out}, R_b], [T_{out}, T_{in}], [R_c, L_b]\} & \mathcal{Q}_{42} &= \{[R_b, T_{in}], [T_{out}, T_{in}], [L_c, T_{in}], [R_c, L_b]\}.
\end{aligned}$$

The i -th web subset $\mathcal{Q}_i \subseteq \mathcal{W}_i \subseteq \mathcal{W}_\square$ is moreover a subset of the i -th web family \mathcal{W}_i (§5.1). More precisely, each of the four Hilbert basis webs $W^H \in \mathcal{Q}_i$ is determined by the schematic picture for the web family \mathcal{W}_i (as in Figure 16) by putting all but one of the variables x, y, z, t to 0 and the remaining variable to 1. Recall that the 9 specific web families denoted (j) in Figure 16 are the families \mathcal{W}_{i_j} as explained in Notation 5.2.

Definition 7.19. For $i = 1, 2, \dots, 42$, let $\mathcal{Q}_i \subseteq \mathcal{W}_i \subseteq \mathcal{W}_\square$ be the set of four webs defined just above, and recall that W_j^H for $j = 1, 2, \dots, 8$ are the 8 corner arcs in the square.

Define the i -th completed KTGS subcone $C_{\mathcal{T}}^i \subseteq C_{\mathcal{T}} \subseteq \mathbb{R}_+^{12}$ as the completion

$$C_{\mathcal{T}}^i = \overline{\mathcal{C}_{\mathcal{T}}^i}$$

of the i -th KTGS submonoid $\mathcal{C}_{\mathcal{T}}^i \subseteq \mathcal{C}_{\mathcal{T}} \subseteq \mathbb{Z}_+^{12}$, defined by

$$\mathcal{C}_{\mathcal{T}}^i = \text{span}_{\mathbb{Z}_+} \left(\{ \Phi_{\mathcal{T}}(W_1^H), \Phi_{\mathcal{T}}(W_2^H), \dots, \Phi_{\mathcal{T}}(W_8^H) \} \cup \{ \Phi_{\mathcal{T}}(W^H); \quad W^H \in \mathcal{Q}_i \} \right),$$

where $\Phi_{\mathcal{T}}(W^H) \in \mathcal{C}_{\mathcal{T}} \subseteq \mathbb{Z}_+^{12}$ is the point in the KTGS positive integer cone $\mathcal{C}_{\mathcal{T}}$ assigned to W^H by the web tropical coordinate map $\Phi_{\mathcal{T}} : \mathcal{W}_\square \rightarrow \mathcal{C}_{\mathcal{T}}$.

The set \mathcal{Q}_i of four webs is called the *topological type* of the completed KTGS subcone $C_{\mathcal{T}}^i$.

By construction of the web tropical coordinate map $\Phi_{\mathcal{T}}$, we can immediately say:

Observation 7.20. For $i = 1, 2, \dots, 42$, we have $\Phi_{\mathcal{T}}(\mathcal{W}_i) = \mathcal{C}_{\mathcal{T}}^i \subseteq \mathbb{Z}_+^{12}$.

The main result of this section is:

Theorem 7.21. Consider the completed KTGS cone $C_{\mathcal{T}} \subseteq \mathbb{R}_+^{12}$ for the triangulated square (\square, \mathcal{T}) ; see Definition 7.16. Then:

- $C_{\mathcal{T}}$ is 12-dimensional. Namely, $C_{\mathcal{T}}$ is a full cone; see Definition 7.2.
- The completed KTGS subcones $C_{\mathcal{T}}^i \subseteq C_{\mathcal{T}}$ are full sectors forming a sector decomposition $\{C_{\mathcal{T}}^i\}_{i=1,2,\dots,42}$ of $C_{\mathcal{T}}$; see Definition 7.5.
- The intersection $C_{\mathcal{T}}^i \cap C_{\mathcal{T}}^\ell$ is a wall if and only if $\mathcal{Q}_i \cap \mathcal{Q}_\ell$ has 3 elements; that is, if and only if the topological types of $C_{\mathcal{T}}^i$ and $C_{\mathcal{T}}^\ell$ differ by a single web. In this case,

(#)

$$C_{\mathcal{T}}^i \cap C_{\mathcal{T}}^\ell = \text{span}_{\mathbb{R}_+} \left(\{ \Phi_{\mathcal{T}}(W_1^H), \Phi_{\mathcal{T}}(W_2^H), \dots, \Phi_{\mathcal{T}}(W_8^H) \} \cup \{ \Phi_{\mathcal{T}}(W^H); \quad W^H \in \mathcal{Q}_i \cap \mathcal{Q}_\ell \} \right) \subseteq \mathbb{R}_+^{12}.$$

Moreover, for each web $W \in \mathcal{Q}_i$, there exists a unique index $i^*(i, W) \in \{1, 2, \dots, 42\}$ such that

$$\mathcal{Q}_i \cap \mathcal{Q}_{i^*(i, W)} = \mathcal{Q}_i - \{W\};$$

that is, such that there is a web $W^*(i, W) \in \mathcal{Q}_{i^*(i, W)}$ satisfying the property that the topological type $\mathcal{Q}_{i^*(i, W)}$ of $C_{\mathcal{T}}^{i^*(i, W)}$ is obtained from the topological type \mathcal{Q}_i of $C_{\mathcal{T}}^i$ by swapping W with $W^*(i, W)$. (One might think of such a swap as a web mutation.)

In particular, each sector $C_{\mathcal{T}}^i$ has 4 walls. See Figure 3.

Example 7.22. As an example of the second paragraph of the third item of the theorem, consider $i = i_1 = 29$, corresponding to family (1) in Figure 16. If $W = [L_b, T_{out}] \in \mathcal{Q}_{29}$, then $i^*(29, W) = i_2 = 30$ corresponding to family (2) in Figure 16, and $W^*(29, W) = [R_b, T_{in}] \in \mathcal{Q}_{30}$. One similarly checks that $i^*(29, [L_b, R_c]) = 28$ and $W^*(29, [L_b, R_c]) = [R_c, T_{out}] \in \mathcal{Q}_{28}$; that $i^*(29, [R_b, L_c]) = 25$ and $W^*(29, [R_b, L_c]) = [T_{out}, R_b] \in \mathcal{Q}_{25}$; and, that $i^*(29, [T_{out}, L_c]) = 31$ and $W^*(29, [T_{out}, L_c]) = [T_{in}, R_c] \in \mathcal{Q}_{31}$.

Note that Figure 3 provides some, but not all, of this topological information; the full information is contained in the definition of the subsets \mathcal{Q}_i above.

Question 7.23. By Theorem 6.10, the Hilbert basis $\mathcal{H}_{(\square, \mathcal{T})}$ of the positive integer cone $\mathcal{C}_{\mathcal{T}} \subseteq \mathbb{Z}_+^{12}$ has 22 elements. It follows by Observation 7.13 that $\text{rank}(C_{\mathcal{T}}) \leq 22$. By Theorem 7.21, $\text{rank}(C_{\mathcal{T}}) \geq 12$. We ask: What is the rank of $C_{\mathcal{T}}$?

Compare Example 7.14 and Corollary 7.18 as well as Example (part 1) in §7.1.2.

We will need to make some preparations before proving the theorem. In particular, we will make use of a generalization of the linear isomorphism used in the proof of Proposition 7.17.

7.3. Proof of Theorem 7.21.

7.3.1. Two linear isomorphisms: second isomorphism $\phi_{\mathcal{T}}$ by tropical \mathcal{X} -coordinates.

In §6.2.3, to each ideal triangulation \mathcal{T} of the square \square we constructed a linear isomorphism $\theta_{\mathcal{T}} : \mathbb{R}^{12} \rightarrow V_{\mathcal{T}} \subseteq \mathbb{R}^{18}$. This map sends 12 real numbers A_1, A_2, \dots, A_{12} , called the (real) tropical \mathcal{A} -coordinates, to their 18 rhombus numbers $\beta_1, \beta_2, \dots, \beta_{18}$. There are 6 relations (see (†) in §6.2.3) defining the 12-dimensional subspace $V_{\mathcal{T}} \subseteq \mathbb{R}^{18}$, which determine four real numbers X_1, X_2, X_3, X_4 , called the (real) tropical \mathcal{X} -coordinates: they are four numbers assigned to any 18-tuple in $V_{\mathcal{T}}$ of rhombus numbers. See Figure 23. See also [Xie13].

Remark 7.24. The tropical \mathcal{X} -coordinates originate in Fock-Goncharov theory as tropicalized double and triple ratios [FG06, FG07b], and can be thought of in the following geometric way. For X_1 , say, consider the hexagon in the top triangle in the top left square of Figure 23. There are six tropical \mathcal{A} -coordinates assigned to the vertices of this hexagon. Then X_1 is the signed sum of these coordinates, as indicated in the figure. Similarly for X_2, X_3, X_4 .

Definition 7.25. Let $V_{\mathcal{T}} \subseteq \mathbb{R}^{18}$ be the 12-dimensional subspace just discussed. Define a linear map

$$\phi_{\mathcal{T}} : V_{\mathcal{T}} \longrightarrow \mathbb{R}^8 \times \mathbb{R}^4$$

by

$$\phi_{\mathcal{T}}(\beta_1, \beta_2, \beta_3, \dots, \beta_{18}) = (\beta_1, \beta_2, \beta_4, \beta_5, \beta_7, \beta_8, \beta_{10}, \beta_{11}; \quad X_1, X_2, X_3, X_4).$$

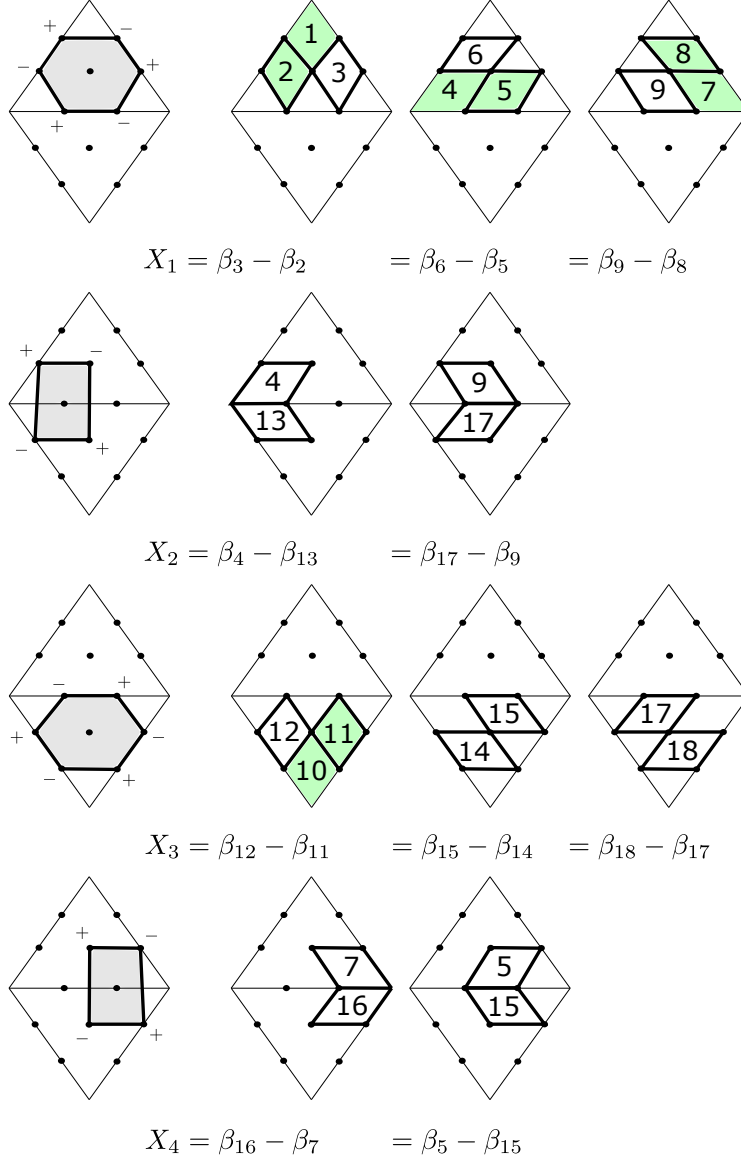


FIGURE 23. Shown are the 18 rhombus numbers $\{\beta_i\}_{i=1,2,\dots,18}$ for the square, and the associated 4 tropical integer \mathcal{X} -coordinates $\{X_i\}_{i=1,2,3,4}$. The latter can be computed either as differences of rhombus numbers, or as alternating sums of the 12 positive tropical integer \mathcal{A} -coordinates $\{A_i\}_{i=1,2,\dots,12}$ around the polygons displayed on the left. The rhombi colored green are those involved in the first 8 coordinates of the isomorphism $\phi_{\mathcal{T}} : V_{\mathcal{T}} \rightarrow \mathbb{R}^{12}$.

See Figure 23, where the eight rhombi appearing in the first eight coordinates of the image of $\phi_{\mathcal{T}}$ are colored green.

For example, the images under $\phi_{\mathcal{T}}$ of $\theta_{\mathcal{T}}$ applied to the 22 Hilbert basis elements, $\theta_{\mathcal{T}}(\Phi_{\mathcal{T}}(W_j^H)) \in V_{\mathcal{T}}$, can be computed from Figure 22 or from the computations in §6.2.3 to be:

- (1) $\phi_{\mathcal{T}}(\theta_{\mathcal{T}}(\Phi_{\mathcal{T}}([R_a]))) = (1, 0, 0, 0, 0, 0, 0, 0; \quad 0, 0, 0, 0)$
- (2) $\phi_{\mathcal{T}}(\theta_{\mathcal{T}}(\Phi_{\mathcal{T}}([L_a]))) = (0, 1, 0, 0, 0, 0, 0, 0; \quad 0, 0, 0, 0)$

$$\begin{aligned}
(3) \quad & \phi_{\mathcal{T}}(\theta_{\mathcal{T}}(\Phi_{\mathcal{T}}([R_b]))) = (0, 0, 1, 0, 0, 0, 0, 0; \quad 0, 0, 0, 0) \\
(4) \quad & \phi_{\mathcal{T}}(\theta_{\mathcal{T}}(\Phi_{\mathcal{T}}([L_b]))) = (0, 0, 0, 1, 0, 0, 0, 0; \quad 0, 0, 0, 0) \\
(5) \quad & \phi_{\mathcal{T}}(\theta_{\mathcal{T}}(\Phi_{\mathcal{T}}([R_c]))) = (0, 0, 0, 0, 1, 0, 0, 0; \quad 0, 0, 0, 0) \\
(6) \quad & \phi_{\mathcal{T}}(\theta_{\mathcal{T}}(\Phi_{\mathcal{T}}([L_c]))) = (0, 0, 0, 0, 0, 1, 0, 0; \quad 0, 0, 0, 0) \\
(7) \quad & \phi_{\mathcal{T}}(\theta_{\mathcal{T}}(\Phi_{\mathcal{T}}([R_d]))) = (0, 0, 0, 0, 0, 0, 1, 0; \quad 0, 0, 0, 0) \\
(8) \quad & \phi_{\mathcal{T}}(\theta_{\mathcal{T}}(\Phi_{\mathcal{T}}([L_d]))) = (0, 0, 0, 0, 0, 0, 0, 1; \quad 0, 0, 0, 0) \\
(9) \quad & \phi_{\mathcal{T}}(\theta_{\mathcal{T}}(\Phi_{\mathcal{T}}([T_{out}, R_b]))) = (0, 0, 0, 0, 0, 0, 0, 0; \quad 1, -1, 0, 0) \\
(10) \quad & \phi_{\mathcal{T}}(\theta_{\mathcal{T}}(\Phi_{\mathcal{T}}([T_{out}, L_c]))) = (0, 0, 0, 0, 0, 0, 0, 0; \quad 1, 0, 0, 0) \\
(11) \quad & \phi_{\mathcal{T}}(\theta_{\mathcal{T}}(\Phi_{\mathcal{T}}([T_{in}, L_b]))) = (0, 1, 0, 1, 0, 1, 0, 0; \quad -1, 0, 0, 0) \\
(12) \quad & \phi_{\mathcal{T}}(\theta_{\mathcal{T}}(\Phi_{\mathcal{T}}([T_{in}, R_c]))) = (0, 1, 0, 1, 0, 1, 0, 0; \quad -1, 0, 0, 1) \\
(13) \quad & \phi_{\mathcal{T}}(\theta_{\mathcal{T}}(\Phi_{\mathcal{T}}([L_b, T_{out}]))) = (0, 0, 0, 1, 0, 0, 0, 0; \quad 0, 0, 1, 0) \\
(14) \quad & \phi_{\mathcal{T}}(\theta_{\mathcal{T}}(\Phi_{\mathcal{T}}([L_c, T_{in}]))) = (0, 0, 0, 0, 0, 1, 0, 1; \quad 0, 0, -1, 0) \\
(15) \quad & \phi_{\mathcal{T}}(\theta_{\mathcal{T}}(\Phi_{\mathcal{T}}([R_b, T_{in}]))) = (0, 0, 1, 0, 0, 0, 0, 1; \quad 0, 1, -1, 0) \\
(16) \quad & \phi_{\mathcal{T}}(\theta_{\mathcal{T}}(\Phi_{\mathcal{T}}([R_c, T_{out}]))) = (0, 0, 0, 0, 1, 0, 0, 0; \quad 0, 0, 1, -1) \\
(17) \quad & \phi_{\mathcal{T}}(\theta_{\mathcal{T}}(\Phi_{\mathcal{T}}([T_{out}, T_{in}]))) = (0, 0, 0, 0, 0, 0, 0, 1; \quad 1, 0, -1, 0) \\
(18) \quad & \phi_{\mathcal{T}}(\theta_{\mathcal{T}}(\Phi_{\mathcal{T}}([T_{in}, T_{out}]))) = (0, 1, 0, 1, 0, 1, 0, 0; \quad -1, 0, 1, 0) \\
(19) \quad & \phi_{\mathcal{T}}(\theta_{\mathcal{T}}(\Phi_{\mathcal{T}}([L_b, R_c]))) = (0, 0, 0, 1, 0, 0, 0, 0; \quad 0, 0, 0, 1) \\
(20) \quad & \phi_{\mathcal{T}}(\theta_{\mathcal{T}}(\Phi_{\mathcal{T}}([R_b, L_c]))) = (0, 0, 1, 0, 0, 0, 0, 0; \quad 0, 1, 0, 0) \\
(21) \quad & \phi_{\mathcal{T}}(\theta_{\mathcal{T}}(\Phi_{\mathcal{T}}([R_c, L_b]))) = (0, 0, 0, 0, 1, 0, 0, 0; \quad 0, 0, 0, -1) \\
(22) \quad & \phi_{\mathcal{T}}(\theta_{\mathcal{T}}(\Phi_{\mathcal{T}}([L_c, R_b]))) = (0, 0, 0, 0, 0, 1, 0, 0; \quad 0, -1, 0, 0).
\end{aligned}$$

Proposition 7.26. *The linear map $\phi_{\mathcal{T}} : V_{\mathcal{T}} \rightarrow \mathbb{R}^8 \times \mathbb{R}^4$ is an isomorphism. Consequently, letting $\theta_{\mathcal{T}} : \mathbb{R}^{12} \rightarrow V_{\mathcal{T}}$ be the isomorphism from §6.2.3, we have that the composition*

$$\phi_{\mathcal{T}} \circ \theta_{\mathcal{T}} : \mathbb{R}^{12} \xrightarrow{\sim} \mathbb{R}^8 \times \mathbb{R}^4$$

is a linear isomorphism.

Proof. Since $V_{\mathcal{T}}$ is 12-dimensional (Proposition 6.14), it suffices to show that the image of $\phi_{\mathcal{T}}$ spans $\mathbb{R}^8 \times \mathbb{R}^4$. Indeed, one checks by elementary linear algebra that the above 22 images $\{\phi_{\mathcal{T}}(\theta_{\mathcal{T}}(\Phi_{\mathcal{T}}(W_j^H)))\}_{j=1,2,\dots,22} \subseteq \mathbb{R}_+^8 \times \mathbb{R}^4$ span $\mathbb{R}^8 \times \mathbb{R}^4$. \blacksquare

Definition 7.27. The linear isomorphism $\phi_{\mathcal{T}} \circ \theta_{\mathcal{T}} : \mathbb{R}^{12} \rightarrow \mathbb{R}^8 \times \mathbb{R}^4$ of Proposition 7.26 maps the completed KTGS cone $C_{\mathcal{T}} \subseteq \mathbb{R}_+^{12}$ to the *isomorphic cone*

$$C := \phi_{\mathcal{T}}(\theta_{\mathcal{T}}(C_{\mathcal{T}})) \subseteq \mathbb{R}_+^8 \times \mathbb{R}^4.$$

Note that C indeed lies in $\mathbb{R}_+^8 \times \mathbb{R}^4$ because $C_{\mathcal{T}} \subseteq \mathbb{R}_+^{12}$ is the completion of the KTGS cone $\mathcal{C}_{\mathcal{T}} \subseteq \mathbb{Z}_+^{12}$, which by definition has all nonnegative (integer) rhombus numbers $\{\beta_i\}_{i=1,2,\dots,18}$.

Observe, in particular, that the 8 corner arcs $W_1^H, W_2^H, \dots, W_8^H$ of Figure 22 (part 1) correspond via $\phi_{\mathcal{T}} \circ \theta_{\mathcal{T}} \circ \Phi_{\mathcal{T}}$ to the first 8 standard basis elements e_i of $\mathbb{R}^8 \times \mathbb{R}^4$.

7.3.2. Sector decomposition of \mathbb{R}^4 via the isomorphism $\phi_{\mathcal{T}} \circ \theta_{\mathcal{T}}$.

Let $C \subseteq \mathbb{R}_+^8 \times \mathbb{R}^4$ be the cone defined in Definition 7.27, which is isomorphic, via the isomorphism $\phi_{\mathcal{T}} \circ \theta_{\mathcal{T}} : \mathbb{R}^{12} \rightarrow \mathbb{R}^8 \times \mathbb{R}^4$, to the completed KTGS cone $C_{\mathcal{T}} \subseteq \mathbb{R}_+^{12}$ for the triangulated square (\square, \mathcal{T}) .

Notation 7.28. Put $k = 8$, $n = 4$, $m = 14$, and $p = 42$ (compare §7.1.2).

For $j = 1, 2, \dots, m$, define cone points $x_j \in C$ by

$$x_j = \phi_{\mathcal{T}}(\theta_{\mathcal{T}}(\Phi_{\mathcal{T}}(W_{k+j}^H))) \in C,$$

where $\Phi_{\mathcal{T}}(W_{j'}^H)$ is the j' -th Hilbert basis element for the triangulated square; see Figure 22. Note that the points $\{x_j\}_{j=1,2,\dots,m} \subseteq C$ are displayed explicitly in §7.3.1.

For $i = 1, 2, \dots, p$, define index sets $J_i \subseteq \{1, 2, \dots, m\}$ of constant size n as follows. Given i , consider the topological type $\mathcal{Q}_i \subseteq \mathcal{W}_i \subseteq \mathcal{W}_{\square}$ of the completed KTGS subcone $C_{\mathcal{T}}^i \subseteq \mathbb{R}_+^{12}$ (Definition 7.19). By definition of the topological type \mathcal{Q}_i , there are four Hilbert basis webs $W_{k+j_1^{(i)}}^H, W_{k+j_2^{(i)}}^H, W_{k+j_3^{(i)}}^H, W_{k+j_4^{(i)}}^H$, where the indices $j_r^{(i)} \in \{1, 2, \dots, m\}$, such that $\mathcal{Q}_i = \left\{ W_{k+j_r^{(i)}}^H \right\}_{r=1,2,3,4}$. We then define the index set J_i by

$$J_i = \left\{ j_1^{(i)}, j_2^{(i)}, j_3^{(i)}, j_4^{(i)} \right\} \subseteq \{1, 2, \dots, m\}.$$

Definition 7.29. Recalling Notation 7.28: for each $i = 1, 2, \dots, 42$, define subcones $D_i \subseteq \mathbb{R}^4$ by (compare §7.1.2)

$$D_i = \text{span}_{\mathbb{R}_+}(\{\pi_4(x_j); \quad j \in J_i\}) \subseteq \mathbb{R}^4.$$

Here, $\pi_4 : \mathbb{R}^8 \times \mathbb{R}^4 \rightarrow \mathbb{R}^4$ is the natural projection.

Just as for the subcones $C_{\mathcal{T}}^i \subseteq C_{\mathcal{T}}$, we call \mathcal{Q}_i the *topological type* of the subcone $D_i \subseteq \mathbb{R}^4$.

Remark 7.30. Note, by the calculations of §7.3.1, that the 14 vectors $\{\pi_4(x_j)\}_{j=1,2,\dots,14} \subseteq \mathbb{R}^4$ are distinct.

Proposition 7.31. *The subcones $D_i \subseteq \mathbb{R}^4$ are full sectors forming a sector decomposition $\{D_i\}_{i=1,2,\dots,42}$ of \mathbb{R}^4 (Definition 7.5).*

Proof. Let us begin by giving some examples of how to describe the subcones D_i . Specifically, we will describe those 9 subcones $D_{i_j} \subseteq \mathbb{R}^4$ corresponding to the topological types $\mathcal{Q}_{i_j} \subseteq \mathcal{W}_{i_j} \subseteq \mathcal{W}_{\square}$, which in particular are subsets of the (j) web families \mathcal{W}_{i_j} displayed in Figure 16; see Notation 5.2 and Remark 5.3.

Remark 7.32. In each of the 9 examples below, note that the ordering of the rows of the matrix does not affect the description of the subcone $D_i \subseteq \mathbb{R}^4$.

i1=29. For \mathcal{Q}_{29} , let us write the four vectors $\pi_4(\phi_{\mathcal{T}} \circ \theta_{\mathcal{T}} \circ \Phi_{\mathcal{T}}(\mathcal{Q}_{29})) \subseteq \mathbb{R}^4$ in rows to form a (4×4) matrix $M_{29} = \begin{pmatrix} 0 & 0 & 1 & 0 \\ 0 & 1 & 0 & 0 \\ 0 & 0 & 0 & 1 \\ 1 & 0 & 0 & 0 \end{pmatrix}$. Then for real numbers $x, y, z, t \geq 0$, we get

$$\begin{pmatrix} x & y & z & t \end{pmatrix} M_{29} = \begin{pmatrix} t & y & x & z \end{pmatrix}.$$

Thus $D_{29} = \{(X_1, X_2, X_3, X_4) \in \mathbb{R}_+ \times \mathbb{R}_+ \times \mathbb{R}_+ \times \mathbb{R}_+\}$.

i2=30. Similarly, for \mathcal{Q}_{30} , writing the four vectors $\pi_4(\phi_{\mathcal{T}} \circ \theta_{\mathcal{T}} \circ \Phi_{\mathcal{T}}(\mathcal{Q}_{30}))$ in rows, we get a (4×4) matrix $M_{30} = \begin{pmatrix} 0 & 1 & -1 & 0 \\ 0 & 1 & 0 & 0 \\ 0 & 0 & 0 & 1 \\ 1 & 0 & 0 & 0 \end{pmatrix}$. Then for $x, y, z, t \geq 0$, we get

$$\begin{pmatrix} x & y & z & t \end{pmatrix} M_{30} = \begin{pmatrix} t & x+y & -x & z \end{pmatrix}.$$

Thus $D_{30} = \{(X_1, X_2, X_3, X_4) \in \mathbb{R}_+ \times \mathbb{R}_+ \times \mathbb{R}_- \times \mathbb{R}_+ \mid X_2 + X_3 \geq 0\}$.

i3=42. For \mathcal{Q}_{42} , writing the four vectors $\pi_4(\phi_{\mathcal{T}} \circ \theta_{\mathcal{T}} \circ \Phi_{\mathcal{T}}(\mathcal{Q}_{42}))$ in rows, we get a (4×4) matrix $M_{42} = \begin{pmatrix} 0 & 1 & -1 & 0 \\ 1 & 0 & -1 & 0 \\ 0 & 0 & -1 & 0 \\ 0 & 0 & 0 & -1 \end{pmatrix}$. Then for $x, y, z, t \geq 0$, we get

$$\begin{pmatrix} x & y & z & t \end{pmatrix} M_{42} = \begin{pmatrix} y & x & -x - y - z & -t \end{pmatrix}.$$

Thus $D_{42} = \{(X_1, X_2, X_3, X_4) \in \mathbb{R}_+ \times \mathbb{R}_+ \times \mathbb{R}_- \times \mathbb{R}_- \mid X_1 + X_2 + X_3 \leq 0\}$.

i4=17. For \mathcal{Q}_{17} , writing the four vectors $\pi_4(\phi_{\mathcal{T}} \circ \theta_{\mathcal{T}} \circ \Phi_{\mathcal{T}}(\mathcal{Q}_{17}))$ in rows, we get a (4×4) matrix $M_{17} = \begin{pmatrix} 1 & -1 & 0 & 0 \\ 1 & 0 & 0 & 0 \\ 0 & 0 & 0 & -1 \\ 0 & 0 & 1 & -1 \end{pmatrix}$. Then for $x, y, z, t \geq 0$, we get

$$\begin{pmatrix} x & y & z & t \end{pmatrix} M_{17} = \begin{pmatrix} x + y & -x & t & -z - t \end{pmatrix}.$$

Thus $D_{17} = \{(X_1, X_2, X_3, X_4) \in \mathbb{R}_+ \times \mathbb{R}_- \times \mathbb{R}_+ \times \mathbb{R}_- \mid X_1 + X_2 \geq 0 \text{ \& } X_3 + X_4 \leq 0\}$.

i5=5. For \mathcal{Q}_5 , writing the four vectors $\pi_4(\phi_{\mathcal{T}} \circ \theta_{\mathcal{T}} \circ \Phi_{\mathcal{T}}(\mathcal{Q}_5))$ in rows, we get a (4×4) matrix $M_5 = \begin{pmatrix} -1 & 0 & 1 & 0 \\ -1 & 0 & 0 & 0 \\ 0 & 0 & 1 & -1 \\ 0 & 1 & 0 & 0 \end{pmatrix}$. Then for $x, y, z, t \geq 0$, we get

$$\begin{pmatrix} x & y & z & t \end{pmatrix} M_5 = \begin{pmatrix} -x - y & t & x + z & -z \end{pmatrix}.$$

Thus $D_5 = \{(X_1, X_2, X_3, X_4) \in \mathbb{R}_- \times \mathbb{R}_+ \times \mathbb{R}_+ \times \mathbb{R}_- \mid -X_1 \geq X_3 + X_4 \geq 0\}$.

i6=6. For \mathcal{Q}_6 , writing the four vectors $\pi_4(\phi_{\mathcal{T}} \circ \theta_{\mathcal{T}} \circ \Phi_{\mathcal{T}}(\mathcal{Q}_6))$ in rows, we get a (4×4) matrix $M_6 = \begin{pmatrix} 0 & 0 & 1 & 0 \\ -1 & 0 & 1 & 0 \\ -1 & 0 & 0 & 1 \\ 0 & 1 & 0 & 0 \end{pmatrix}$. Then for $x, y, z, t \geq 0$, we get

$$\begin{pmatrix} x & y & z & t \end{pmatrix} M_6 = \begin{pmatrix} -y - z & t & x + y & z \end{pmatrix}.$$

Thus $D_6 = \{(X_1, X_2, X_3, X_4) \in \mathbb{R}_- \times \mathbb{R}_+ \times \mathbb{R}_+ \times \mathbb{R}_+ \mid -X_3 \leq X_1 + X_4 \leq 0\}$.

i7=2. For \mathcal{Q}_2 , writing the four vectors $\pi_4(\phi_{\mathcal{T}} \circ \theta_{\mathcal{T}} \circ \Phi_{\mathcal{T}}(\mathcal{Q}_2))$ in rows, we get a (4×4) matrix $M_2 = \begin{pmatrix} 1 & 0 & 0 & 0 \\ 0 & 0 & 1 & -1 \\ 0 & 0 & 0 & -1 \\ 0 & 1 & 0 & 0 \end{pmatrix}$. Then for $x, y, z, t \geq 0$, we get

$$\begin{pmatrix} x & y & z & t \end{pmatrix} M_2 = \begin{pmatrix} x & t & y & -y - z \end{pmatrix}.$$

Thus $D_2 = \{(X_1, X_2, X_3, X_4) \in \mathbb{R}_+ \times \mathbb{R}_+ \times \mathbb{R}_+ \times \mathbb{R}_- \mid X_3 + X_4 \leq 0\}$.

i8=1. For \mathcal{Q}_1 , writing the four vectors $\pi_4(\phi_{\mathcal{T}} \circ \theta_{\mathcal{T}} \circ \Phi_{\mathcal{T}}(\mathcal{Q}_1))$ in rows, we get a (4×4) matrix $M_1 = \begin{pmatrix} -1 & 0 & 0 & 0 \\ 0 & 0 & 1 & -1 \\ 0 & 0 & 0 & -1 \\ 0 & 1 & 0 & 0 \end{pmatrix}$. Then for $x, y, z, t \geq 0$, we get

$$\begin{pmatrix} x & y & z & t \end{pmatrix} M_1 = \begin{pmatrix} -x & t & y & -y - z \end{pmatrix}.$$

Thus $D_1 = \{(X_1, X_2, X_3, X_4) \in \mathbb{R}_- \times \mathbb{R}_+ \times \mathbb{R}_+ \times \mathbb{R}_- \mid X_3 + X_4 \leq 0\}$.

i9=33. For \mathcal{Q}_{33} , writing the four vectors $\pi_4(\phi_{\mathcal{T}} \circ \theta_{\mathcal{T}} \circ \Phi_{\mathcal{T}}(\mathcal{Q}_{33}))$ in rows, we get a (4×4) matrix $M_{33} = \begin{pmatrix} 1 & -1 & 0 & 0 \\ 1 & 0 & 0 & 0 \\ 0 & 0 & 1 & 0 \\ 0 & 0 & 1 & -1 \end{pmatrix}$. Then for $x, y, z, t \geq 0$, we get

$$\begin{pmatrix} x & y & z & t \end{pmatrix} M_{33} = \begin{pmatrix} x + y & -x & z + t & -t \end{pmatrix}.$$

Thus $D_{33} = \{(X_1, X_2, X_3, X_4) \in \mathbb{R}_+ \times \mathbb{R}_- \times \mathbb{R}_+ \times \mathbb{R}_- \mid X_1 + X_2 \geq 0 \text{ \& } X_3 + X_4 \geq 0\}$.

In the same way as the 9 examples just demonstrated, we compute directly by hand the subcones $D_i \subseteq \mathbb{R}^4$ for $i = 1, 2, \dots, 42$ as follows:

$$D_1 = \{(X_1, X_2, X_3, X_4) \in \mathbb{R}_- \times \mathbb{R}_+ \times \mathbb{R}_+ \times \mathbb{R}_- \mid X_3 + X_4 \leq 0\}$$

$$D_2 = \{(X_1, X_2, X_3, X_4) \in \mathbb{R}_+ \times \mathbb{R}_+ \times \mathbb{R}_+ \times \mathbb{R}_- \mid X_3 + X_4 \leq 0\}$$

$$D_{39} = \{(X_1, X_2, X_3, X_4) \in \mathbb{R}_+ \times \mathbb{R}_- \times \mathbb{R}_- \times \mathbb{R}_+ \mid X_1 + X_2 + X_3 \geq 0\}$$

$$D_{40} = \{(X_1, X_2, X_3, X_4) \in \mathbb{R}_+ \times \mathbb{R}_+ \times \mathbb{R}_- \times \mathbb{R}_+ \mid X_1 + X_2 + X_3 \leq 0\}$$

$$D_{41} = \{(X_1, X_2, X_3, X_4) \in \mathbb{R}_+ \times \mathbb{R}_- \times \mathbb{R}_- \times \mathbb{R}_- \mid X_1 + X_2 + X_3 \geq 0\}$$

$$D_{42} = \{(X_1, X_2, X_3, X_4) \in \mathbb{R}_+ \times \mathbb{R}_+ \times \mathbb{R}_- \times \mathbb{R}_- \mid X_1 + X_2 + X_3 \leq 0\}.$$

In particular, each subcone $D_i \subseteq \mathbb{R}^4$ has dimension 4, since its explicit description via inequalities shows that it has nonempty interior in \mathbb{R}^4 . Equivalently, one can check directly by hand that the corresponding 4×4 matrix, such as in the 9 examples above, has rank 4.

Since, by Definition 7.29, the subcones $D_i \subseteq \mathbb{R}^4$ are generated by 4 elements, we gather that each D_i is a full subsector of \mathbb{R}^4 .

One checks directly by hand that the 16 orthants $\mathbb{R}_\pm \times \mathbb{R}_\pm \times \mathbb{R}_\pm \times \mathbb{R}_\pm \subseteq \mathbb{R}^4$ decompose as:

- (1) $\mathbb{R}_- \times \mathbb{R}_- \times \mathbb{R}_- \times \mathbb{R}_- = D_{24}$
- (2) $\mathbb{R}_+ \times \mathbb{R}_+ \times \mathbb{R}_+ \times \mathbb{R}_+ = D_{29}$
- (3) $\mathbb{R}_+ \times \mathbb{R}_+ \times \mathbb{R}_+ \times \mathbb{R}_- = D_2 \cup D_{28}$
- (4) $\mathbb{R}_- \times \mathbb{R}_+ \times \mathbb{R}_- \times \mathbb{R}_- = D_3 \cup D_{18}$
- (5) $\mathbb{R}_- \times \mathbb{R}_+ \times \mathbb{R}_+ \times \mathbb{R}_+ = D_6 \cup D_{31} \cup D_{35}$
- (6) $\mathbb{R}_- \times \mathbb{R}_- \times \mathbb{R}_+ \times \mathbb{R}_- = D_7 \cup D_{23} \cup D_{38}$
- (7) $\mathbb{R}_- \times \mathbb{R}_- \times \mathbb{R}_- \times \mathbb{R}_+ = D_{10} \cup D_{19}$
- (8) $\mathbb{R}_+ \times \mathbb{R}_- \times \mathbb{R}_+ \times \mathbb{R}_+ = D_{11} \cup D_{25}$
- (9) $\mathbb{R}_+ \times \mathbb{R}_+ \times \mathbb{R}_- \times \mathbb{R}_+ = D_{14} \cup D_{30} \cup D_{40}$
- (10) $\mathbb{R}_+ \times \mathbb{R}_- \times \mathbb{R}_- \times \mathbb{R}_- = D_{15} \cup D_{22} \cup D_{41}$
- (11) $\mathbb{R}_- \times \mathbb{R}_+ \times \mathbb{R}_+ \times \mathbb{R}_- = D_1 \cup D_5 \cup D_{36}$
- (12) $\mathbb{R}_+ \times \mathbb{R}_+ \times \mathbb{R}_- \times \mathbb{R}_- = D_4 \cup D_{16} \cup D_{42}$
- (13) $\mathbb{R}_- \times \mathbb{R}_- \times \mathbb{R}_+ \times \mathbb{R}_+ = D_8 \cup D_{12} \cup D_{37}$
- (14) $\mathbb{R}_+ \times \mathbb{R}_- \times \mathbb{R}_- \times \mathbb{R}_+ = D_9 \cup D_{13} \cup D_{39}$
- (15) $\mathbb{R}_+ \times \mathbb{R}_- \times \mathbb{R}_+ \times \mathbb{R}_- = D_{17} \cup D_{20} \cup D_{21} \cup D_{33}$
- (16) $\mathbb{R}_- \times \mathbb{R}_+ \times \mathbb{R}_- \times \mathbb{R}_+ = D_{26} \cup D_{27} \cup D_{32} \cup D_{34}.$

It follows that $\mathbb{R}^4 = \cup_{i=1}^{42} D_i$. It remains to show that $D_i \cap D_\ell$ has empty interior for all pairwise-distinct i, ℓ . Since this is true if D_i and D_ℓ lie in different orthants, we only need to check those pairs D_i, D_ℓ lying in the same orthant.

This is done directly by hand; however, the cases fall into only four types. First, for orthants 1, 2: There is nothing to check. Second, for orthants 3, 4, 7, 8: In 3, say, the inequalities $X_3 + X_4 \leq 0$ and $X_3 + X_4 \geq 0$ have codimension 1 intersection even when defined on all of \mathbb{R}^4 , so they do as well when restricted to the orthant. The other cases go the same. Third, for orthants 15, 16: This is similar to the second type. Lastly, for orthants 5, 6, 9, 10, 11, 12, 13, 14: In 5, say, the sectors D_6 and D_{31} similarly have codimension 1 intersection, as do the sectors D_6 and D_{35} . This is also true for $D_{31} (X_1 + X_4 \geq 0)$ and $D_{35} (X_1 + X_3 + X_4 \leq 0)$ so long as $D_{31} \cap D_{35}$ implies $X_3 = 0$, which it does, since it implies $X_3 \leq -X_1 - X_4 \leq 0$ whereas we are restricted to the orthant $\mathbb{R}_- \times \mathbb{R}_+ \times \mathbb{R}_+ \times \mathbb{R}_+$. The other cases go the same. ■

We now analyze the walls (Definition 7.5) in the sector decomposition $\{D_i\}_{i=1,2,\dots,42}$ of \mathbb{R}^4 . Recall (Definition 7.29) that \mathcal{Q}_i is called the topological type of the sector D_i .

Proposition 7.33. *The third item of Theorem 7.21 holds word-for-word, except with $C_{\mathcal{T}}^i$ replaced by D_i , and replacing $(\#)$ by $(*)$ below.*

In particular, $D_i \cap D_\ell$ is a wall if and only if the intersection $J_i \cap J_\ell$ of their corresponding index sets has 3 elements (see the beginning of this sub-subsection, §7.3.2). In this case,

$$(*) \quad D_i \cap D_\ell = \text{span}_{\mathbb{R}_+}(\{\pi_4(x_j); \quad j \in J_i \cap J_\ell\}) \subseteq \mathbb{R}^4.$$

Proof. Any wall $D_i \cap D_\ell$ must, by definition, be 3 dimensional. This restricts which indices $\{i, \ell\}$ can yield walls. Through a direct by hand check, using the explicit description by inequalities of the sector decomposition $\{D_i\}_i$ as in the proof of Proposition 7.31, one verifies that a necessary condition for $D_i \cap D_\ell$ to be a wall is for D_i and D_ℓ to be connected by an edge in the graph \mathcal{G} depicted in Figure 3. We show this is also a sufficient condition.

More precisely, the goal is to show, for any two sectors D_i and D_ℓ connected by an edge in \mathcal{G} , that $J_i \cap J_\ell$ has 3 elements and $(*)$ holds. In particular, $D_i \cap D_\ell$ is a cone of dimension 3. Note the inclusion \supseteq in $(*)$ holds automatically; see Definition 7.29.

We checked this directly by hand. There are two types of calculations, depending on whether the sectors are in different orthants or the same orthant.

As an example where the sectors are in different orthants: We demonstrate this for D_{29} and D_{30} , which were computed in detail in the proof of Proposition 7.31. There, one sees that three rows of the corresponding 4×4 matrix M_{29} appear as rows in the matrix M_{30} (recall also Remark 7.32). This means that $J_i \cap J_\ell$ has 3 elements; see Remark 7.30. Note that the row in M_{29} that is not in M_{30} corresponds to the variable x , and the row in M_{30} that is not in M_{29} corresponds to the variable x' . The inclusion \subseteq in $(*)$ is true since

$$(t, y, x, z) = (t', x' + y', -x', z') \in \mathbb{R}^4 \quad (x, y, z, t, x', y', z', t' \geq 0)$$

implies $x = x' = 0$. The other different-orthant cases are similar.

As an example where the sectors are in the same orthant: We demonstrate this for D_5 and D_1 , which were also computed in detail in the proof of Proposition 7.31. There, one sees that three rows of the corresponding 4×4 matrix M_5 appear as rows in the matrix M_1 (recall also Remark 7.32). This means that $J_i \cap J_\ell$ has 3 elements; see Remark 7.30. The row in M_5 not in M_1 corresponds to the variable x , and the row in M_1 not in M_5 corresponds to the variable z' . The inclusion \subseteq in $(*)$ is true since

$$(-x - y, t, x + z, -z) = (-x', t', y', -y' - z') \in \mathbb{R}^4 \quad (x, y, z, t, x', y', z', t' \geq 0)$$

implies, by adding the third and fourth entries, that $x = -z'$ hence $x = z' = 0$. The other same-orthant cases are similar.

We gather $D_i \cap D_\ell$ is a wall if and only if D_i and D_ℓ are connected by an edge of the graph \mathcal{G} , in which case $J_i \cap J_\ell$ has 3 elements. In particular, since \mathcal{G} is 4-valent, the last paragraph of the third item of Theorem 7.21 holds (again, with D_i in place of $C_{\mathcal{T}}^i$).

To finish justifying the second paragraph of Proposition 7.33 (equivalently, the first paragraph of the third item of Theorem 7.21, appropriately substituted), we need to show that if $J_i \cap J_\ell$ has 3 elements (equivalently, $\mathcal{Q}_i \cap \mathcal{Q}_\ell$ has 3 elements), then $D_i \cap D_\ell$ is a wall.

So far, we have exhibited, for each i , 4 topological types \mathcal{Q}_ℓ such that $\mathcal{Q}_i \cap \mathcal{Q}_\ell$ has 3 elements, all corresponding to walls $D_i \cap D_\ell$. We thus need to show there are no more indices ℓ such that $\mathcal{Q}_i \cap \mathcal{Q}_\ell$ has 3 elements. For this, it suffices to establish the second paragraph of the third item of Theorem 7.21, which is a purely topological statement about webs in good position

on the triangulated square; compare Observation 3.8 and Proposition 5.1. We checked this directly by hand; compare Example 7.22. \blacksquare

7.3.3. Bringing everything together.

We are now prepared to prove the main result of this section.

Proof of Theorem 7.21. Let $C \subseteq \mathbb{R}_+^8 \times \mathbb{R}^4$ be the cone isomorphic to the completed KTGS cone $C_{\mathcal{T}} \subseteq \mathbb{R}_+^{12}$ via the linear isomorphism $\phi_{\mathcal{T}} \circ \theta_{\mathcal{T}} : \mathbb{R}^{12} \rightarrow \mathbb{R}^8 \times \mathbb{R}^4$; see Definition 7.27.

Recall also Notation 7.28 from the discussion at the beginning of §7.3.2, which should help with comparing the general lemmas of §7.1.2 to the current application.

By the explicit calculation of the Hilbert basis elements $\phi_{\mathcal{T}} \circ \theta_{\mathcal{T}} \circ \Phi_{\mathcal{T}}(W_i^H) \in C$ for $i = 1, 2, \dots, 22$ in §7.3.1, together with Proposition 7.31, we see that $C \subseteq \mathbb{R}_+^8 \times \mathbb{R}^4$ satisfies the hypotheses of Lemma 7.9. Indeed, $D_i \subseteq \pi_4(C)$ by definition, for each i . Therefore, C is 12 dimensional, so the isomorphic completed KTGS cone $C_{\mathcal{T}}$ is 12 dimensional as well. This establishes the first item of Theorem 7.21.

Let us prove that $C_{\mathcal{T}} = \cup_{i=1}^{42} C_{\mathcal{T}}^i \subseteq \mathbb{R}_+^{12}$; see Definition 7.19. This follows by Theorem 3.9, Proposition 5.1, and Lemma 7.15. Indeed, by Theorem 3.9, every point in the KTGS positive integer cone $\mathcal{C}_{\mathcal{T}} \subseteq \mathbb{Z}_+^{12}$ is equal to $\Phi_{\mathcal{T}}(W)$ for some reduced web $W \in \mathcal{W}_{\square}$ in the square. By Proposition 5.1, the web W is an element of one of the 42 web families: $W \in \mathcal{W}_i \subseteq \mathcal{W}_{\square}$. By Observation 7.20, we have that $\Phi_{\mathcal{T}}(W) \in \mathcal{C}_{\mathcal{T}}^i$. We gather that $\mathcal{C}_{\mathcal{T}} = \cup_{i=1}^{42} \mathcal{C}_{\mathcal{T}}^i \subseteq \mathbb{Z}_+^{12}$. Note that the monoid $\mathcal{C}_{\mathcal{T}} \subseteq \mathbb{Z}_+^{12}$ is finitely generated, since it admits a Hilbert basis (Theorem 6.10). The submonoids $\mathcal{C}_{\mathcal{T}}^i \subseteq \mathcal{C}_{\mathcal{T}}$ are also finitely generated, by Definition 7.19. We conclude by Lemma 7.15 that we have the equality $C_{\mathcal{T}} = \cup_{i=1}^{42} C_{\mathcal{T}}^i \subseteq \mathbb{R}_+^{12}$ of completions, as desired.

We return to the isomorphic cone $C \subseteq \mathbb{R}_+^8 \times \mathbb{R}^4$. Let $\{x_j\}_{j=1,2,\dots,14}$ and $\{J_i\}_{i=1,2,\dots,42}$ be defined as in the beginning of §7.3.2. For $i = 1, 2, \dots, 42$, let the subcones $C_i \subseteq C$ be defined as in the statement of Lemma 7.10. Equivalently, the subcone $C_i = \phi_{\mathcal{T}} \circ \theta_{\mathcal{T}}(C_{\mathcal{T}}^i) \subseteq \mathbb{R}_+^8 \times \mathbb{R}^4$ is the isomorphic counterpart to the subcone $C_{\mathcal{T}}^i \subseteq C_{\mathcal{T}} \subseteq \mathbb{R}_+^{12}$. It follows by the previous paragraph that $C = \cup_{i=1}^{42} C_i \subseteq \mathbb{R}_+^8 \times \mathbb{R}^4$ in the isomorphic cone C . By this, together with another application of Proposition 7.31, we see that the hypotheses of Lemma 7.10 are satisfied. Therefore, by Lemma 7.10, we obtain the second item of Theorem 7.21, except with $C_{\mathcal{T}}$ and $C_{\mathcal{T}}^i$ replaced by C and C_i , respectively. Since this property is preserved by linear isomorphisms, we conclude the second item of Theorem 7.21 as stated.

Lastly, by Proposition 7.33, in particular (*), the hypothesis of Lemma 7.11 is satisfied. Therefore, by Lemma 7.11, the set $\{\text{walls of } \{C_i\}_i \text{ in } C\}$ is in one-to-one correspondence with the set $\{\text{walls of } \{D_i\}_i \text{ in } \mathbb{R}^n\}$ in the obvious way by the projection π_4 . Moreover, a given wall $C_i \cap C_{\ell}$ can be computed by (%) in Lemma 7.11. We conclude by the remainder of Proposition 7.33 that the first and third paragraphs of the third item of Theorem 7.21 are valid, except with $C_{\mathcal{T}}$, $C_{\mathcal{T}}^i$, and (#) replaced by C , C_i , and (%), respectively. Since the inverse of the linear isomorphism $\phi_{\mathcal{T}} \circ \theta_{\mathcal{T}}$ preserves these properties, and maps (%) to (#) (see the beginning of §7.3.2), we conclude the first and third paragraphs of the second item of Theorem 7.21 as stated. The second paragraph is a purely topological statement about webs in the square, and was already established during the proof of Proposition 7.33. \blacksquare

The following consequence is immediate from the proof of Theorem 7.21.

Corollary 7.34. *The function*

$$\pi_4 \circ \phi_{\mathcal{T}} \circ \theta_{\mathcal{T}} : C_{\mathcal{T}} \rightarrow \mathbb{R}^4$$

is a surjection from the completed KTGS cone $C_{\mathcal{T}} \subseteq \mathbb{R}_+^{12}$ (in fact, from a “4 dimensional” proper subset of $C_{\mathcal{T}}$) onto \mathbb{R}^4 . \blacksquare

Recall the notion of a cornerless web $W = W_c$ in the square; see Definition 4.8. Let $\mathcal{W}_{\square}^c \subseteq \mathcal{W}_{\square}$ denote the set of cornerless webs up to equivalence. Note for each $i = 1, 2, \dots, 42$ that $\mathcal{Q}_i \subseteq \mathcal{W}_i \cap \mathcal{W}_{\square}^c$.

Consider also the function $\pi_4 \circ \phi_{\mathcal{T}} \circ \theta_{\mathcal{T}} \circ \Phi_{\mathcal{T}} : \mathcal{W}_{\square} \rightarrow \mathbb{Z}^4 \subseteq \mathbb{R}^4$ defined on \mathcal{W}_{\square} . See for example the nine computations at the beginning of the proof of Proposition 7.31.

Another consequence of the proof of Theorem 7.21 is:

Corollary 7.35. *The restricted function*

$$\pi_4 \circ \phi_{\mathcal{T}} \circ \theta_{\mathcal{T}} \circ \Phi_{\mathcal{T}} : \mathcal{W}_{\square}^c \twoheadrightarrow \mathbb{Z}^4,$$

restricted to the cornerless webs $\mathcal{W}_{\square}^c \subseteq \mathcal{W}_{\square}$, is a surjection onto the integer lattice $\mathbb{Z}^4 \subseteq \mathbb{R}^4$.

In particular, the function $\pi_4 \circ \phi_{\mathcal{T}} \circ \theta_{\mathcal{T}}$ from Corollary 7.34 maps (a “4 dimensional” proper subset of) the KTGS cone $\mathcal{C}_{\mathcal{T}} \subseteq \mathbb{Z}_+^{12}$ surjectively onto \mathbb{Z}^4 .

Proof. We know that $\mathbb{R}^4 = \cup_{i=1}^{42} D_i$ and $D_i = \pi_4 \circ \phi_{\mathcal{T}} \circ \theta_{\mathcal{T}}(C_{\mathcal{T}}^i)$ where $C_{\mathcal{T}}^i \supseteq \mathcal{C}_{\mathcal{T}}^i$ (Definition 7.19). We also know that the cone points $\Phi_{\mathcal{T}}(W_j^H)$ in $\mathcal{C}_{\mathcal{T}}^i$ for $j = 1, 2, \dots, 8$, corresponding to the 8 corner arcs in the square, are sent by $\phi_{\mathcal{T}} \circ \theta_{\mathcal{T}}$ to the first 8 standard basis elements e_j of $\mathbb{R}_+^8 \times \mathbb{R}^4$. We gather $\pi_4 \circ \phi_{\mathcal{T}} \circ \theta_{\mathcal{T}}$ is still a surjection onto D_i when restricted to the subset

$$C_{\mathcal{T}}^{\prime i} := \text{span}_{\mathbb{R}_+}(\{\Phi_{\mathcal{T}}(W^H); \quad W^H \in \mathcal{Q}_i\}) \subseteq C_{\mathcal{T}}^i \subseteq \mathbb{R}_+^{12}.$$

Note also that (similar to Observation 7.20)

$$\Phi_{\mathcal{T}}(\mathcal{W}_i \cap \mathcal{W}_{\square}^c) = \text{span}_{\mathbb{Z}_+}(\{\Phi_{\mathcal{T}}(W^H); \quad W^H \in \mathcal{Q}_i\}) \subseteq C_{\mathcal{T}}^{\prime i}.$$

It thus suffices to show: for any $c \in C_{\mathcal{T}}^{\prime i}$, if $\pi_4 \circ \phi_{\mathcal{T}} \circ \theta_{\mathcal{T}}(c) \in \mathbb{Z}^4 \cap D_i$, then $c \in \Phi_{\mathcal{T}}(\mathcal{W}_i \cap \mathcal{W}_{\square}^c)$.

Once again, we work in the isomorphic cone $C_i = \phi_{\mathcal{T}} \circ \theta_{\mathcal{T}}(C_{\mathcal{T}}^i) \subseteq \mathbb{R}_+^8 \times \mathbb{R}^4$, which projects to D_i by π_4 . Put (see the beginning of §7.3.2)

$$C_i' := \phi_{\mathcal{T}} \circ \theta_{\mathcal{T}}(C_{\mathcal{T}}^{\prime i}) = \text{span}_{\mathbb{R}_+}(\{x_j; \quad j \in J_i\}) \subseteq C_i \subseteq \mathbb{R}_+^8 \times \mathbb{R}^4$$

and note also that

$$\phi_{\mathcal{T}} \circ \theta_{\mathcal{T}} \circ \Phi_{\mathcal{T}}(\mathcal{W}_i \cap \mathcal{W}_{\square}^c) = \text{span}_{\mathbb{Z}_+}(\{x_j; \quad j \in J_i\}) \subseteq C_i'.$$

The above property is then equivalent to showing: for any $c \in C_i'$ such that $\pi_4(c) \in \mathbb{Z}^4 \cap D_i$, we have $c \in \phi_{\mathcal{T}} \circ \theta_{\mathcal{T}} \circ \Phi_{\mathcal{T}}(\mathcal{W}_i \cap \mathcal{W}_{\square}^c)$; that is, if such a $c \in C_i'$ is written $c = xx_{1(i)} + yy_{2(i)} + zx_{3(i)} + tx_{4(i)}$ for $x, y, z, t \geq 0$ (see the beginning of §7.3.2), we want to show $x, y, z, t \in \mathbb{Z}$.

This is accomplished through a direct by hand check, taking advantage of the explicit description of the sectors D_i provided in §7.3.2. As before, although there are 42 cases, these fall into only five types, each represented among the 9 examples demonstrated in the proof of Proposition 7.31: Type 1 corresponds to i_1 ; Type 2 corresponds to i_2, i_7, i_8 ; Type 3 corresponds to i_3 ; Type 4 corresponds to i_4, i_9 ; and Type 5 corresponds to i_5, i_6 . We will only demonstrate the most nontrivial case, Type 5 (for i_5 , say); the other cases are similar.

So consider $i_5 = 5$, and assume $\pi_4(c) = x\pi_4(x_{1(5)}) + y\pi_4(x_{2(5)}) + z\pi_4(x_{3(5)}) + t\pi_4(x_{4(5)}) \in D_i$ is, in addition, in \mathbb{Z}^4 for some $x, y, z, t \geq 0$. Note the vector $\pi_4(x_{j(5)})$ is the j -th row of the matrix displayed in the i_5 example in the proof of Proposition 7.31. From this example, we gather that $\pi_4(c) = (-x - y, t, x + z, -z) \in \mathbb{Z}^4$. So $t, z \in \mathbb{Z}$; implying by $x + z \in \mathbb{Z}$ that $x \in \mathbb{Z}$; implying by $-x - y \in \mathbb{Z}$ that $y \in \mathbb{Z}$, as desired. \blacksquare

Remark 7.36. We believe that the restricted function from Corollary 7.35 is also an injection. We suspect that there may be a proof of this result via a conjectural generalization of (#) to higher codimension intersections.

Conceptual Remark 7.37. Recall Remark 6.15. Recall also (§2.3) $\mathcal{A}_{\mathrm{PGL}_3, \square}^+(\mathbb{R}^t) = \mathcal{A}_{\mathrm{SL}_3, \square}^+(\mathbb{R}^t)$.

We view the real cone $C_{\mathcal{T}} \subseteq \mathbb{R}_+^{12}$ as the isomorphic \mathcal{T} -chart $C_{\mathcal{T}} \cong -\mathcal{A}_{\mathrm{SL}_3, \square}^+(\mathbb{R}^t)_{\mathcal{T}} (\cong -\mathcal{A}_{\mathrm{PGL}_3, \square}^+(\mathbb{R}^t)_{\mathcal{T}})$.

On the other hand, via the isomorphism $\theta_{\mathcal{T}} : \mathbb{R}^{12} \rightarrow V_{\mathcal{T}} \subseteq \mathbb{R}^{18}$ we view the real cone $\theta_{\mathcal{T}}(C_{\mathcal{T}}) \subseteq V_{\mathcal{T}}$ as the isomorphic \mathcal{T} -chart $\theta_{\mathcal{T}}(C_{\mathcal{T}}) \cong -\mathcal{A}_{\mathrm{PGL}_3, \square}^+(\mathbb{R}^t)_{\mathcal{T}} (\cong -\mathcal{A}_{\mathrm{SL}_3, \square}^+(\mathbb{R}^t)_{\mathcal{T}})$.

Recall, in addition to the 12 dimensional \mathcal{A} -moduli spaces $\mathcal{A}_{\mathrm{SL}_3, \square}$ and $\mathcal{A}_{\mathrm{PGL}_3, \square}$ (§2), Fock-Goncharov [FG06] and Goncharov-Shen [GS15, GS19] defined the \mathcal{X} - and \mathcal{P} -moduli spaces $\mathcal{X}_{\mathrm{PGL}_3, \square}$ and $\mathcal{P}_{\mathrm{PGL}_3, \square}$, which are 4- and 12-dimensional, respectively. In addition, there are canonical maps $p : \mathcal{A}_{\mathrm{SL}_3, \square} \rightarrow \mathcal{X}_{\mathrm{PGL}_3, \square}$ and $\bar{p} : \mathcal{A}_{\mathrm{SL}_3, \square} \rightarrow \mathcal{P}_{\mathrm{PGL}_3, \square}$ (the overline notation \bar{p} may be nonstandard). The tropical points $\mathcal{X}_{\mathrm{PGL}_3, \square}(\mathbb{R}^t)$ and $\mathcal{P}_{\mathrm{PGL}_3, \square}(\mathbb{R}^t)$ of these spaces are also defined, inducing tropicalizations $p^t : \mathcal{A}_{\mathrm{SL}_3, \square}(\mathbb{R}^t) \rightarrow \mathcal{X}_{\mathrm{PGL}_3, \square}(\mathbb{R}^t)$ and $\bar{p}^t : \mathcal{A}_{\mathrm{SL}_3, \square}(\mathbb{R}^t) \rightarrow \mathcal{P}_{\mathrm{PGL}_3, \square}(\mathbb{R}^t)$ of the canonical maps.

In terms of \mathcal{T} -charts, we view $\mathcal{X}_{\mathrm{PGL}_3, \square}(\mathbb{R}^t)_{\mathcal{T}} \cong \mathbb{R}^4$ and $\mathcal{P}_{\mathrm{PGL}_3, \square}(\mathbb{R}^t)_{\mathcal{T}} \cong \mathbb{R}^8 \times \mathbb{R}^4$. We think of the projection $\pi_4 \circ \phi_{\mathcal{T}} \circ \theta_{\mathcal{T}} : \mathbb{R}^{12} \rightarrow \mathbb{R}^8 \times \mathbb{R}^4 \rightarrow \mathbb{R}^4$ as the canonical map p^t written in coordinates. The isomorphism $\phi_{\mathcal{T}} \circ \theta_{\mathcal{T}} : \mathbb{R}^{12} \rightarrow \mathbb{R}^8 \times \mathbb{R}^4$ could be viewed as a coordinate version of the canonical map \bar{p}^t .

We can interpret Corollary 7.34 as saying that, when expressed in coordinates, the canonical map $p^t (\approx \pi_4 \circ \phi_{\mathcal{T}} \circ \theta_{\mathcal{T}})$ also projects the subset $-\mathcal{A}_{\mathrm{SL}_3, \square}^+(\mathbb{R}^t)_{\mathcal{T}} \subseteq -\mathcal{A}_{\mathrm{SL}_3, \square}(\mathbb{R}^t)_{\mathcal{T}} (\approx C_{\mathcal{T}} \subseteq \mathbb{R}^{12})$ of positive points onto $\mathcal{X}_{\mathrm{PGL}_3, \square}(\mathbb{R}^t)_{\mathcal{T}} (\approx \mathbb{R}^4)$.

In addition, since the positive integer cone $\mathcal{C}_{\mathcal{T}} \subseteq \mathbb{Z}_+^{12}$ is in bijection with the set of reduced webs \mathcal{W}_{\square} via the web tropical coordinate map $\Phi_{\mathcal{T}}$, and since $\mathcal{C}_{\mathcal{T}} \cong -3\mathcal{A}_{\mathrm{PGL}_3, \square}^+(\mathbb{Z}^t)_{\mathcal{T}}$ by Remark 3.4: we can interpret Corollary 7.35 as saying that, in coordinates, the canonical map $p^t (\approx \pi_4 \circ \phi_{\mathcal{T}} \circ \theta_{\mathcal{T}})$ projects (a proper subset of) $-3\mathcal{A}_{\mathrm{PGL}_3, \square}^+(\mathbb{Z}^t)_{\mathcal{T}} (\approx \mathcal{C}_{\mathcal{T}})$ onto $\mathcal{X}_{\mathrm{PGL}_3, \square}(\mathbb{Z}^t)_{\mathcal{T}} (\approx \mathbb{Z}^4)$.

REFERENCES

- [AF17] N. Abdiel and C. Frohman. The localized skein algebra is Frobenius. *Algebr. Geom. Topol.*, 17:3341–3373, 2017.
- [AK17] D. G. L. Allegretti and H. K. Kim. A duality map for quantum cluster varieties from surfaces. *Adv. Math.*, 306:1164–1208, 2017.
- [Bul97] D. Bullock. Rings of $\mathrm{SL}_2(\mathbb{C})$ -characters and the Kauffman bracket skein module. *Comment. Math. Helv.*, 72:521–542, 1997.
- [CKM14] S. Cautis, J. Kamnitzer, and S. Morrison. Webs and quantum skew Howe duality. *Math. Ann.*, 360:351–390, 2014.
- [Dou21] D. C. Douglas. Quantum traces for $\mathrm{SL}_n(\mathbb{C})$: the case $n = 3$. <https://arxiv.org/abs/2101.06817>, 2021.
- [DS20] D. C. Douglas and Z. Sun. Tropical Fock-Goncharov coordinates for SL_3 -webs on surfaces I: construction. <https://arxiv.org/abs/2011.01768>, 2020.
- [FG06] V. V. Fock and A. B. Goncharov. Moduli spaces of local systems and higher Teichmüller theory. *Publ. Math. Inst. Hautes Études Sci.*, 103:1–211, 2006.
- [FG07a] V. V. Fock and A. B. Goncharov. Dual Teichmüller and lamination spaces. *Handbook of Teichmüller theory*, 1:647–684, 2007.
- [FG07b] V. V. Fock and A. B. Goncharov. Moduli spaces of convex projective structures on surfaces. *Adv. Math.*, 208:249–273, 2007.
- [FG09] V. V. Fock and A. B. Goncharov. Cluster ensembles, quantization and the dilogarithm. *Ann. Sci. Éc. Norm. Supér.*, 42:865–930, 2009.

- [FKK13] B. Fontaine, J. Kamnitzer, and G. Kuperberg. Buildings, spiders, and geometric Satake. *Compos. Math.*, 149:1871–1912, 2013.
- [FS22] C. Frohman and A. S. Sikora. $SU(3)$ -skein algebras and webs on surfaces. *Math. Z.*, 300:33–56, 2022.
- [FZ02] S. Fomin and A. Zelevinsky. Cluster algebras. I. Foundations. *J. Amer. Math. Soc.*, 15:497–529, 2002.
- [GHKK18] M. Gross, P. Hacking, S. Keel, and M. Kontsevich. Canonical bases for cluster algebras. *J. Amer. Math. Soc.*, 31:497–608, 2018.
- [GMN13] D. Gaiotto, G. W. Moore, and A. Neitzke. Spectral networks. *Ann. Henri Poincaré*, 14:1643–1731, 2013.
- [GS15] A. B. Goncharov and L. Shen. Geometry of canonical bases and mirror symmetry. *Invent. Math.*, 202:487–633, 2015.
- [GS19] A. B. Goncharov and L. Shen. Quantum geometry of moduli spaces of local systems and representation theory. <https://arxiv.org/abs/1904.10491>, 2019.
- [Hil90] D. Hilbert. Ueber die Theorie der algebraischen Formen. *Math. Ann.*, 36:473–534, 1890.
- [HS19] Y. Huang and Z. Sun. McShane identities for Higher Teichmüller theory and the Goncharov-Shen potential, to appear in Mem. Amer. Math. Soc. <https://arxiv.org/abs/1901.02032>, 2019.
- [IK22] T. Ishibashi and S. Kano. Unbounded \mathfrak{sl}_3 -laminations and their shear coordinates. <https://arxiv.org/abs/2204.08947>, 2022.
- [Kim20] H. K. Kim. SL_3 -laminations as bases for PGL_3 cluster varieties for surfaces. <https://arxiv.org/abs/2011.14765>, 2020.
- [KS08] M. Kontsevich and Y. Soibelman. Stability structures, motivic Donaldson-Thomas invariants and cluster transformations. <https://arxiv.org/abs/0811.2435>, 2008.
- [KT99] A. Knutson and T. Tao. The honeycomb model of $GL_n(\mathbb{C})$ tensor products. I. Proof of the saturation conjecture. *J. Amer. Math. Soc.*, 12:1055–1090, 1999.
- [Kup96] G. Kuperberg. Spiders for rank 2 Lie algebras. *Comm. Math. Phys.*, 180:109–151, 1996.
- [Le16] I. Le. Higher laminations and affine buildings. *Geom. Topol.*, 20:1673–1735, 2016.
- [MFK94] D. Mumford, J. Fogarty, and F. Kirwan. *Geometric invariant theory. Third edition.* Springer-Verlag, Berlin, 1994.
- [Pen87] R. C. Penner. The decorated Teichmüller space of punctured surfaces. *Comm. Math. Phys.*, 113:299–339, 1987.
- [Prz91] J. H. Przytycki. Skein modules of 3-manifolds. *Bull. Polish Acad. Sci. Math.*, 39:91–100, 1991.
- [PS00] J. H. Przytycki and A. S. Sikora. On skein algebras and $SL_2(\mathbb{C})$ -character varieties. *Topology*, 39:115–148, 2000.
- [Sch81] A. Schrijver. On total dual integrality. *Linear Algebra Appl.*, 38:27–32, 1981.
- [Sik01] A. S. Sikora. SL_n -character varieties as spaces of graphs. *Trans. Amer. Math. Soc.*, 353:2773–2804, 2001.
- [Sik05] A. S. Sikora. Skein theory for $SU(n)$ -quantum invariants. *Algebr. Geom. Topol.*, 5:865–897, 2005.
- [SSW] L. Shen, Z. Sun, and D. Weng. In preparation.
- [SW07] A. S. Sikora and B. W. Westbury. Confluence theory for graphs. *Algebr. Geom. Topol.*, 7:439–478, 2007.
- [SWZ20] Z. Sun, A. Wienhard, and T. Zhang. Flows on the $PGL(V)$ -Hitchin component. *Geom. Funct. Anal.*, 30:588–692, 2020.
- [Thu97] W. P. Thurston. *Three-dimensional geometry and topology. Vol. 1.* Princeton University Press, Princeton, NJ, 1997.
- [Tur89] V. G. Turaev. Algebras of loops on surfaces, algebras of knots, and quantization. In *Braid group, knot theory and statistical mechanics*, pages 59–95. World Sci. Publ., Teaneck, NJ, 1989.
- [Wie18] A. Wienhard. An invitation to higher Teichmüller theory. In *Proceedings of the International Congress of Mathematicians—Rio de Janeiro 2018. Vol. II. Invited lectures*, pages 1013–1039. World Sci. Publ., Hackensack, NJ, 2018.
- [Wit89] E. Witten. Quantum field theory and the Jones polynomial. *Comm. Math. Phys.*, 121:351–399, 1989.
- [Xie13] D. Xie. Higher laminations, webs and $N=2$ line operators. <https://arxiv.org/abs/1304.2390>, 2013.

DEPARTMENT OF MATHEMATICS, YALE UNIVERSITY, NEW HAVEN CT 06511, U.S.A.
Email address: `daniel.douglas@yale.edu`

IHES, 35 ROUTE DE CHARTRES, 91440 BURES-SUR-YVETTE, FRANCE
Email address: `sun.zhe@ihes.fr`

SCHOOL OF MATHEMATICAL SCIENCES, UNIVERSITY OF SCIENCE AND TECHNOLOGY OF CHINA, 96
 JINZHAI ROAD, 230026 HEFEI, CHINA
Email address: `sunz@ustc.edu.cn`

APPENDIX A. TWO FLIP EXAMPLES

In Figures 24 and 25 below, we display the bigon drawing procedure, putting a web into good position after flipping the diagonal, for two examples in the web families (3) and (7), respectively, as explained in detail in §5.2.

APPENDIX B. PENTAGON RELATION FOR SL_3

The Mathematica notebook presented in Figure 26 below provides the expression for $f_5(x_1, x_2, \dots, x_{17})$ as defined in Example (part 5) from §4.3.2. See Remark 4.15.

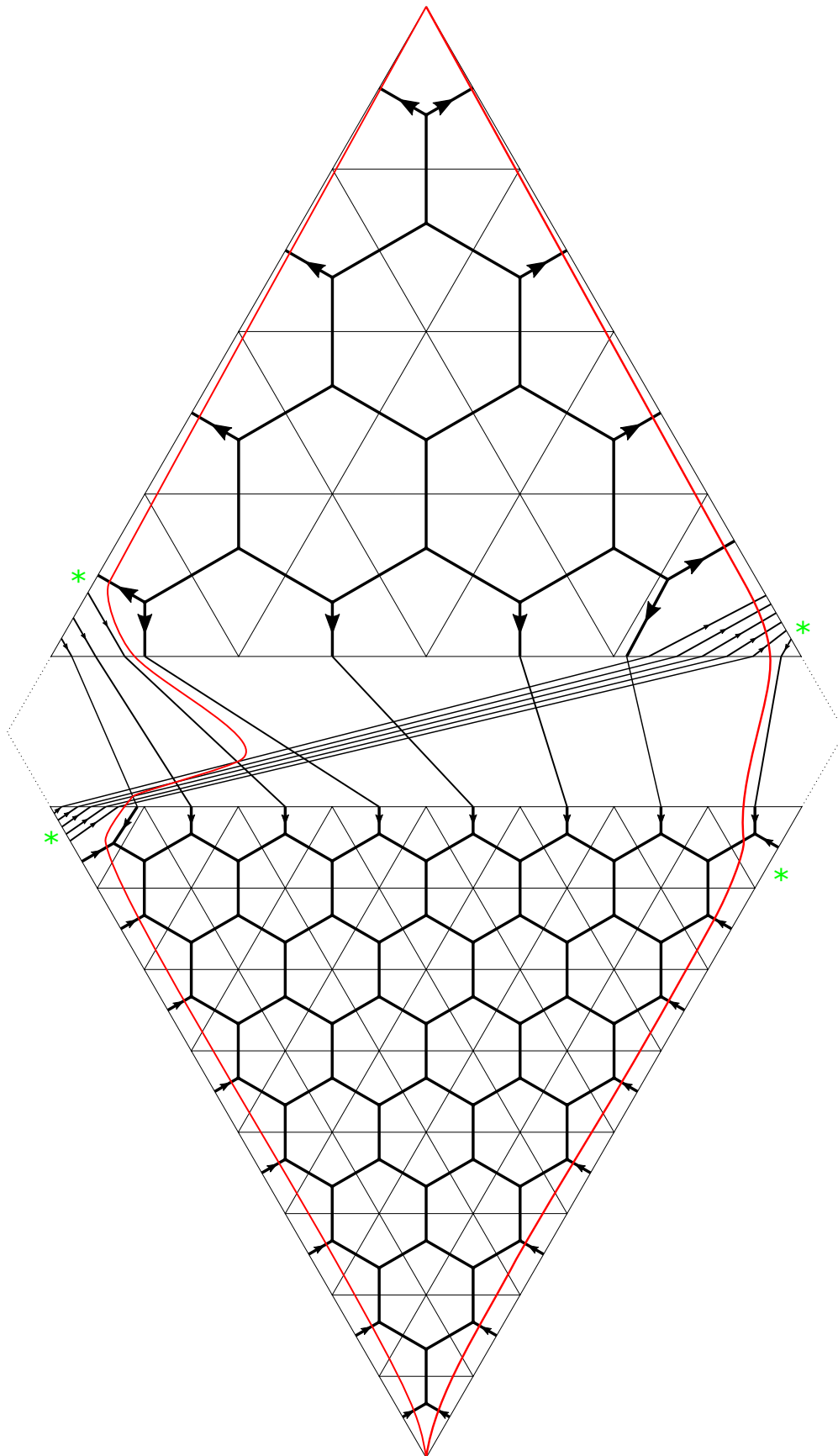


FIGURE 24. **Family (3).** Bigon drawing procedure in the example $x = 3, y = 4, z = 1, t = 5$. The web represented by the schematic is in good position with respect to the red bigon. The green asterisks separate the honeycombs from the corner arcs in the flipped triangulation. Compare Figures 18 and 19.

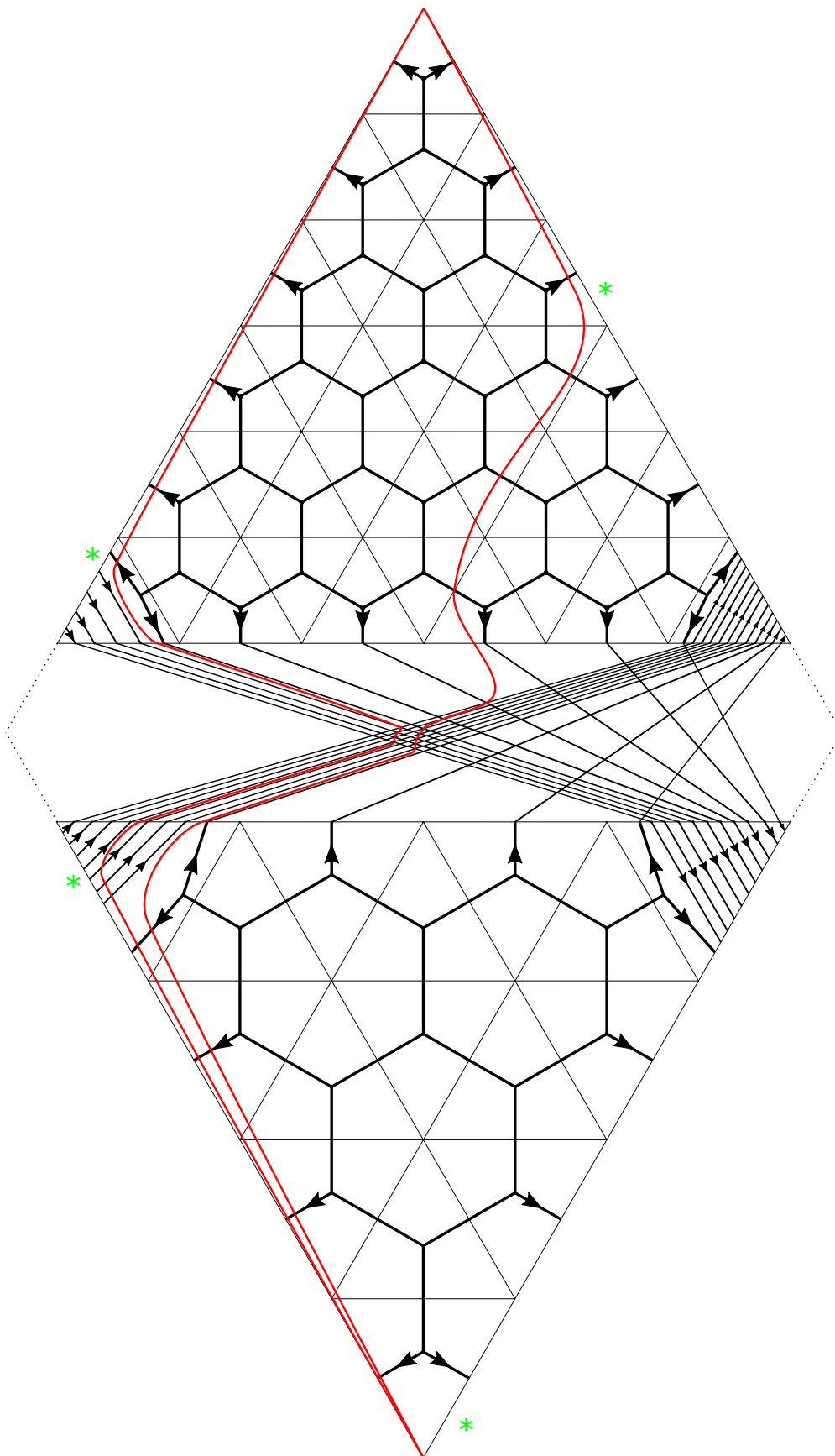


FIGURE 25. **Family (9).** Bigon drawing procedure in the example $x = 6, y = 4, z = 7, t = 4$. The web represented by the schematic is in good position with respect to the red bigon. The green asterisks separate the honeycombs from the corner arcs in the flipped triangulation. Compare Figures 20 and 21.

```
(* f_5(x1, x2, ..., x17), namely the piecewise-linear expression below *)
```

FIGURE 26. (Page 1 of 2.)

FIGURE 26. (Page 2 of 2.)